AD_____

Award Number: DAMD17-99-1-9001

TITLE: Clinical Evaluation of Digital Mammography

PRINCIPAL INVESTIGATOR: Laurie L. Fajardo, M.D.

CONTRACTING ORGANIZATION: The Johns Hopkins University
School of Medicine
Baltimore, Maryland 21205-2196

REPORT DATE: February 2000

TYPE OF REPORT: Annual

PREPARED FOR: U.S. Army Medical Research and Materiel Command
Fort Detrick, Maryland 21702-5012

REPORT DOCUMENTATION PAGE

Form Approved
OMB No. 074-0188

1. AGENCY USE ONLY (Leave blank)	2. REPORT DATE	3. REPORT TYPE AND DATES COVERED
	February 2000	Annual (1 Feb 99 - 31 Jan 00)

4. TITLE AND SUBTITLE
Clinical Evaluation of Digital Mammography

5. FUNDING NUMBERS
DAMD17-99-1-9001

6. AUTHOR(S)
Laurie L. Fajardo, M.D.

7. PERFORMING ORGANIZATION NAME(S) AND ADDRESS(ES)
The Johns Hopkins University School of Medicine
Baltimore, Maryland 21205-2196

E-MAIL: LFAJARDO@JHMI.edu

8. PERFORMING ORGANIZATION REPORT NUMBER

9. SPONSORING / MONITORING AGENCY NAME(S) AND ADDRESS(ES)
U.S. Army Medical Research and Materiel Command
Fort Detrick, Maryland 21702-5012

10. SPONSORING / MONITORING AGENCY REPORT NUMBER

11. SUPPLEMENTARY NOTES
This report contains colored photographs

12a. DISTRIBUTION / AVAILABILITY STATEMENT
Approved for public release; distribution unlimited

12b. DISTRIBUTION CODE

13. ABSTRACT ***(Maximum 200 Words)***

Our study entails two aspects of translational research related to the clinical application of digital mammography: technology optimization (Phase 1) and a clinical evaluation (Phase 2).

The technology/system optimization work is near completion and has focused on optimizing the operational parameters most likely to impact mammographic image quality for radiodense breasts, including x-ray tube target material, filter composition, tube voltage, and x-ray exposure level/radiation dose. We have evaluated digital mammography systems from 3 different manufacturers - comprising the systems to be used in the Phase 2 portion of this research. Expert physicists collaborating in this work have developed optimization parameters for each system to enable the best image quality within reasonable x-ray dose ranges. In addition, quality control standards have also been established to maintain optimized system performance and control the above cited parameters during the Phase 2 clinical study.

The second phase of this project is a multicenter clinical evaluation comparing optimized digital mammography to SFM in women with moderate or marked breast density who present for problem-solving mammography. Eligible women consenting to participate will undergo a 4-view screen-film and digital mammogram. Total accrual will be 1075 women with moderately or markedly dense breasts. The clinical trial is scheduled to open July 1,2000.

Our Phase 1 results demonstrate that successful system optimization and quality control of digital mammography systems can be efficiently achieved in a manner similar to conventional screen-film mammography. The clinical research to be carried out during Phase 2 will determine whether digital mammography has the same or better diagnostic accuracy as conventional mammography in the population of women who have radiodense breast tissue.

14. SUBJECT TERMS
Breast Cancer, Digital Mammography, System Optimization - Digital Mammography, Quality Control - Digital Mammography, Clinical Evaluation - Digital Mammography.

15. NUMBER OF PAGES
163

16. PRICE CODE

17. SECURITY CLASSIFICATION OF REPORT	18. SECURITY CLASSIFICATION OF THIS PAGE	19. SECURITY CLASSIFICATION OF ABSTRACT	20. LIMITATION OF ABSTRACT
Unclassified	Unclassified	Unclassified	Unlimited

FOREWORD

Opinions, interpretations, conclusions and recommendations are those of the author and are not necessarily endorsed by the U.S. Army.

N/A Where copyrighted material is quoted, permission has been obtained to use such material.

N/A Where material from documents designated for limited distribution is quoted, permission has been obtained to use the material.

N/A Citations of commercial organizations and trade names in this report do not constitute an official Department of Army endorsement or approval of the products or services of these organizations.

N/A In conducting research using animals, the investigator(s) adhered to the "Guide for the Care and Use of Laboratory Animals," prepared by the Committee on Care and use of Laboratory Animals of the Institute of Laboratory Resources, national Research Council (NIH Publication No. 86-23, Revised 1985).

X For the protection of human subjects, the investigator(s) adhered to policies of applicable Federal Law 45 CFR 46.

N/A In conducting research utilizing recombinant DNA technology, the investigator(s) adhered to current guidelines promulgated by the National Institutes of Health.

N/A In the conduct of research utilizing recombinant DNA, the investigator(s) adhered to the NIH Guidelines for Research Involving Recombinant DNA Molecules.

N/A In the conduct of research involving hazardous organisms, the investigator(s) adhered to the CDC-NIH Guide for Biosafety in Microbiological and Biomedical Laboratories.

Laurie Fajardo 6-18-00

PI - Signature Date

Table of Contents

Cover.....p1

SF 298.....p2

Foreword.....p3

Table of Contents.....p4

Introduction.....p5

Body..... p5

Key Research Accomplishments..... p15

Reportable Outcomes..... p16

Conclusions.....p17

References..... p18

Appendices.....

APPENDIX A: ACCEPTANCE TESTS AND QUALITY CONTROL PROCEDURES FOR FULL-BREAST DIGITAL MAMMOGRAPHY

Appendix B: Protocol Manual – "CLINICAL EVALUATION OF DIGITAL MAMMOGRAPHY"

Appendix C: Case Report/Data Forms

Appendix D: Abstracts Presented

Appendix E: Manuscripts in Preparation

ANNUAL REPORT FOR AWARD NUMBER DAMD17-99-1-9001

"CLINICAL EVALUATION OF DIGITAL MAMMOGRAPHY"

INTRODUCTION:

The investigations being conducted under DAMD award 17-999-1-9001 involve a unique group of expert physicists and clinical researchers who have previously collaborated to establish a research group known as the International Digital Mammography Group. Our study entails two aspects of translational research related to the clinical application of digital mammography: technology optimization (Phase 1) and a clinical evaluation (Phase 2).

The technology/system optimization work is near completion and has focused on optimizing the operational parameters most likely to impact mammographic image quality for radiodense breasts (x-ray tube target material, filter composition, tube voltage, and exposure level/radiation dose). Because the dynamic range of x-ray signals recorded with standard screen-film mammography systems is greatly exceeded by digital systems, one of the most promising contributions of digital mammography is improved imaging of moderate to markedly dense breast tissue.

The second phase of this project is a multicenter clinical evaluation comparing optimized digital mammography to SFM in women with moderate or marked breast density who present for problem-solving mammography. Eligible women consenting to participate will undergo a 4-view screen-film and digital mammogram. Total accrual will be 1075 women with moderately or markedly dense breasts and either (1) a palpable breast lesion scheduled for biopsy, (2) a nonpalpable lesion detected on SFM and scheduled for biopsy, or (3) a nonpalpable lesion detected on SFM and scheduled for diagnostic imaging and mammographic follow-up only. The primary outcome of interest—lesion detectability on digital versus screen-film mammograms—will be evaluated based on a receiver operating characteristic curve analysis of 12 readers' assessments of the likely presence of malignant lesions based on mammographic findings. Secondarily, differences in case management between the two imaging modalities will be measured.

It is anticipated that optimized digital mammography will improve radiologists' detection of breast cancer over screen-film mammography results, which will in turn demonstrate benefits to the patient and the health-care system as a result of more accurately prescribed clinical management and follow-up.

BODY: RESEARCH ACCOMPLISHMENTS:

PHASE I: Technical evaluations/system optimization:

The specific aims for Phase 1 are as follows:

Task 1: Optimize technical parameters for operating DM systems with respect to x-ray beam/image acquisition, dose considerations, and image quality as a function of signal-to-noise ratio.

Task 1a) Identify preliminary exposure techniques for early patient accrual.
Task 1b) Refine the exposure techniques to optimize imaging performance.

Task 2): To ensure quality control of the digital mammographic units during clinical image acquisition.

Our goal is to ensure uniform and consistent imaging performance from the digital units at the six clinical sites during clinical image acquisition. Where applicable, performance evaluation is based on existing American College of Radiology (ACR) guidelines for conventional mammography. Because of the specialized nature of the digital mammography systems, some of the tests have been modified and new guidelines for performance have been defined.

Description of the Digital Mammographic Systems

Fischer system

This system consists of a long, narrow detector that moves in an arc behind the breast in synchrony with a fan-shaped beam of x-rays. The detector consists of a cesium iodide (Csl) phosphor material, coupled to multiple CCD arrays through glass fiber optic tapers. The CCDs are operated in time delay integration (TDI) mode. The images from the individual CCD modules are combined or "stitched" together to form the complete two-dimensional digital mammogram. At this time, Fischer systems have been installed at Brooke Army Hospital, Thomas Jefferson University Hospital, the University of North Carolina at Chapel Hill and Sunnybrook Health Science Centre.

General Electric system

This system incorporates an area detector that is the full size of the desired image field. The detector consists of a layer of CsI deposited on a photodiode array formed on an amorphous silicon thin film transistor array. The image is initially acquired as integrated charge in each pixel, and then read out and digitized by activating a set of control and data lines that connect to the pixel transistors from the sides of the array. A GE system is operational at the University of Pennsylvania.

Trex system

The current detector incorporates an area array formed as a matrix of 12 (3x4) smaller modules. Each module is composed of a fiber optic taper, which has an input face that is approximately square. The fibers conduct the image, formed by a CsI layer that covers all of the modules, to 12 square format CCDs. The digitized subimages from the CCDs are then stitched together. Trex units are installed at Johns Hopkins, Good Samaritan Hospital, and at UCLA. These systems are second generation prototype systems. A report

of the performance characteristics of the first generation system was published [Williams 1996].

Although these systems differ in their technical details, they have many factors in common. Each uses CsI(Tl) as an x-ray converter. For all three systems, the mechanical patient positioning is similar to that of conventional mammography systems. The x-ray generators and tubes are also similar to those of conventional units, however, the available targets and filters differ among the three. The following table summarizes some of the characteristics of the three systems.

	FISCHER	GE	TREX
Active Area	18.1 cm x 23.4 cm	18.0 cm x 23.0 cm	19.2 cm x 25.6 cm
Image Matrix Size	3348 x 4340	1800 x 2304 (100 μm mode) 3600 x 4608 (50 μm mode)	4800 x 6400
Pixel Size	54 μm	100 μm or 50 μm (effective)	40 μm
X-ray Targets	Tungsten	Molybdenum, Rhodium	Molybdenum
Filters	Mo, Rh, Cd	Mo, Rh, Al	Mo, Rh

Task 1a: Beam Optimization

Criteria for optimization of tube voltage and external filtration in digital mammography (DM) differ from those used in screen-film mammography. This is because the separation of the processes of acquisition and display in the former permits the contrast of individual structures to be adjusted when the image is viewed. It is therefore possible to detect objects with low subject contrast provided that the image signal to noise ratio (SNR) is adequate. Thus, rather than maximization of contrast within the constraint of acceptable film darkening and patient dose, beam optimization in digital mammography requires maximization of the image SNR, constrained by acceptable patient dose.

The goal of this study is to identify, for each of several currently available DM systems, technique factors that result in the highest SNR per unit radiation dose, and to do so for a range of breast thickness and adipose/fibroglandular ratio. Data from three different early commercial DM systems, located at three different university test sites, are presented here. Each of these sites is participating in a coordinated clinical evaluation of the DM systems, and a major purpose of our study is to provide guidelines for technique factors to be used during the clinical evaluation.

To identify optimum technique factors, we have chosen the following figure of merit (FOM),

$$FOM = (SNR)^2/MGD,$$

where MGD is the mean dose to the glandular portion of the breast, and the SNR is as defined in section 2.2 below. This FOM is independent of exposure (in the x-ray

quantum-limited regime of operation), and has been used previously by others in mammographic beam optimization studies (Jennings et al., 1993; Boone et al., 1990).

A set of customized mammographic phantoms was circulated among the group of physicists at the participating clinical sites. The phantom set consists of blocks of three different fibroglandular/fat breast tissue compositions- 30/70,50/50 and 70/30. One block of each type contains test objects including step wedges of two types (microcalcification and mass equivalent compositions), and several other types of targets.

At each site, 9 different phantoms are tested (3 compositions x 3 thicknesses: 3, 5, and 7 cm). For each phantom, a wide range of kVp, along with all applicable target/filter combinations, is tested. The goal is to find the kVp, target and filtration that will provide the highest signal-to-noise (SNR) for a given dose. We are using the quantity $(SNR)^2/MGD$ as a figure of merit (FOM), where MGD is the calculated mean glandular dose. The signal is taken as the difference between average pixel values in regions of interest (ROIs) centered on steps in the step wedges, and of ROIs in the nearby phantom background area. The MGD for each setup is calculated from the measured half-value layer (HVL), entrance exposure, phantom composition and thickness, kVp and target/filter combination, according to the tables given by Sobol and Wu.

Initial Results: Data from the TREX Digital Mammography System at Johns Hopkins Medical Institution:

Following are example plots of measured signal, SNR, and the FOM, as a function of kVp, for a 70/30 fibroglandular/fat equivalent phantom composition, using the signal from the microcalcification-equivalent material. These data were obtained from the DM system at Johns Hopkins. The results of these studies will be presented at the 5th International Workshop on Digital Mammography, Toronto, CA, June 11-14, 2000.

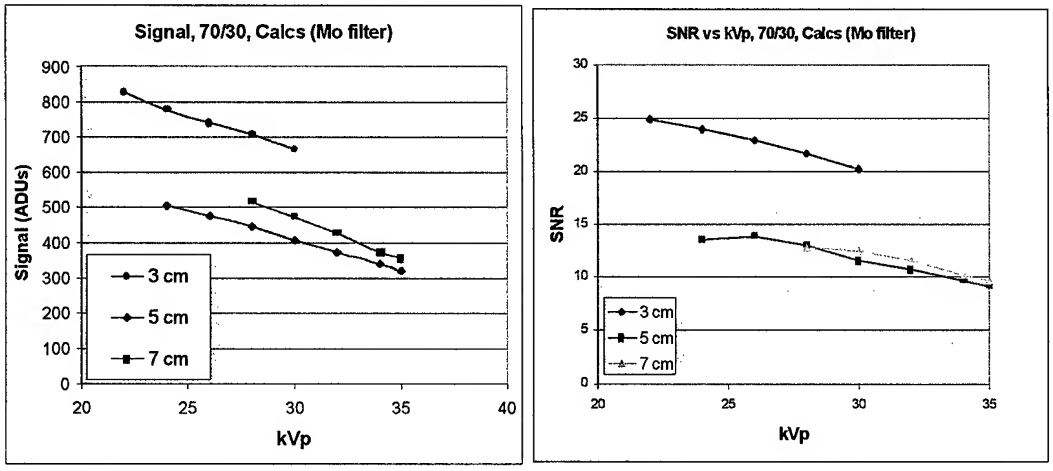

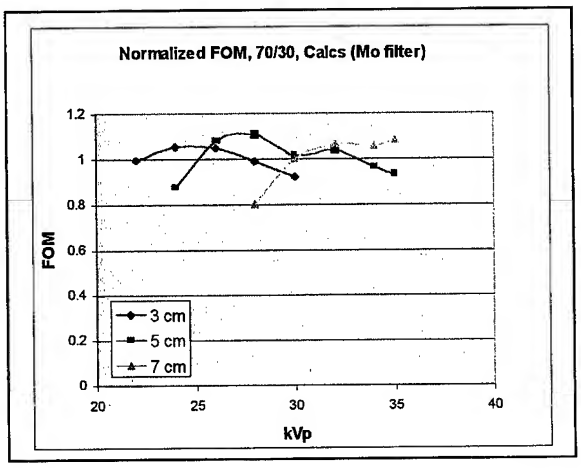

Subsequent Data Acquisition: Three different Digital Mammography (DM) Systems

Three DM units from three different manufacturers were subsequently evaluated and optimized. The units from Fischer, GE, and Trex will hereafter be referred to as Systems 1, 2, and 3, respectively. A common set of phantoms was circulated between the physicists participating in the study. The phantoms were assembled from stacks of blocks of breast equivalent material (CIRS, Inc., Norfolk, VA). Nine different phantoms were assembled and imaged, simulating breasts of three different thicknesses (3 cm, 5 cm, and 7 cm), and three different attenuation equivalent adipose/fibroglandular mass ratios (30/70, 50/50, and 70/30). All blocks of a given phantom had the same adipose /fibroglandular ratio, except for two 5 mm thick blocks, common to all phantoms, that are 100% adipose equivalent. These blocks were placed at the top and bottom of the stack to simulate skin (see figure 1). In each phantom stack assembled, the centrally located block in the stack (the signal block) contained a series of test objects. For the data reported here, the test objects of interest were two stepwedges, one each of calcification equivalent and mass equivalent material. The mass equivalent stepwedge has the same x-ray attenuation as 100% glandular equivalent material, and the microcalcification equivalent step wedge is composed of calcium carbonate. Figure 2 is a schematic of a signal block showing the dimensions of the block and step wedges (other test objects present in the signal block have been omitted for clarity). The thickness of all signal blocks is 2 cm. Images were obtained in manual mode with the phantoms positioned at the chest wall edge of the receptor, centered left to right. Exposure time was selected to give approximately the same average pixel value in the phantom background area for each phantom/technique combination. For each combination two images were obtained with identical exposure times for the purpose of image subtraction, taking care not to move the phantom between the two exposures. At each site, entrance exposures (mR/mAs) and half value layers (HVLs) were measured for each target/filter/kVp combination used.

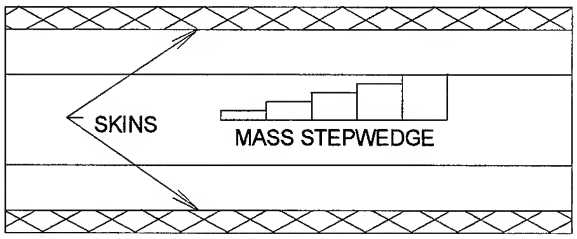

Figure 1: Side view of a 5 cm thick phantom, comprised of one 2 cm thick signal block, two 1 cm thick blank blocks, and two 0.5 cm thick skins.

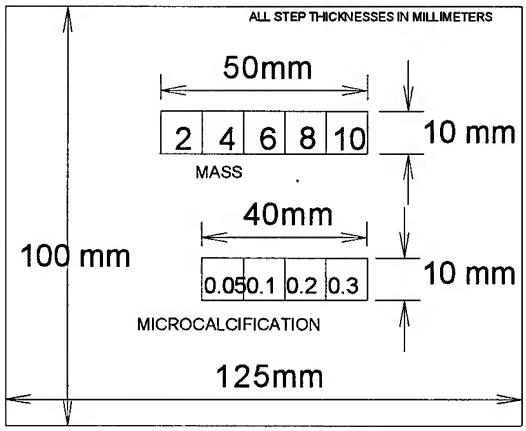

Figure 2: Schematic diagram of a signal block

Image Analysis:

Signal was defined as the difference between the average pixel values in a region of interest (ROI) centered on an individual step (but not including the step boundaries), and an equal sized ROI located immediately adjacent to the step, but containing only background. To quantify the image noise, the two images of a given phantom, obtained at a common technique, were subtracted. Image subtraction was performed to

remove fixed pattern noise associated with phantom defects, detector nonuniformity, and the heel effect. Noise in a single image was defined as the rms pixel-to-pixel fluctuations in an ROI of 1109 x 511 pixels in the difference image, divided by the square root of two.

Calculation of MGD:

Table I lists each of the target and filter combinations tested in the study. Also given for each target/filter combination are the range of kVps used, and the corresponding HVL

Table I

Target	Filter	kVp range	HVL range (mm Al)
Molybdenum	Molybdenum	22-35	0.26-0.43
Molybdenum	Rhodium	24-39	0.37-0.51
Rhodium	Rhodium	25-35	0.36-0.52
Tungsten	Aluminum	29-45	0.46-0.77
Tungsten	Rhodium	32-45	0.47-0.58

Target/filter combinations, kVp ranges, and HVL ranges of the systems tested. Two of the three mammographic systems used Mo/Mo and Mo/Rh combinations. In those cases, the kVp and HVL ranges given represent the pooled values from both systems.

range. In several cases, the same target/filter combination was available on more than one DM system. Table I lists the combined kVp and HVL ranges from all systems.

The MGD for each phantom was calculated using its known thickness and composition, and the measured HVL and mR/mAs values from each DM system. For Mo/Mo and Mo/Rh spectra, the parameterized dose tables of Sobol and Wu were utilized to obtain the glandular dose per unit exposure (Sobol and Wu, 1997). For the W/Al spectra, normalized (to entrance exposure) MGD values were obtained from the data of Stanton et al. (Stanton et al., 1984). Their data were extrapolated to 3 cm breast thickness, and interpolation between their published HVL curves was used to obtain correction factors for the particular glandular volume fractions (0.22, 0.40, and 0.61, corresponding to glandular mass fractions of 0.30, 0.50, and 0.70, respectively) used in our study. For the W/Rh spectra, the calculations of Boone were utilized, interpolating between his published HVL and adipose/fibroglandular composition values (Boone, 1999). All FOM values were obtained by dividing the square of the SNR by the MGD, expressed in units of 10^{-5} Gy (1 mrad).

The measured HVL values for the seven specific target/filter combinations tested at the three sites, as a function of kVp, are shown in Figure 3. Figure 4 shows the corresponding normalized MGD, D_{gN}, calculated for each of the seven spectra, plotted versus the measured HVL. Similarly, Figure 5 shows D_{gN} for each target/filter combination tested, plotted versus kVp. The general tradeoff between loss of contrast and reduction in MGD with increasing kVp is illustrated in Figure 6. In this example, the measured contrast of the 0.3 mm thick (thickest) calcification step in shown for the 5 cm thick, 50/50 phantom.

For each of the three DM systems, SNR versus kVp, and the corresponding FOM values vs. kVp have been determined. Figures 7-12 show the results obtained for the 300 micron thick step of the calcification stepwedge in the three 50/50 composition phantoms, for each of the three imaging systems. To illustrate the applicability of these data to objects, the dependence of the FOM on the step thickness for both types of stepwedges is presented in Figures 13 and 14. These data are from images obtained on System 3, using a Mo/Mo target/filter combination to image a 5 cm thick, 50/50 composition phantom. Finally, Figures 15-17 illustrate the effect on the FOM of changing breast composition, holding breast thickness fixed. These data were obtained using System 1, and signals were calculated using the 10 mm thick mass equivalent step.

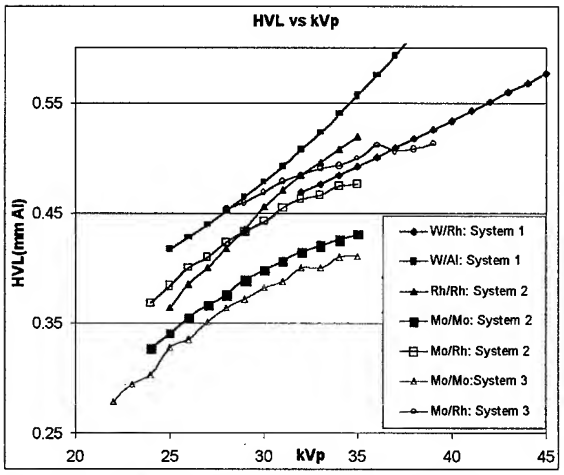

Figure 3: Measured HVLs for the three DM systems, plotted versus kVp.

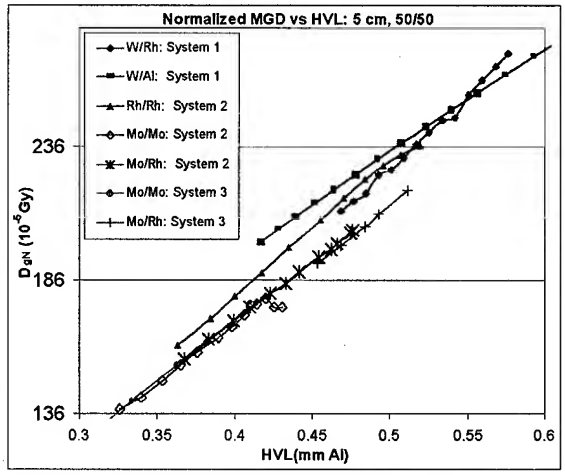

Figure 4: Normalized mean glandular dose versus HVL, for the DM units tested, assuming a 5 cm thick, 50/50phantom.

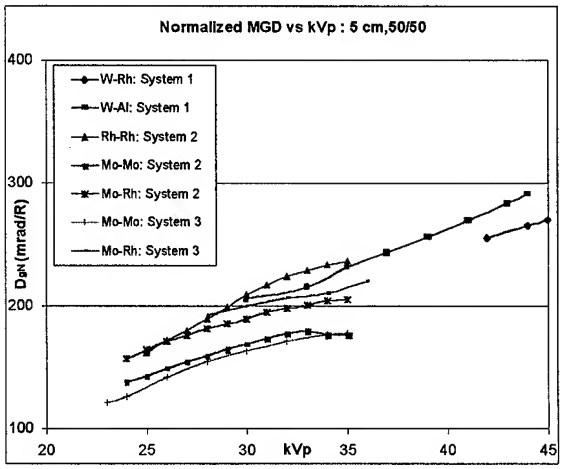

Figure 5: Normalized mean glandular dose vs. kVp for the DM units tested, assuming a 5 cm thick, 50/50 phantom.

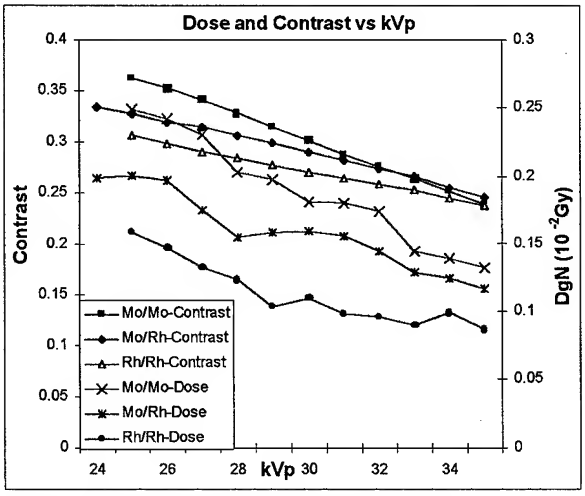

Figure 6: Dose and contrast versus kVp for System 2, using the 0.3 mm calcification step in a 5 cm thick, 50/50 phantom

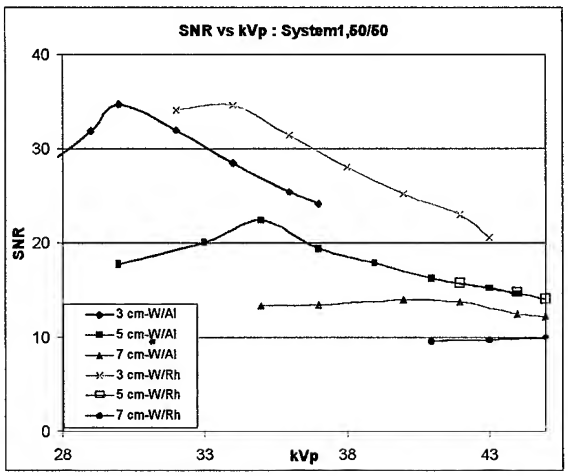

Figure 7: System 1, SNR vs. kVp.

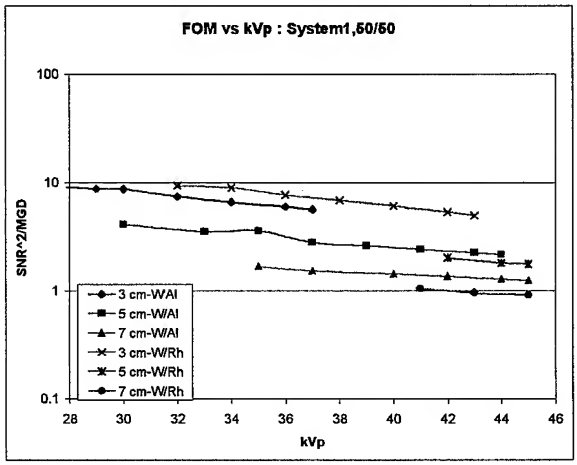

Figure 8: System 1, FOM vs. kVp.

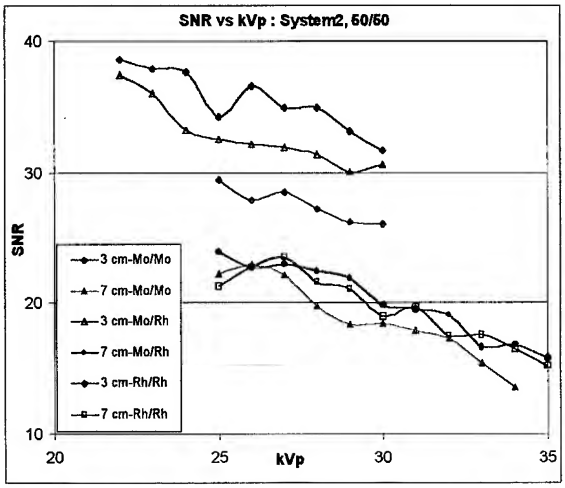

Figure 9: System 2, SNR vs. kVp. 5 cm phantom data have been omitted for clarity, and fall between the 3 cm and 7 cm phantom data shown.

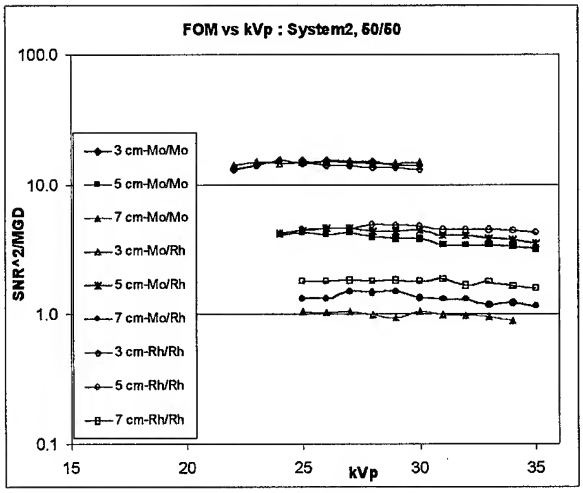

Figure 10: System 2, FOM vs. kVp.

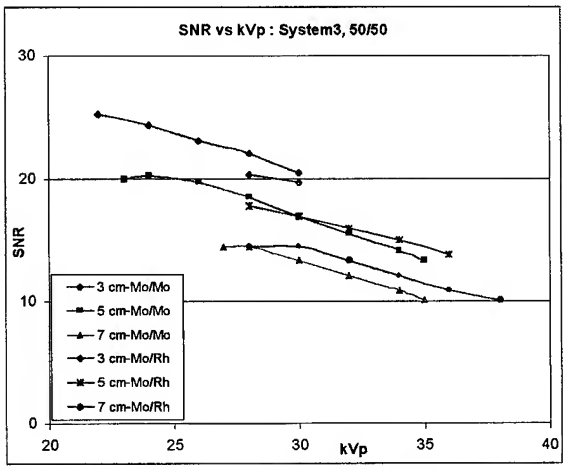

Figure 11: System 3, SNR vs. kVp

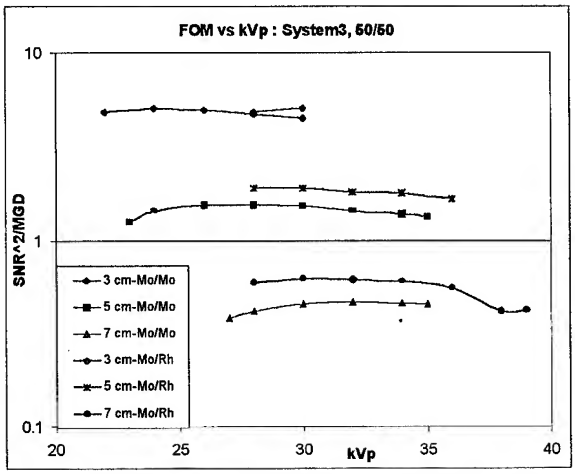

Figure 12: System 3, FOM vs. kVp.

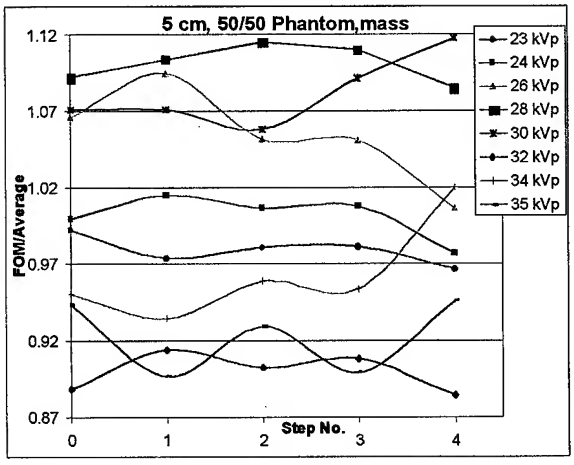

Figure 13: FOM values for the five steps of the mass stepwedge, normalized by the average value for each step. The average FOM values ranged from 0.2 (step 0) to 0.011 (step 4). Data are from System 3, imaging the 5 cm 50/50 phantom.

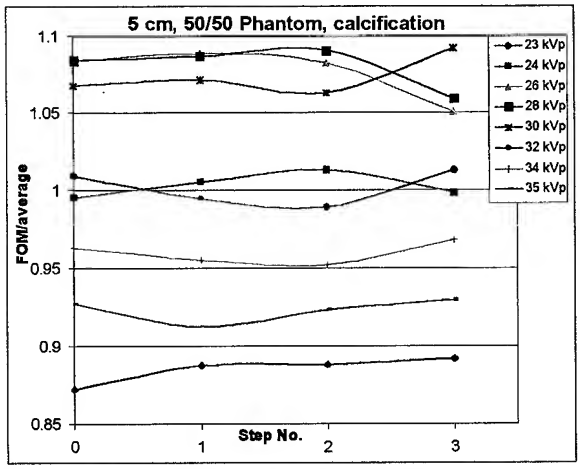

Figure 14: FOM values for the four steps of the calcification stepwedge, normalized by the average value for each step. The average FOM values ranged from 1.4 (step 0) to 0.64 (step 3). Data are from System 3, imaging the 5 cm 50/50 phantom.

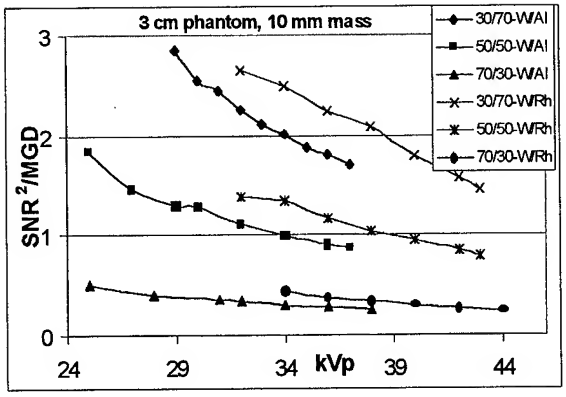

Figure 15: FOM vs kVp for 3 cm thick phantoms of three compositions, imaged on System 1.

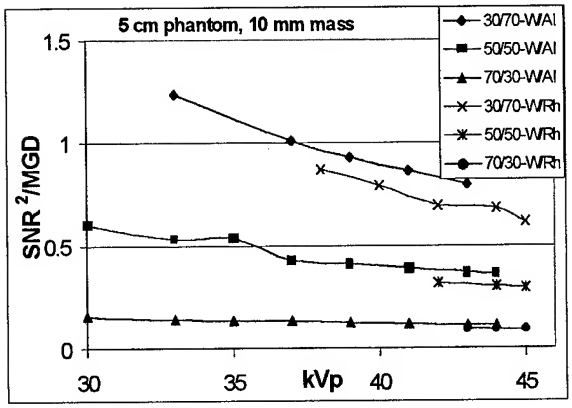

Figure 16: FOM vs kVp for 5 cm thick phantoms of three compositions, imaged on System 1.

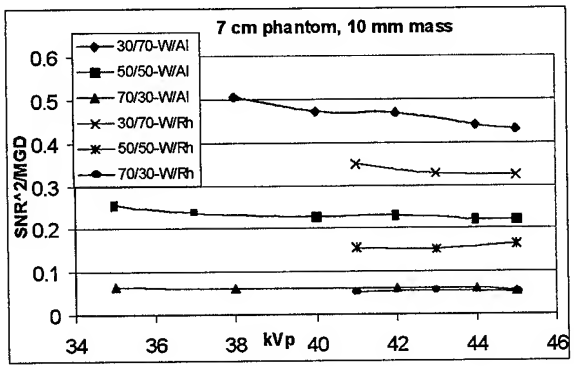

Figure 17: FOM vs kVp for 7 cm thick phantoms of three compositions, imaged on System 1.

Task 2: Quality Control:
We have developed and tested several new phantoms and test tools for quality control of DM systems. Description and preliminary results from application of these tools has been presented at the 1998 RSNA [Development of a quality control system for full-field digital mammography, MJ Yaffe, MB Williams, LT Niklason, GE Mawdsley, AD Maidment, Radiology 209(P) (1998) 160]. We have appended the current version of the Quality Control Manual in Appendix B.

Phase II. Clinical Trial:
During year one of this study, a standardized clinical protocol (Protocol Manual is provided in Appendix A) was established and institutional IRB approvals and DAMB Human Investigations approvals for all six clinical sites were obtained. In addition, the case report forms for data collection were pilot tested and electronically programmed into laptop computers that were then distributed to the clinical site (the case report/data collection forms are provided in Appendix C). Training sessions on the laptop computers for the research assistants and site radiologist investigators have been completed. Each clinical site has recruited and performed data entry on five clinical "test" cases. The digital mammography archive at Johns Hopkins Medical Institution has been established and tested. All digital mammograms are now being backed up and archived onto CDs, rather than magneto-optical disks as originally planned.

In addition, we have completed the data analysis on the 200 patients we recruited in our pilot study (which was sponsored by the Office of Women's Health and provided the preliminary experience and data for this research – manuscripts I preparation provided in Appendix E).

Our full clinical trial is scheduled to open on July 1st, when the Principal Investigator returns from maternity leave.

Key Research Accomplishments:

PHASE I: Technical evaluations/system optimization:

- Phase I technical evaluations are completed and optimization work is nearly complete for the three types of digital mammography systems that will be used in the clinical trial.

- A detailed manual has been written that describes the qualitative tests that should be performed by a qualified physicist prior to accepting a particular digital mammography system for clinical use. Such evaluations are critical as this new technology diffuses into routine clinical use. Due to the complexities of digital imagers and their distinct differences from conventional film imagers, it is likely that variability in manufacture and performance will exist. Radiologists and physicists

must be aware of these issues and understand how their particular system performs relative to the benchmarks our research group is establishing. We plan to publish a complete guideline on acceptance testing after an additional year of monitoring performance and quality assurance measurements on all systems utilized in our study.

- The manual devised for this research study also details quality control procedures for digital mammography. This is an obvious and important parameter to control in our study. Additionally, it is likely that digital mammography will be regulated nationally, similar to current regulatory programs for conventional mammography. Thus, our research group will be in a unique position to spearhead these efforts.

PHASE II: Clinical Trial:

- These were fully described above.

REPORTABLE OUTCOMES:

Abstracts & Presentations: Three scholarly presentations related to this study have been presented in the last six months (see Appendix D).

The 1999 Radiological Society of North America, Chicago, IL, November 27- December 3, 1999:
"Development of a quality control system for full-field digital mammography".
MJ Yaffe, MB Williams, LT Niklason, GE Mawdsley, AD Maidment, Radiology 209(P) (1999) 160.

The 5th International Workshop on Digital Mammography, Toronto, CA, June 11-14, 2000:
"Beam Optimization for Digital Mammography".
MB Williams, M More, V Venkatakrishnan, L Niklason, MJ Yaffe, G Mawdsley, A Bloomquist, A Maidment, D Chakraborty, C Kimme-Smith, LL Fajardo

"Accuracy of digital mammography vs. screen-film mammography in a diagnostic mammography population".
The International Digital Mammography Group

Manuscripts in Preparation:
Two manuscripts, authored by the International Digital Mammography Group and reporting data from the pilot study that preceded this Clinical Translational Research Trial are provided in Appendix E.

Informatics - Databases:
All digital mammography studies performed in this trial and biopsy results will be backed-up in an archive at Johns Hopkins University. This repository of over 1000 digital mammograms, the majority of which will be from women who also have pathology

information, will provide a rich data set for future studies (e.g., the application of computer assisted diagnosis programs to digital mammograms, etc.).

CONCLUSIONS:

PHASE I: Technical evaluations/system optimization:

The analysis of SNR and FOM as a function of kVp, shown in Figures 7-12, indicates that although the image SNR tends to decrease monotonically for all systems with increasing kVp, the accompanying MGD reduction results in fairly flat FOM curves. Note, however, in the case of System 1, the SNR falls at low kVp. This is primarily due to tube loading, since it was not possible to obtain the same exit exposure at all kVps (that is, the tube output was insufficient to compensate for the lower transmission through the phantoms). Thus the falling SNR (and the falling MGD) with decreasing kVp are really consequences of falling exposure.

For a given phantom/technique combination, the SNR, and thus the *magnitude* of the FOM, increases with increasing step thickness for both types of stepwedge. However, the *shape* of the FOM vs. kVp curves for a given target/filter/phantom combination are essentially independent of step thickness, and are similar for mass and calcification equivalent signals. This is illustrated by the example shown in figures 13 and 14. This implies that the result of the optimization is not sensitively dependent on signal amplitude.

Figures 15-17 illustrate that, at least in the case of System 1, there is a clear advantage to using rhodium filtration for thin breasts, but that for breasts 5 cm or thicker, aluminum filtration becomes increasingly advantageous. Similar statements can be made for the molybdenum target systems tested, where molybdenum filtration was superior for 3 cm phantoms of all compositions, but rhodium filtration produced better results for 5 and 7 cm thick phantoms of all compositions. These data suggest that the choice of external filtration is potentially more significant in determination of the overall FOM of a DM system than is choice of tube voltage.

Fahrig and Yaffe developed a model for optimizing spectral shape in digital mammography, and used it to calculate kVp values producing maximum SNR at a fixed dose for W and Mo spectra (Fahrig and Yaffe, 1994). They found that, for a fixed MGD of 0.6 mGy (60 mrads), the peak SNR occurred in the 24-31 kVp range (W spectrum) and 25-29 kVp range (Mo spectrum) for 4 – 8 cm breast thickness, and 50/50 breast composition. Their results were the same, whether the lesion type modeled was infiltrating ductal carcinoma or microcalcification.

Jennings et al. used a computational approach to identify maximum FOM values ($FOM = SNR^2/MGD$) for a variety of target/filter combinations, and breast thicknesses. They found that for a Mo/Mo beam used to image 3-6 cm, 50/50 breasts, the FOM peaks at 27-28 kVp, and changes slowly with changing kVp near the peak values. Very similar FOM vs. kVp curves were obtained for Mo/Mo, Mo/Rh, and W/Al spectra, applied to 6 cm

thick, 50/50 composition breasts. The general trends in our data appear to be consistent with those of these previous studies.

Using the data from these measurements, the expert physicists collaborating in this study have designed operating parameters and quality control guidelines that maintain and control peak performance for each of the 3 different types of digital mammography systems that will be used in our clinical evaluation. Our Phase 1 results demonstrate that successful system optimization and quality control of digital mammography systems can be efficiently achieved in a manner similar to conventional screen-film mammography.

PHASE II: Clinical Trial:
Laptop computers, programmed with the data collection forms (Appendix C), have been provided to each of the six clinical sites. Several training session, conducted by telephone conference calls, have been conducted to train the research assistants at each site. Each site has successfully "enrolled" 5 test cases and the clinical trial will open on July 15, 2000.

The physicist and radiologist investigators comprising the International Digital Mammography Group communicate monthly by conference call.

REFERENCES:

Boone, J. (1999). Glandular breast dose for monoenergetic and high-energy x-ray beams: Monte Carlo assessment. Radiology 213, 23-37.

Boone, J., Shaber, G., and Tecotzky, M. (1990). Dual energy mammography: A detector analysis. Med.Phys. 17, 665-675.

Fahrig, R. and Yaffe, M. (1994). Optimization of spectral shape in digital mammography: Dependence on anode material, breast thickness, and lesion type. Med.Phys. 21, 1473-1481.

Jennings, R.L., Quinn, P.W., Gagne, R.M., and Fewell, T.R. (1993). Evaluation of x-ray sources for mammography. Proc SPIE 1896, 259-268.

Sobol, WT and Wu, X. Parameterization of mammography normalized average glandular dose tables. Medical Physics 24(4), 547-555. 1997.

Stanton, L., Villafana, T., Day, J., and Lightfoot, D. (1984). Dosage evaluation in mammography. Radiology 150, 577-584.

APPENDIX A:

ACCEPTANCE TESTS AND QUALITY CONTROL PROCEDURES FOR FULL-BREAST DIGITAL MAMMOGRAPHY

ACCEPTANCE TESTS
AND
QUALITY CONTROL PROCEDURES
FOR
FULL-BREAST DIGITAL MAMMOGRAPHY

International Digital Mammography Evaluation Group

TABLE OF CONTENTS

1 INTRODUCTION 3

1.1 TABLE 1 - FFDM TECHNOLOGIST'S QC PROCEDURES AND MINIMUM FREQUENCIES 4
1.2 TABLE 2 – FFDM MEDICAL PHYSICIST'S ANNUAL QC PROCEDURES 4

2 ACCEPTANCE TESTING 5

2.1 RATIONALE 5
2.2 STANDARDS FOR ACCEPTANCE 5

3 DAILY FFDM TECHNOLOGIST QC PROCEDURES 6

3.1 MECHANICAL INSPECTION 6
3.2 PHANTOM IMAGE QUALITY TEST 7
3.3 LASER PRINTER DAILY QUALITY CONTROL CHECK 9

4 WEEKLY FFDM TECHNOLOGIST QC PROCEDURES 11

4.1 FLAT FIELD UNIFORMITY AND SNR TEST 11
4.2 DISPLAY MONITOR TEST 12
4.3 VIEWING CONDITIONS 12

5 MONTHLY FFDM TECHNOLOGIST QC PROCEDURES 13

5.1 VISUAL CHECKLIST 13

6 QUARTERLY FFDM TECHNOLOGIST QC PROCEDURES 14

6.1 COMPRESSION FORCE TEST 14
6.2 REPEAT ANALYSIS 15

7 MEDICAL PHYSICISTS FFDM QC PROCEDURES 17

7.1 MAMMOGRAPHIC UNIT ASSEMBLY EVALUATION 17
7.2 MAMMOGRAPHIC ACCREDITATION PHANTOM IMAGE QUALITY EVALUATION 17
7.3 CHEST WALL MISSED TISSUE, NPS, CONTRAST, RESOLUTION 19
7.4 SYSTEM LIMITING SPATIAL RESOLUTION 20
7.5 MTF 21
7.6 COLLIMATION EVALUATION 22
7.7 KVP ACCURACY AND REPRODUCIBILITY 23
7.8 TUBE OUTPUT - MR/MAS VS. KVP 24
7.9 BEAM QUALITY ASSESSMENT - HVL 24
7.10 BREAST ENTRANCE EXPOSURE AND MEAN GLANDULAR DOSE 26
7.11 THICKNESS TRACKING 27
7.12 NOISE, LINEARITY AND REPRODUCIBILITY 27
7.13 SPATIAL LINEARITY AND GEOMETRIC DISTORTION 28
7.14 MONITOR DISPLAY QUALITY SMPTE PATTERN 29
7.15 ARTIFACT EVALUATION TEST 30
7.16 LASER PRINTER EVALUATION 31

1. INTRODUCTION

This document lists the quality control (QC) procedures, their frequencies, and action limits that should be used for clinical Full Field Digital Mammography (FFDM). All QC procedures listed here should be performed at the frequencies indicated. All QC procedures should be documented using the forms provided in this manual. If any problems are encountered in performing these procedures or in documenting your results, please contact one of the people listed above.

This program has been designed to be compliant with requirements of MQSA certification and ACR accreditation insofar as they can be met by digital mammography units. It is also designed to collect information on which tests are effective indicators of image quality degradation and which tests may not be required for future operation of digital mammography facilities.

This QC Manual is divided into Technologist's Procedures with frequencies ranging from daily to quarterly, and Medical Physicist's Tests that are to be performed annually during the trial or more frequently if indicated by image quality considerations. All Technologist Procedures (except Repeat Analysis) should be performed at the start of participation and then repeated at the recommended frequencies. Data collection for repeated exposures should also begin immediately. QC results will need to be kept at your site and a copy of all results will need to be submitted on a monthly basis to the Physics QC Core if you are involved in this clinical trial.

As in conventional mammography, FFDM QC is only effective if the procedures are performed correctly, results are charted and compared to previous results and to action limits as data are collected, and appropriate corrective actions are taken when needed. QC is ineffective if procedures are not performed regularly, if tests are performed but results are not charted, or if the charted results are not looked at carefully to determine if corrective actions are needed. To aid in recognizing when corrective actions should be taken, specific action limits are given for all QC test results. Because these action limits have been developed from the performance of only a few units of each design, it is important that we make sure that action limits are appropriate. If action limits are exceeded in your initial performance of these tests, please let us know immediately so we can see if this is a system problem or a problem with the level at which action limits have been set.

The Technologist's Procedures for FFDM for all units are shown in **Table 1** below. Each unit will have specific tests which are appropriate to that design. The first three tests are daily QC procedures and are covered by two data collection sheets (**Charts 1 and 2**) which permit entry of a month's worth of daily QC data on each. These procedures are discussed in more detail below under the **Daily QC Procedures** section. Similarly, a separate data collection sheet (**Chart 3**) and discussion section are included below for the **Weekly QC Procedures**. A fourth chart (**Chart 4**) is included to indicate performance of the **Monthly and Quarterly QC Procedures**. The Unit Visual Checklist (**Chart 5**) is the only **Monthly Technologist QC Procedure**. Compression force and repeat analysis are the only **Quarterly Technologist QC Procedures**. To aid in collection of data for repeat analysis, a form is included (**Chart 6**) to log each repeated exposure and its cause. Data collection using this repeat log should begin immediately. A separate form is included to summarize the causes of repeated exposures at the end of each quarter (**Chart 7**) based on the data collected in the repeat log.

1.1 Table 1 - FFDM Technologist's QC Procedures and Minimum Frequencies

Procedure	Minimum Frequency	Relevant Forms
Mechanical Inspection	Daily	Chart 1
Phantom Image Quality Test	Daily	Chart 1
Laser Printer Daily Quality Control Check	Daily	Chart 2
Flat-field Uniformity and SNR Test	Weekly	Chart 3
Display Monitor Test	Weekly	Chart 3
Viewing Conditions	Weekly	Chart 3
Visual Checklist	Monthly	Charts 4 & 5
Compression Force Test	Quarterly	Chart 4
Repeat Analysis	Quarterly	Charts 4, 6 & 7

1.2 Table 2 – FFDM Medical Physicist's Annual QC Procedures

	Relevant Forms
Mammographic Unit Assembly Evaluation	Chart 8.1
Mammographic Accreditation Phantom Image Quality Evaluation	Chart 8.2
Chest Wall Missed Tissue, NPS, Contrast, Resolution	Chart 8.3
System Limiting Spatial Resolution	Chart 8.4
Modulation Transfer Function (MTF) Measurement	Chart 8.5
Collimation Evaluation	Chart 8.6
kVp Accuracy And Reproducibility	Chart 8.7
Tube Output mR/mAs vs. kVp	Chart 8.8
Beam Quality Assessment - HVL	Chart 8.9
Breast Entrance Exposure and Mean Glandular Dose	Chart 8.10
Thickness Tracking	Chart 8.11
Noise, Linearity and Reproducibility	Chart 8.12
Spatial Linearity and Geometric Distortion	Chart 8.13
Monitor Display Quality – SMPTE Pattern	Chart 8.14
Artifact Evaluation Test	Chart 8.15
Laser Printer – If Available	Chart 8.16

2. ACCEPTANCE TESTING

Rationale

Acceptance testing must be performed on all units before the unit is used on patients. This is to be performed by a medical physicist qualified in digital mammography. Acceptance testing involves the performance of all QC procedures in this manual, ensuring that the basic minimum criteria are met for each test. The values obtained during the acceptance testing are to be used as baseline values, and will be referred to during future evaluations to determine if equipment function is degrading.

2.2 Standards for Acceptance

Unit Assembly
The digital mammography unit must be safely installed, and present no undue hazards.

Mean Glandular Dose
Must be below 3.0 mGy per view for a 4.2 cm equivalent phantom.

Accreditation Phantom Score
Fibres >= 5, Specks >= 3, Masses >= 3

Effective Limiting Spatial Resolution
100 um systems – 4.5 lp/mm
50 um systems – 9 lp/mm

Tube Output and Reproducibility
At least 800 mR/s at all settings
Tube output linear with mAs +/- 10%
Coefficient of variation for exposure < 0.05.
actual kVp must be within +/- 1.5 kV of the indicated kVp over the full working range

Half-value Layer (HVL) Measurement
HVL should be within the ACR recommended limits: kVp/100 < HVL (in mm Al) < kVp/100 + C where C=0.12 for Mo/Mo, C=0.19 for Mo/Rh and C= 0.22 for Rh/Rh.

Noise
The ratio of the average pixel value to the rms pixel-to-pixel fluctuations for a ROI 1 cm^2 in area of a 4 cm thick uniform phantom image using clinical technique factors must be greater than 50.

Display Quality
The 5% squares at bright and dark levels in the SMPTE test pattern must be visible.

Artifacts
There will be no visible dead pixels, missing lines, or missing columns of data.
There will be no visually distracting structured noise patterns in a uniformity test image acquired after dark current and flat-field detector calibration.

3. DAILY FFDM TECHNOLOGIST QC PROCEDURES

Make sure all FFDM System equipment is turned on, so that it can warm up (approximately 10 minutes) prior to acquiring the daily phantom image.

Recording of all daily FFDM QC procedure results should be done using **Charts 1and 2** found under the **Daily** tab in your site's FFDM QC Manual. The Mechanical Inspection and Phantom Image Quality Test are procedures are listed in order here; the corresponding data forms are on **Chart 1**. The third daily QC test, the Laser Printer Daily Quality Control Check , is described below and the corresponding data forms are on Chart 2.

3.1 Mechanical Inspection

Objective

To ensure that the unit is safe, and that hoses and cables are not crimped or knotted.

Frequency

Daily

Required Equipment

None

Procedure

1. Check that all hoses and cables are free from breaks, crimps, or knots. Hoses and cables should not be under other heavy equipment.
2. Visually inspect the unit for loose parts, cracks in the paddle, compressor cleanliness and integrity.
3. Record on **Chart 1**

Suggested Performance Criteria

Items that are hazardous, inoperative, out of alignment or operate improperly should be repaired by appropriate service personnel.

3.2 Phantom Image Quality Test

Objective

To ensure that image quality is adequate and has not degraded over time.

Frequency

Daily

Required Equipment

ACR Mammography Accreditation Phantom (RMI-156 or Nuclear Associates 18-220). Use the same phantom each time.

Procedure

1. Open a test patient.

2. Set technical factors that would be used for a 4.5 cm compressed breast. Once a setting is selected, this setting should be maintained.

3. Place the ACR phantom in its normal orientation, with the labeled edge of the phantom aligned with the chest wall edge of the digital image receptor, centered left to right, and lightly compress the phantom with the compression paddle.

4. Acquire an image of the phantom.

5. Check that the phantom image is essentially artifact free before accepting it.

6. Evaluate the phantom image using the Radiologist's review station, if available. It is useful to rotate the phantom by 90° and to magnify the phantom. Use the window and level adjustment as well as magnification to display the test objects in the phantom optimally.

7. Scoring of the ACR phantom should use the following criteria. Count the number of visible objects from the largest object of a given type (fiber, speck group, or mass) downward, until a score of 0 or 0.5 is reached, then stop counting for that object type.

(i) Count each fiber as one point if the full length of the fiber is visible and the location and orientation of the fiber are correct. Count a fiber as 0.5 point if not all, but more than half, of the fiber is visible and its location and orientation are correct. If a fiber-like artifact appears anywhere in the insert area of the image but is not in an appropriate location or orientation, deduct the "artifactual" fiber from the last "real" fiber scored if the artifactual fiber is equally or more apparent.

(ii) Count each speck group as 1 point. A full speck group is counted if 4 or more specks are visible in the group in the proper locations. Count a speck group as 0.5 if two or three specks of the group are visible. If noise or speck-like artifacts are visible in the wrong locations in the phantom insert but are as apparent as the "real" specks you are counting, deduct them one for one from the individual specks that you counted. Artifactual specks should only be deducted from "real" specks in the last group counted.

(iii) Count each mass as 1 point if a density difference is visible in the correct location and the mass appears to be generally circular against the background. Count each mass as 0.5 point if a density difference is visible in the correct location but the mass does not have a generally circular appearance. If there is a mass-like artifact appearing in the wrong location anywhere in the phantom insert, deduct the "artifactual" mass from the last "real" mass scored if the artifactual mass is equally or more apparent.

(iv) Enter the results in each category (fibers, specks, and masses) on **Chart 1**.

8. Examine the phantom image carefully for artifacts, including grid lines or other equipment-induced artifacts, and note their presence or absence on the daily control chart (**Chart 1**).

Suggested Performance Criteria

The System should easily meet the ACR and FDA requirement of demonstrating the largest 4 fibers, the largest 3 speck groups, and the largest 3 masses with the techniques and scoring methods described above.

The phantom score should be at least 5 fibers, 3 speck groups, and 3 masses. If phantom image scores on your system are less than this, or you notice a decrease in phantom scores by more than 0.5 in any category, you should contact your medical physicist or authorized service representative.

If any significant artifacts are observed, re-flat-fielding may be needed. If significant artifacts are still observed, contact your authorized service representative.

3.3 Laser Printer Daily Quality Control Check

Objective

To confirm and verify that the laser film processing system is working in a consistent manner according to pre-established specifications (manufacturer's specifications) so that printed image quality is consistently high.

Printing should be conducted directly from the review station to evaluate the entire printing chain integrity.

Frequency

Daily or on days before clinical images are to be printed.

Required Equipment

Densitometer.
Control chart (Chart 2).

Procedure – Establishment of Processor Quality Control Operating Levels

1. Expose and process a SMPTE film and/or a sensitometric film.
2. Repeat step 1 for 5 days, obtaining 5 films.

3. For the SMPTE pattern, read and record the densities on the pattern for the 0% box (D_{max}), 50% box (mid-density or MD), 80%-20% boxes (density difference or DD), and the 100% box (base+fog). For the sensitometric strip, read and record the densities for step 1 (base+fog), for the step with OD reading closest to 1.60 (mid-density step MD), the difference between ODs for steps closest to 2.20 and closest to but not less than 0.45 (the density difference DD), and the highest optical density step (Dmax). Once the mid-density and density difference steps have been selected, the same step numbers should be used for each repeating measurement, until the operating levels are re-established.

Determine the averages for these four values (base+fog, mid-density, density difference, and D_{max}) over the first week, and use them as the operating levels on Chart 2, the Laser Printer Daily Quality Control Chart.

Procedure – Daily Laser Printer Quality Control

1. Expose and process a single SMPTE film or a sensitometric strip following the same procedures as used in Steo 1 above.

2. For the SMPTE pattern, read and record the densities on the pattern for the 0% box (D_{max}), 50% box (mid-density or MD), 80%-20% boxes (density difference or DD), and the 100% box (base+fog). For the sensitometric strip, read and record the densities from the same base+fog, mid-density step (MD), density difference steps, and highest density step (Dmax) used above.

3. Record these four values (base+fog, mid-density, density difference, and D_{max}) on Chart 2, the Laser Printer Daily Quality Control Chart.

Suggested Performance Criteria

If the MD and DD are within +/- 0.10 of their respective operating levels, and the B+F is within +/-0.03 of its operating level, the processor is in control and no further action is required. If the MD or DD fall outside of the +/- 0.10 control limit but with +/- 0.15 limit, the test should be repeated immediately. If the same result is obtained it is acceptable to process films, but the processor should be monitored closely. If the MD or DD exceeds the control limit of +/- 15, the source of the problem must be determined and corrected before digital mammograms are processed. Likewise, if the B+F exceeds +0.03, immediately corrective action must be taken before clinical mammograms are processed.

If a change in the mid-density, density difference, or base+fog exceeds the suggested performance criteria, it will be necessary to determine the source or sources of this change and the problems should be corrected immediately. In addition, the out-of-control data point should be circled, the cause of the problem noted in the "Remarks" section of the control chart, and the in-control data point plotted. On wet processors, the most likely sources of change are processing chemistry, replenishment, and temperature changes. For example, if few films have been printed for some time, the processing chemistry may have oxidized and may not have been properly replenished. On dry processors, the most likely source of change might be the drum temperature. On either processor, a change in film emulsion batches may lead to a change in film optical densities.

4. WEEKLY FFDM TECHNOLOGIST QC PROCEDURES

These procedures should be conducted at the beginning of each week, before patient imaging begins. It is suggested that approximately one hour be set aside each Monday morning before patients are scheduled to conduct these procedures. Allow the system to stabilize before acquiring phantom images. It may be helpful to conduct these weekly procedures for the first time with your medical physicist present to answer any questions that arise.

Record all Weekly FFDM QC Procedures using **Chart 3** found under the **Weekly** tab in your site's FFDM QC Manual. The weekly procedures to be performed are listed in order here and on **Chart 3**. All procedures should be conducted with the compression paddle in place and grid if available.

4.1 Flat Field Uniformity and SNR Test

Objective

To ensure that uniform artifact-free image are produced.

Frequency

Weekly

Required Equipment

One 2 – 5 cm thick sheet of acrylic large enough to cover the entire detector system.

Procedure

1. Place the sheet of acrylic on the breast support tray so that it covers the entire image receptor. The compression paddle should be in place.
2. Acquire an image using a pre-established technique.
3. Measure the average pixel value and standard deviation for 1cm^2 ROIs and record on Chart 3.
4. View the images on the Review Workstation. This may require major adjustment of window level and width to display images properly. Use a narrow window width so that you will be sensitive to artifacts if they exist. To separate image artifacts from monitor-caused artifacts, you may need to rotate images with significant artifacts. If the artifacts rotate, then they are in the image. If the artifacts keep a fixed orientation relative to the monitor, then they are monitor-caused artifacts. Record a checkmark for Pass or record the details of the artifacts observed in the Comments section of Chart 3.

Suggested Performance Criteria

If there are significant artifacts for any images that remain fixed relative to the detector (not the monitor), flat fielding should be redone. If the same artifacts re-appear, the cause should be determined by a medical physicist or service engineer. If artifacts keep a fixed orientation relative to the monitor even after image rotation, there are likely to be problems with the monitor.

4.2 Display Monitor Test

Objective

To ensure that uniform artifact-free image are displayed on the monitor at adequate contrast and resolution.

Frequency

Weekly

Required Equipment

SMPTE pattern

Procedure

Display the image of the SMPTE pattern on all monitors used for diagnosis.

View the images on each Workstation.

Suggested Performance Criteria

The 5% squares should be visible in both the light and dark squares.

Resolution at all corners of the image should be uniform.

The images on all monitors should appear to be the same brightness and contrast.

4.3 Viewing Conditions

Objective

To ensure that displays and viewboxes are clean, viewboxes are uniform and that masking is available.

Frequency

Weekly

Procedure

Clean the screens and panels.
Ensure masking materials are available.
Ensure that background lighting is subdued.

Suggested Performance Criteria

TBA

5. MONTHLY FFDM TECHNOLOGIST QC PROCEDURES

Record the summary of monthly techologist QC test procedures on Chart 4.

5.1 Visual Checklist

Objective

To assure that mammographic X-ray system indicator lights, displays, and mechanical locks and detents are working properly and that the system is mechanically stable.

Frequency

This test should be carried out monthly or after any service or maintenance on the mammographic X-ray system.

Required Equipment

Visual checklist (**Chart 5**)

Procedure

1. Review all of the items listed on the visual checklist and indicate the status.
2. Date and initial the checklist where indicated.
3. Note on **Chart 4** the completion of the Visual Checklist.

Suggested Performance Criteria

Some of the items on the visual checklist are operator convenience features. Some of the items, however, are essential for patient safety and high-quality diagnostic images.

Each of the items listed in the Visual Checklist should pass or receive a check mark. Items not passing the visual check should be replaced or corrected immediately.

Items missing from the room should be replaced immediately. Malfunctioning equipment should be reported to the Service Engineer for repair or replacement as soon as possible.

6. QUARTERLY FFDM TECHNOLOGIST QC PROCEDURES

Record the summary of quarterly techologist QC tests, along with the monthly QC tests, on Chart 4.

6.1 Compression Force Test

Objective

To assure that the mammographic system can provide adequate compression in power driven and manual modes and that the equipment does not allow too much compression to be applied.

Frequency

This test should be carried out initially, then quarterly, and when reduced compression is suspected.

Required Test Equipment

Bathroom scale: the scale must be flat and must be a conventional, analog type, not digital. The digital scales sample the data and may not respond properly as additional pressure is applied slowly to the scale.
Several towels

Procedure

1. Place a towel on the breast support assembly (to protect the breast support), then place the bathroom scale on the towel with the dial or read-out positioned for easy reading. Locate the center of the scale directly under the compression device.

2. Place one or more towels on top of the scale to prevent damage to the compression device.

3. Using the power drive, activate the compression device and allow it to operate until it stops automatically.

4. Read and record this compression force on **Chart 4**.

5. Using the manual drive, continue increasing the compression until the compression device stops.

7. Read and record this compression force on **Chart 4**.

8. Release the compression device.

Note: 1 decaNewton (daN) = 2.2 lbs force.

If the safety mechanism is not properly adjusted, it may be possible to damage the compression device and associated components. If the compression exceeds 18 daN (or approximately 40 pounds) in the power drive mode, immediately release the compression device and ask a service engineer to make the appropriate adjustments.

For adequate compression of the breast, the compression force should range from 11 to 18 daN (25 to 40 lb.) in the power drive mode. Under manual adjustment of compression, a compression force of at least 25 lb. should be achievable and compression forces in excess of 40 lb. are acceptable.

If the suggested performance criteria are not met in both the manual and power driven modes, a service engineer should make the appropriate internal adjustments of compression force.

6.2 Repeat Analysis

Objective

To determine the number and cause of repeated digital mammograms. Analysis of these data should help identify ways to improve system efficiency and reduce digital image retakes and patient exposure.

Frequency

This test should be carried out quarterly. For the repeat rates to be meaningful, a patient volume of at least 250 patients or 1,000 exposures is needed.

Required Equipment

Repeat record sheet(s) (**Chart 6**)
Repeat analysis data sheet (**Chart 7**)

Procedure

1. Record each repeated exposure on **Chart 6**, entering the Study Number, cause of repeated exposure, date, etc.

2. At the end of each quarter, use the repeat analysis form (**Chart 7**) to summarize the number of repeats in each category.

4. Estimate the number of exposures taken during the quarter. This can be done by subtracting the patient number at the beginning of the quarter from the patient number at the end of the quarter (assuming sequential patient numbering of all patients) and multiplying by 4 (assuming 4 exposures per patient on average).

4. Calculate the overall repeat rate as the total of repeated exposures divided by the total number of exposures during the analysis period, multiplied by 100%.

5. Determine the percentage of repeats in each category by dividing the repeats in the category by the total number of repeated exposures from all categories.

6. Note on **Chart 4** completion of the Repeat Analysis Test.

Suggested Performance Criteria

The repeat rate should be less than 5%. If the repeat rate exceeds 5%, the sources of repeated exposures

should be investigated. If the primary cause of excessive repeated exposures is an equipment or detector problem, it should be brought to the attention of the service engineer. If the primary cause of excessive repeated exposures is a positioning or other motion problem, corrective actions such as additional training on positioning and compression should be taken.

7. MEDICAL PHYSICISTS FFDM QC PROCEDURES

All forms for the Medical Physicist's QC Tests are included in Charts 8.0-8.16.

7.1 Mammographic Unit Assembly Evaluation

Objective

To ensure that all locks, detents, angulation indicators, and mechanical support devices for the X-ray tube and breast support assembly are operating properly.

Test Procedure Steps (record results on Chart 8.1)

1. Verify that the free-standing dedicated mammography unit is mechanically stable under normal operating conditions.
2. Verify that all moving parts move smoothly, without undue friction, that cushions or bumpers limit the range of available motions and that no obstructions hinder the full range of motions within these limits.
3. Set and test each lock and detent independently to ensure that mechanical motion is prevented when the lock or detent is set.
4. Verify that the image receptor holder assembly is free from wobble or vibration during normal operation and for any orientation of the image receptor holder assembly.
5. If provided, verify that the compressed breast thickness scale (analog or digital) is accurate to within +/- 0.5 cm under conditions of moderate compression (15 to 20 lb) and reproducible to within +/- 2 mm between 1 and 8 cm.
6. Verify that manual release of the compression paddle is available in the case of a power failure.
7. Verify that in normal operation, the patient and operator are not exposed to sharp or rough edges or other hazards including electrical hazards.
8. Using a screen-film cassette, XTL film or a large ion chamber, verify that: with the tube port blocked with at least 3 mm lead, there is less than .1mR exposure at the external housing for the largest technique to used in practice.
9. Verify that the operator is protected from radiation by adequate shielding.
10. Verify that operator technique charts are posted.
11. Place a lead sheet on the breast support plate, and make an AEC exposure. Verify that the exposure is less than 2000mAs, and that there is indication of hitting the limit which requires resetting.

Suggested Performance Criteria and Corrective Action

Items that are hazardous, inoperative, or operate improperly should be repaired by appropriate service personnel.

7.2 Mammographic Accreditation Phantom Image Quality Evaluation

Objective

To assess mammographic image quality and to detect temporal changes in image quality.

Required Test Equipment

Mammographic phantom (approximately equivalent to a 4.2 cm- thick 50/50 tissue equivalent breast phantom) containing appropriate details ranging from visible to invisible on the mammographic image, e.g., the RMI-156 or Nuclear Associates 18-220 Mammographic Phantom used for the ACR Mammography Accreditation Program (MAP) or a similar phantom. Use the same phantom each time.

Images should be viewed on the same display media used clinically. If a printed film is used for diagnosis, the phantom image should be read on the viewbox used by the radiologist, properly masked.

Original phantom image and the previous phantom image acquired on this unit.

Magnifying lens of the same type used clinically (for film display only).

Test Procedure Steps

1. Prepare the system for a single image acquisition using a patient name such as "ACR Phantom" and a patient number completely different than those used for clinical imaging.
2. Place the phantom on the breast support plate, positioning the phantom laterally centered in the X-ray field with one edge coincident with the chest wall edge of the breast support.
3. Lower the compression paddle so that it is just in contact with the top of the phantom. Do not exert excessive compression force on the phantom, as this may damage the compression paddle.
4. For units using phototimed techniques, verify that the phototimer detector or region is centered on the phantom and in the same location as used for previously acquired phantom images.
5. For sites using manual techniques, select the appropriate exposure time and mA setting (or mAs setting) for the phantom thickness, matching technique factors used for previously acquired phantom images. Initial selection of phantom technique should be based on the technique used for an average breast of 4.2 cm thickness. If the clinical technique changes, the phantom technique should be adjusted to follow the clinical technique.
6. Make an exposure, recording all technique factors on the image quality evaluation form, Chart 8.2.
7. Check on the acquisition station that the phantom image is essentially artifact free before accepting it.
8. For soft-copy diagnosis, record on Chart 8.2 the mean pixel value in a region .5 cm x .5cm in the center of the phantom insert.
9. Evaluate the phantom image using the Radiologist's review station, if available. It is useful to rotate the phantom by 90° and to magnify the phantom to a magnification factor of approximately 1.7. Some re-centering of the phantom is likely to be needed to center the phantom on the monitor. Use the window and level adjustment to display the test objects in the phantom optimally.
10. Using appropriate viewing conditions (film masking, clinical lookup-tables), determine the number of test objects of each type that are visible in the phantom image. Record the phantom test scores on Chart 8.2.
11.

Scoring Criteria

Always count the number of visible objects from the largest object of a given type (fiber, speck group, or mass) downward, until a score of 0 or 0.5 is reached, then stop counting for that object type.

a) Count each fiber as one point if the full length of the fiber is visible and the location and orientation of the fiber are correct. Count a fiber as 0.5 point if not all, but more than half, of the fiber is visible and its location and orientation are correct. If a fiber-like artifact appears anywhere in the insert area of the image but is not in an appropriate location or orientation, deduct the "artifactual" fiber from the last "real" fiber scored if the artifactual fiber is equally or more apparent.

b) Use a large field of view magnifying lens if required (approximately 2x) to assist in the visualization of specks. Count each speck group as one point. A full speck group is counted if four or more specks are visible in the group in the proper locations. Count a speck group as 0.5 if two or three specks of the group are visible. If noise or speck-like artifacts are visible in the wrong locations in the phantom insert but are as apparent as the "real" specks you are counting, deduct them one for one from the individual specks that you counted. Artifactual specks should only be deducted from "real" specks in the last group counted.

c) Count each mass as one point if a density difference is visible in the correct location and the mass appears to be generally circular against the background. Count each mass as 0.5 point if a density difference is visible in the correct location but the mass does not have a generally circular appearance. If there is a mass-like artifact appearing in the wrong location anywhere in the phantom insert, deduct the "artifactual" mass from the last "real" mass scored if the artifactual mass is equally or more apparent.

d) Enter the results in each category (fibers, specks, and masses) on the image quality evaluation form.

1. Examine the phantom images carefully for artifacts, including dust or dirt, stitching artifacts, spatial non-uniformities, film handling artifacts, processing artifacts, grid lines, and other equipment-induced artifacts

NOTE: Mammography phantom images, like mammograms, should always be viewed under good viewing conditions, consisting of:

1. Masking of the viewbox/monitor so that extraneous light does not come to the viewer's eye without passing through the exposed portion of the phantom image. A mask is essential for appropriate viewing of phantom images.
2. Ambient room lighting reflecting off the film or display monitor should be minimized.

3. Use of a large field of view magnifying lens or window (2x is recommended), preferably the same type of magnifying lens used for reading clinical mammograms.

Precautions and Caveats

This test measures all components of the imaging chain, other than breast positioning by the technologist; patient-induced errors such as motion; and image interpretation by the radiologist. Observed changes in phantom image quality may be due to any component of the imaging chain, from X-ray generator or tube to processor or display monitor. As a result, other tests will be needed to determine the component(s) of the imaging chain that is at fault and in need of corrective action. Because the medical physicist may not have the opportunity to measure phantom image quality as frequently as the QC technologist, it is important to review the phantom images acquired by the technologist since the previous visit, comparing results with your own assessment of image quality.

Suggested Performance Criteria and Corrective Action

The optical density of the film in the centre of the phantom image should be greater than 1.4. The mean pixel value measured from phantom image to phantom image is the crucial factor. If the exposure is made identically to previous phantom images, the optical density in the centre of the phantom should not change by more than +/- 0.20 and the pixel value should not change by more than 1.0% of full scale. The exposure time or mAs noted on the generator read-out should not change by more than +/- 15% from one phantom image exposure to another.

The minimum score (with deductions for artifacts) is 5 fibers, 4 speck groups, and 3.5 masses. The number of objects detected in each group (fibers, specks, and masses) should not change by more than 0.5 if viewed under ideal conditions by the same observer. If the observed number of test objects in one or more groups changes by more than 0.5, then further comparison with the original or previous phantom image and previously acquired phantom images should be made to determine whether the change is real.

Any change between the current phantom image and the original or previous phantom image in density, density difference, or number of test objects that exceeds the suggested performance criteria should be investigated to determine the source or sources for the change. Once the source has been identified, the problem or problems should be corrected immediately.

7.3 Chest Wall Missed Tissue, NPS, Contrast, Resolution

Objective

To determine the amount of tissue which is not imaged by the mammographic unit when a patient is positioned as closely to the unit as possible. To evaluate the contrast sensitivity and dynamic range of the unit. To evaluate the limiting resolution at the top surface of the breast of a medium contrast object. To provide a measure of the spatial noise power in a region of uniform thickness imaged under normal conditions.

Required Test Equipment

IDMDG digital test phantom

Test Procedure Steps

1. Position the phantom on the breast support plate with the chest wall edge of the phantom pushed as close to the edge of the table as possible. The compression paddle should be lowered and compressed to a pressure of 15 dN, while holding the phantom tightly to the table and compressor edges. The phantom should be allowed to be pushed out if the flexing of the compressor paddle forces it to slide against firm pressure from the operator's hand.
2. An image should be acquired using a technique suitable for a breast 1 cm thicker than the Accreditation Phantom.
3. Record results on Chart 8.3.

Data Interpretation and Analysis

1. The image of the phantom should be viewed, and amount of missing tissue read off the angled scales at the chest wall side of the phantom.
2. The pixel values (and OD values) for the 2nd (1.7mm total PMMA) and 8th step (5.4 cm total PMMA) on the step wedge should be measured and recorded. The difference should be recorded as an index of contrast.
3. The effective medium contrast resolution at the top surface of the breast should be read from the resolution pattern. The last resolved pattern must be visualized at least 50% of its length. Contrast, magnification and level may be adjusted in order to see the pattern.
4. The NPS should be calculated in an area enclosed by the 10 cm box on the center of the phantom.
5. The number of stars visualized should be recorded for both strips over 5.4 cm PMMA and 2.8 cm PMMA.
6. The number of stars on which points are fully visualized should be recorded for both strips over 5.4 cm PMMA and 2.8 cm PMMA.

Suggested Performance Criteria and Corrective Action

Closest tissue visualized at chest wall- 7 mm
Contrast - TBA
Resolution – no worse than 2 lp/mm less than pixel size Nyquist limit.

7.4 System Limiting Spatial Resolution

Objective

To evaluate the system limiting resolution by using a high-contrast resolution test pattern.

Required Test Equipment

High-contrast resolution pattern providing a test up to 10 lp/mm (either a bar pattern or a wedge pattern marked to identify the number of lp/mm in the image at the appropriate points).

Procedures

1. Place the line pair pattern or wedge-shaped line pair pattern 4.5 cm above the breast support plate, with a homogeneous phantom supporting the pattern. Position the pattern within 1 cm of the chest wall edge of the image receptor, centered laterally. The pattern's bars should lie parallel to the anode-cathode axis for the first image. It is important that the test pattern be positioned in a reproducible manner. A test stand may be helpful.
2. Select the kVp, mAs, target/filter, and focal spot for imaging an average breast during normal radiography.
3. Make an exposure and record techniques on Chart 8.4.
4. Repeat step 3 with the bars oriented perpendicular to the anode-cathode axis.
5. Repeat steps 1 through 4 for other focal spots and other geometries. In magnification mode, the bar pattern should be positioned 4.5 cm above the magnification breast support. Be sure to record the magnification factor.

Data Interpretation and Analysis

1. Under optimal viewing conditions at the review station, view the high-contrast resolution pattern images at an appropriate magnification and window and level setting.
2. Note the highest frequency pattern whose lines are distinctly visible throughout at least half of the bar length and has the correct number of bars and spaces (for bar pattern) or the lowest frequency at which the lines blur (for the wedge shaped pattern) and record the highest frequency visible for each test image. Record results on Chart 8.4.

Suggested Performance Criteria

In contact mode, measurements made with the bars parallel to the anode-cathode axis should be at least 4.5 lp/mm for 100 um pixel size and 9 lp/mm for 50um pixel size; measurements with the bars perpendicular to the anode-cathode axis should be at least 4.5 lp/mm for 100 um and 8 lp/mm for 50um. If the above specifications are not met, a service engineer should be called.

7.5 Modulation Transfer Function (MTF) Measurement

Objective

To determine the Modulation Transfer Factor for the overall imaging system. This allows determination of limiting resolution, as well as calculation of DQE.

Test Phantom Requirements

Medium Contrast Edge Phantom 27 μm Niobium with four ground edges, each at least 50 mm long arranged in a square and supported on .8 mm Aluminum sheet 10 cm square.

Test Procedure Steps

1. Place edge tool directly on the breast support, angled at approximately 3-4 degrees from one of the pixel matrix axes. This should result in a slant ratio of about 16:1 in the image of the edge.
2. Select a kVp and filtration that is representative of one used on that system for a typical (i.e. 50/50 fat/glandular, 4.5 cm compressed thickness) breast (Use the accreditation phantom technique). Select an mAs that results in pixel values under the aluminum base and under the niobium edge that are within the detector linear dynamic range. Ideally, these levels would be about 80% and 20% of the linear range. There should be no values in the image which are above maximum bright value or below minimum dark level both of which can be determined in the linearity test. This is to ensure that there is no effect due to clipping of signals.
3. Enter results on Chart 8.5.

Data Interpretation and Analysis

1. Using standard techniques (c.f. Fujita et al., IEEE Med. Imag. 11(1) 34-39 (1992), sample the edge image to generate a presampling edge spread function (ESF).
2. Numerically differentiate the presampling ESF to generate the presampling line spread function (LSF).
3. If desired, noise in the LSF can be smoothed using a boxcar (rect) function.
4. Note: The effect of long range background trends on the MTF calculations are likely to be system-specific, and are being investigated.
5. Calculate the FFT of the presampling LSF, and normalize it to 1.0 at zero frequency to obtain the presampling MTF.
6. If the LSF was smoothed in step 5. by a rect function of unity height and width a (in units of presampling LSF bins), then the calculated MTF should be divided by sinc(au) to correct for the effects of the smoothing.
7. Repeat 1. – 6. for the orthogonal space dimension.
8. Repeat 1. – 7. with the slit rotated perpendicular to the anode-cathode direction.

Suggested Performance Criteria and Corrective Action

1. The MTF should be consistent with the pixel size. For systems with pixels around 100 um in size, the 10% MTF value should be no less than 4 lp/mm and for 50 um pixel size, 9 lp/mm.

7.6 Collimation Evaluation

Objective

To ensure that the collimator or cone does not allow significant radiation beyond the edges of the breast support assembly and/or image receptor.

Required Test Equipment

Five radiographic rulers, 1 cm markings
Film cassette (24 x 30 cm)

Procedure Steps

1. Place a large cassette (24 x 30 cm) above the breast support, tube side of cassette toward tube.
2. Remove the compression device and tape one ruler to the underside of the compression paddle, with the marked middle line on the ruler tangent to the inner lip.
3. Turn on the light field and place one ruler on each of the four borders of the light field such that the line on the center of the ruler lines up with edge of the light field or with the markings on the unit which indicate the field location.
4. Replace the compression paddle and adjust the compression paddle height to be 6 cm above the breast support.
5. Make a low dose exposure using the standard kVp, target and filter. mAs should be approximately 5-10% of the ACR phantom exposure.
6. Process the film and use this film to determine light field - x-ray field co-registration.
7. Determine the extent of the field compared to the active area of the detector, the active area of the detector is defined as the area visible on the image - verify that all rows and columns are visible using the display.
8. Enter results on Chart 8.6.

Data Interpretation and Analysis

1. Measure the distance that the radiation field deviates from the centres of the rulers.
2. Determine from the digital image soft copy display the position of the edges of the detector active area with respect to the rulers.
3. Determine the position of the compression device relative to the chest wall side of the detector. Use the position of the ruler on the compression paddle in the digital image. Add to this value the amount of the overhang (either beyond + or inside -) from the chest wall edge ruler to the inner lip of the chest wall side of the compression paddle.

Suggested Performance Criteria And Corrective Action

1. The sum of the absolute values of differences between light field and radiation field on left and right sides must be less than 2% of SID (13 mm).
2. The sum of the absolute values of differences between light field and radiation field on chest wall and anterior sides must be less than 2% of SID (13 mm).
3. The x-ray field shall cover the entire active (displayed) area and not extend beyond the active area by more than 2% of the SID in any direction.
4. Extension of the compression paddle into the chest wall should be no more than 1% of the SID and the inner lip of the compression paddle should not be visible on the image.
5. Proper alignment of the edge of the compression paddle with the chest wall edge of the image receptor holder assembly is necessary for proper positioning and compression of the breast. If the edge of the compression paddle extends too far beyond the image receptor edge, the patient's chest is pushed away from the image receptor and some breast tissue will not be recorded on the image. If the edge of the compression paddle does not extend far enough, the breast tissue will not be properly pulled away from the chest wall and compressed for visualization in the image, and a shadow of the vertical edge of the compression paddle will be visible in the image, possibly obscuring clinical information. The chest wall edge of the compression paddle should be aligned just beyond the chest wall edge of the image receptor such that the chest wall edge of the compression paddle does not appear in the mammogram. In addition, the chest wall edge of the compression paddle should not extend beyond the chest wall edge of the image receptor by more than 1% of the SID.

If the Suggested Performance Criteria are exceeded, then a qualified service engineer should be called to correct the problem as soon as possible.

7.7 kVp Accuracy And Reproducibility

Objective

To ensure that the kVp is accurate (within +/- 5% of the indicated kVp) and that the kVp is reproducible, having a coefficient of variation equal to or less than 0.02.

Required Test Equipment

Test device capable of measuring kVp to an accuracy of
±1.5 kVp and a precision of 0.5 kVp within the mammographic kVp range.

RMI 232 kVp meter (non-invasive) or comparable kVp meter
or Oscilloscope connected to generator monitor output.

Test Procedure Steps

1. Place a lead sheet (to protect the image receptor) on top of the breast support plate and on top of the lead sheet set up the test device following the manufacturer's instructions.
2. Place kVp meter so that the sensitive area is at the chest wall, but completely irradiated.
3. In manual timing mode,select the kVp at which the system is normally used clinically and record on Chart 8.7. The line voltage should be checked and adjusted so that it is within tolerance. Also record nominal focal spot size, exposure time, and mA (or mAs) setting on Chart 8.7.
4. Make four exposures in the same manual mode settings and record the measured kVp values.
5. Repeat the procedure at other clinically important kVp's and mA's used clinically, ensuring that the minimum kVp and maximum kVp used clinically are measured

Data Interpretation and Analysis

1. Calculate Coefficient of Variation (S.D./mean) on the four exposures.
2. Evaluate difference from nominal kVp.

Suggested Performance Criteria and Corrective Action

1. Coefficient of variation should not exceed 0.02 for any kVp setting.
2. Measured kVp should be within +/- 5% of nominal setting.

To determine kVp accuracy, average the four kVp readings for each kVp setting tested and compare this average value with the value of the preset nominal kVp. If the average measured kVp differs by more than ±5% (±1.5 kVp at 30 kVp) from the nominal kVp setting, the unit should be checked by appropriate service personnel.

To determine kVp reproducibility, compute the standard deviation of the kVp values for each kVp setting and then calculate the coefficient of variation (standard deviation divided by the average value). If the coefficient of variation exceeds 0.02 for any kVp setting, the unit should be checked by appropriate service personnel.

NOTE: If the accuracy or reproducibility results with four exposures are questionable, make six (6) additional readings and recalculate using all 10 readings.

7.8 Tube Output - mR/mAs vs. kVp

Objective

To determine radiation outupt from the unit. This may be used to estimate mean glandular dose for given exposure factors.

Required Test Equipment

Pancake-style ionization Chamber and electrometer calibrated at mammographic energies.

Lead sheet to protect the image receptor.

Test Procedure Steps

1. Place a lead sheet (to protect the image receptor) on the breast support surface and place the compressor paddle to support the ionization chamber approximately 4.5 cm above the lead sheet, centered left to right and 20 mm in from the chest wall edge of the image receptor. The ionization chamber should be fully within the X-ray field, and should have no more than 1 mm of low density material between the back side of the chamber and the lead sheet. Use full-field collimation.
2. Measure the exposure at the techniques which are used clinically, ensuring that the maximum and minimum kVps are used. The exposure time should be long enough to measure at least 500mR.

9. 3. Enter results on Chart 8.8.

Data Interpretation and Analysis

Multiply the exposure reading from the dosimeter by any correction factors required.

Calculate mR/mAs.

Suggested Performance Criteria and Corrective Action

Output at 28 kVp will be no less than 800 mR/s.

mR/mAs should increase monotonically with kVp.

7.9 Beam Quality Assessment - HVL

Objective

To ensure that the half-value layer of the X-ray beam is adequate to minimize patient breast dose, while providing sufficient radiographic contrast.

Required Test Equipment

Pancake- style ionization Chamber and electrometer calibrated at mammographic energies.

Aluminum filters (99.99% pure Aluminum) of sufficient area to fully cover the beam of length and width sufficient to fully cover the ionization chamber. The stated thicknesses should be accurate to within ±1%.

NOTE: The use of type 1100 aluminum alloy for HVL measurement can give (depending on specific samples) HVL values up to 7.5% lower than those measured using pure aluminum. If type 1100 aluminum is used, results should be corrected to agree with those obtained using pure aluminum.

Test Procedure Steps

3. The compression paddle should be placed as close as possible to the X-ray tube.
4. Place a lead sheet (to protect the image receptor) on the breast support surface and place the ionization chamber approximately 4.5 cm above the lead sheet, centered left to right and 20 mm in from the chest wall edge of the image receptor. The ionization chamber should be fully within the X-ray field, and should have no more than 1 mm of low density material between the back side of the chamber and the lead sheet. Use a diaphragm to collimate the X-ray beam so that the ionization chamber is just fully exposed (to minimize backscatter production).
5. Two measurements with the compression paddle in place should be made at each pre-selected kVp. Measure at no more than 3 kVps used for clinical image for each anode-filter combination. mAs should be set so that readings of about 500 mR are recorded.
6. Place appropriate thicknesses of aluminum on top of the compression paddle, ensuring that the beam is completely blocked by the sheet. Record readings for each kVp on Chart 8.9.
7. Add Al filters until the reading is below 50% of un-attenuated reading.

Data Interpretation and Analysis

1. HVL should be calculated using logarithmic interpolation for each of the kVps. This may be performed for both exposure data as well as pixel value data.
2. The average exposure (with no aluminum) divided by the mAs for each kVp will give the mR/mAs.

To calculate the HVL by logarithmic interpolation, use the following notation and procedure. Denote the direct exposure reading, without any added aluminum, as E_0. Divide this value in half and find the two exposure readings and added aluminum thicknesses that bracket the $E_0/2$ exposure. Let E_a be the exposure reading that is just greater than one-half of E_0 and t_a be the corresponding aluminum thickness. Let E_b be the exposure reading that is just less than one-half of E_0 and t_b the corresponding aluminum thickness. E_a will be greater than E_b, while t_a will be less than t_b. With this notation, the HVL may be computed using the formula:

$$HVL = \frac{t_b \ln[2E_a/E_0] - t_a \ln[2E_b/E_0]}{\ln[E_a/E_b]}$$

where the HVL will be given in the same units as t_a and t_b, usually millimeters of aluminum. Graphical methods of interpolation may also be used to determine the HVL to a reasonable degree of accuracy if high precision is used.

Suggested Performance Criteria and Corrective Action

1. HVL should meet the Federal performance standard HVL>= kVp/ 100
2. HVL should be within the ACR recommended limits HVL< kVp100 +C where C=0.12 for Mo/Mo, C=0.19 for Mo/Rh and C= 0.22 for Rh/Rh.

If these parameters are outside the limits, the x-ray tube, filters and mirror should be inspected, and the unit should not be used until corrected.

7.10 Breast Entrance Exposure and Mean Glandular Dose

Objective

To measure the typical entrance exposure for an average patient (approximately 4.2-cm compressed breast thickness—50% adipose, 50% glandular composition), to calculate the associated mean glandular dose.

Required Test Equipment

Ionization chamber and electrometer calibrated at mammographic X-ray beam energies (calibration factor constant to within ±1% over the HVL range from 0.2 to 0.5 mm Al)

Mammographic phantom (equivalent to approximately 4.2-cm compressed breast tissue—50/50 composition—at screen-film energies; for example, Radiation Measurement, Inc., Model 156 or Nuclear Associates, Model 18-220 Mammographic Phantom)

Procedure

1. Prepare the mammographic imaging system for operation in the imaging mode (e.g., contact, grid). This step includes appropriate field limitation for the imaging mode. Record the conditions onChart 8.10.
2. For mammographic imaging systems with a variable source-to-image receptor distance (SID), Adjust the system to the SID most commonly used for mammographic imaging and record the SID on the data form.
3. Position the mammographic phantom on the image receptor assembly at the position which would normally be occupied by the patient's breast (laterally centered in the X-ray field with one edge coincident with the chest wall edge of the cassette holder assembly).
4. Position the ionization chamber in the X-ray field beside the mammographic phantom, centered 4 cm in from the chest wall edge of the image receptor and with the center of the chamber level with the top surface of the phantom. Assure that the entire chamber is exposed.
5. Secure the chamber in position and do not change the position of the chamber during the following measurements.

NOTE: Mammographic imaging systems have a significant X-ray intensity gradient in the X-ray field along the anode-cathode direction. Maintaining a constant chamber position during measurements is critical. When measurements are to be compared with others made previously, it is also critical that the original measurement position be re-established as closely as possible.

6. Position the compression device in the X-ray beam, just in contact with the phantom and chamber.
7. Select the kVp, mAs, and target/filter at which the system is normally used clinically and record the settings on Chart 8.9
8. Make an exposure.
9. Repeat the procedure at other clinically utilized target/filter combinations and kVp's (assure that HVL values have been measured at these additional target/filter and kVp combinations).

Data Interpretation and Analysis

Using each exposure value, calculate the mean glandular dose as follows:

1. If necessary, correct the exposure reading with the chamber's appropriate energy correction factor.

2. Determine whether the target is molybdenum, tungsten, or rhodium and find the appropriate column in Tables 1, 2, or 3 from the ACR Mammography Quality Control Manual for the target and filtration combination used clinically.

3. Find the HVL of the system (see the **Beam Quality Assessment** procedure) in the left-hand column of Tables 1 to 3 in the ACR Mammography Quality Control Manual. In the right-hand column of the table appropriate for the target, filter and kVp setting, find the exposure to mean glandular dose conversion factor for a 4.2-cm compressed breast thickness. Multiply this factor by the entrance exposure value computed above. The product obtained represents the mean dose received by the glandular tissue for that specific energy, breast composition, and compressed thickness and is an approximation of the actual patient dose.

NOTE: The conversion factor and the mean glandular dose change substantially for other breast thicknesses, so these factors only apply to a 4.2-cm compressed breast thickness. Conversion factors for other breast or phantom thicknesses may be found in the listed references by Dance and by Wu et al.

Suggested Performance Criteria

The mean glandular dose to an average (4.2-cm compressed) breast should not exceed 3 mGy (0.3 rads) per view. It is recommended that the mean glandular dose should be less than 1 mGy per view for non-grid image receptors and less than 3 mGy per view for grid imaging modes.

If the values exceed these levels, action should be taken to evaluate and eliminate the cause of excessive dose.

7.11 Thickness Tracking

Objective

To evaluate the ability of the system to image a clinically expected range of breast thicknesses.

Required Test Equipment

A set of uniform PMMA slabs at least 10 cm x 10 cm of thicknesses: 2,4,6 and 8 cm, which are free from defects. The Accreditation phantom may also be imaged.

Test Procedure Steps

Place each uniform phantom on the tabletop so that it covers the entire detector and use collimation which allows the full field to be imaged.
Set the AEC, kV, target and filter to the appropriate technique for that thickness of phantom.
Use appropriate window width and window level settings that allows visualization of the entire flat field image.
Choose a central ROI and measure signal and standard deviation.
Enter results on Chart 8.11.

Data Interpretation and Analysis

Calculate the SNR by dividing the signal by the standard deviation.

Suggested Performance Criteria and Corrective Action

The SNR value for 2, 4 and 6 cm should be greater than 50. For 6 cm and 8 cm, the SNR should be greater than 40. If lower SNR's are measured for any thickness, then technique factors for those breast thicknesses should be revised.

7.12 Noise, Linearity And Reproducibility

Objective

To evaluate the spatial and electrical noise characteristics of the entire imaging chain.

Required Test Equipment

2.5 or 5 cm uniform lucite slab free from defects that covers the entire image receptor.

Test Procedure Steps

Note: These tests should be performed on flat-fielded, but un-enhanced (no peripheral or resolution enhancement) images.

1. Place the uniform phantom on the breast support tray so that it covers the entire detector and use collimation which allows the full field to be imaged.
2. Place an ionization chamber on the phantom such that the chamber will not interfere with the ROI measurements of noise and ADU's as described below.
3. Set the kV, target and filter to the accreditation phantom technique. Using the set kVp, obtain one image at each mAs value. Use mAs values of 20, 50, 100, 200, 400 if possible. At least one measurement should be taken on each of the available filters at typical exposure factors.
4. At 100 mAs obtain an additional 3 images for a total of four images at this station.
5. Use appropriate window width and window level settings that allows visualization of the entire flat field image. 6. Choose positions for ROI's as shown on **Chart 8.12**. For systems with multiple detector modules, test each module with 1 cm x 1 cm ROIs, both at the center and one corner of the module. For systems which have only a single module test in the center and also near each edge of the field (5 total).

Data Interpretation and Analysis

1. Linearity: Record the mean and standard deviation for each ROI. Plot mean pixel value versus measured exposure for each ROI.
2. Raw Noise: Plot the SD vs exposure for each ROI on log-log plot
3. Image Noise: For the 100 mAs images, subtract one image from the other three averaged together, and calculate the SD, as well as examining the image for noise patterns.
4. SNR: divide the signal by the SD.
5. Reproducibility:
   a) Determine the COV for the exposures for the four 100 mAs images.
   b) Determine the COV for the signal measured in ROIs from the four 100 mAs flat fielded images.
   c) The reproducibility measurements are made in the same positions as the linearity testing. The pixel values should be corrected for exposure differences prior to determining the COV.

Suggested Performance Criteria and Corrective Action

1. Linearity: Pixel value versus exposure should be linear with less than 1% deviation from the best straight-line fit.
2. Noise: Standard Deviation versus exposure - linear least square fit must have $r > 0.9$. If one area is not linear and displays an excess of noise – set limits on the allowable operating range of the system.
3. The COV for exposure reproducibility and pixel values should be less than 0.05. This limit would apply to each module or ROI measured.
4. If any ROI signal value differs by more than ± 5% from the middle (#4) location, then the source of signal non-uniformity should be identified and corrected.
5. If the SNR changes by more than ± 20% from the middle (#4) location then the source of SNR non-uniformity should be identified and corrected.
6. If the SNR changes by more than ± 10% from the previous SNR measurement made at the same location then the source of SNR non-uniformity should be identified and corrected.

7.13 Spatial Linearity and Geometric Distortion

Objective

To determine the absolute image magnification and straightness of lines.

Test Phantom Requirements

Medium Contrast PCB with parallel lines at 20 mm spacing, angled at 45 degrees.

Test Procedure Steps

1. Place the PCB on the breast support plate, approximately centered L-R.
2. Make an exposure using the accreditation phantom technique.
3. Record the target/filtration, kVp setting, mAs setting, and grid use on Chart 8.13.

Data Interpretation and Analysis

1. At the review station, bring up the wire mesh image and use the appropriate window width and window level settings and magnification that allow visualization of the image.
2. Examine the image for resolution uniformity and pattern distortion.
3. The width and length of the image should be calculated using the breast support plate as the reference position. The intersections of the lines will be spaced 20 mm* sqrt 2 apart.
4. Effective pixel size at the support plate should be calculated.
5. A number of lines should be fit using linear regression.

Suggested Performance Criteria and Corrective Action

1. The image should be within 5% of the manufacturers stated nominal image size.
2. There should be less than 2 pixels deviation along a line.
4. If there is any significant resolution non-uniformity or pattern distortion, rotate the image on the monitor 90°. If the resolution non-uniformity or distortion persists seek service from a qualified service engineer to have the problem corrected.

7.14 Monitor Display Quality SMPTE Pattern

Objective

To assure that digital softcopy review workstation monitors are of adequate brightness and contrast and that the brightness and contrast of multiple monitors match one another so that images are displayed and printed consistently.

Required Test Equipment

Photometer, either stand-alone or one that plugs into the display controller board for each monitor.

Procedure

1. Display an SMPTE pattern, or another appropriate pattern provided by the manufacturer. Set the brightness and contrast on the monitors appropriately.
2. Verify the 0%-5% contrast box is clearly discernible. Record results on Chart 8.14.
3. Verify the 95%-100% contrast box is clearly discernible. Record results on Chart 8.14.
4. Verify the line-pair images at the center and corners of the SMPTE pattern are distinguishable. Record results on Chart 8.13.
5. Verify there is no bleeding throughout the image. Record results on Chart 8.14.
6. Measure the intensity of the 100% (white) square, the 80, 50, 20 and black squares. Record these values and compare to previous measurements.
7. Display the same SMPTE pattern, phantom image or clinical image on both (or all) monitors.
8. Measure and record the ambient illuminance.

Suggested Performance Criteria

If the SMPTE test pattern and low contrast targets are not discernible or there is bleeding on the pattern, the source should be identified and corrected by a qualified service engineer.

The "White" value should be at least 70 ft-Lamberts and the black should be at most 4 ft-Lamberts.

If the same image displayed on both monitors shows distinct visual differences, the two monitors need to be recalibrated.

In the graph of Luminance Response, if the targeted and actual curves are very different, your monitor requires re-calibration.

7.15 Artifact Evaluation Test

Objective

To assess the degree and source of artifacts visualized in full field digital mammograms or phantom images. To assure that the flat field image is uniform.

Test Phantom Requirements

4 cm PMMA uniform slab or 1-2 cm thick sheet of high-grade, uniform BR-12 free from defects that covers the entire image receptor.

Test Procedure Steps

1. Place the phantom on the tabletop and expose using the technique for the Accreditation Phantom.
2. Record the technique factors on Chart 8.15.
3. View the images in the same manner as used for diagnosis, being careful to use a typical window width as for clinical images Record the window level and window width settings for future reference.
4. Note any visible artifacts on Chart 8.15.
5. Repeat for all three target/filter combinations.

Data Interpretation and Analysis

1. Use appropriate window width and window level settings that allow visualization of artifacts if present.
2. Examine the phantom images carefully for artifacts, including: dust or dirt, "phantom" images left over from repeated test or clinical exposures, filter blotchiness, stitching artifacts, clipping/electronic noise, spatial non-uniformities, film handling artifacts, plus or minus signal variations, processing artifacts, grid lines, streaking in the horizontal or vertical directions, bad pixels, and other equipment-induced artifacts.
3. The image should be examined for flat field uniformity ensuring that the image does not have non-uniformities across the field of view.
4. Review all three images for the three target filter combinations
5. If any artifacts or non-uniformities are present, rotate the phantom 90° and repeat the exposure and acquisition procedure.
6. Any artifacts or non-uniformities that keep a fixed orientation relative to the image receptor in both images and deemed significant requires a re-calibration of the gain file specific to the target/filter combination in question.
7. The artifact evaluation should be repeated and the image reviewed.
8. If the artifact or non-uniformity is still present, service by a qualified service engineer should be obtained and the problem fixed.

7.16 Laser Printer Evaluation

Objective

To ensure that uniform artifact-free image are produced.

Required Equipment

One 2 – 5 cm thick sheet of acrylic large enough to cover the entire detector system.

Procedure

Print images of the Accreditation Phantom, a uniform flat field and the SMPTE pattern.
Record the results on **Chart 8.16.**

Suggested Performance Criteria

If there are significant artifacts, the source should be identified.

APPENDIX B:

PROTOCOL MANUAL

CLINICAL EVALUATION OF DIGITAL MAMMOGRAPHY

Clinical Evaluation of Digital Mammography

Sponsor: U.S. Army Medical Research and Materiel Command

(DAMB 17-99-1-9001)

TABLE OF CONTENTS

Key Personnel 4

Overall Objectives of the Protocol Manual 5

Purpose/Hypotheses 5

Research Objectives: Technical & Clinical 6

Protocol: Technical Evaluations/System Optimization 8

Protocol: Clinical Trial 9

A. Participating Clinical Sites 9

B. Eligibility and Exclusion Criteria 9

C. Flow Chart for Accrual 11

Overview of Data to be Collected 12

A. Patient Recruitment & Enrollment 12

B. Summary: Data Collected on all Patient Groups at Time Of Enrollment 15

C. Submitting Screen-Film Mammograms for Confirmation of Lesion Eligibility 16

D. Submitting Digital Mammograms for Archival 17

E. Reporting of Serious and Unexpected Adverse Events 18

F. Patient Follow-up Information 18

G. Patient Confidentiality 19

H. Submitting Pathology Reports for Pathology Review 20

I. Submitting Back-up Discs of Computer Data 21

Reader Performance Study 22

Radiologist Interpretation Protocol 23

Disagreement Resolution 24

APPENDIX A: Data Acquisition Forms .....

APPENDIX B: Acceptance Tests and Quality Control for Digital Mammography Systems.....

APPENDIX C: Directory of Participating Investigators and Site Personnel.....

KEY PERSONNEL

(For Complete Directory See Appendix C)

Co-Principal Investigators:

Johns Hopkins University

Laurie L. Fajardo, M.D.

Univ. of North Carolina at Chapel Hill:

Etta D. Pisano, M.D.

Co-Investigators:

Lead Statistician: Bahjat Qaqish, Ph.D., University of North Carolina

Lead Physicist: Mark Williams, Ph.D.

Collaborating Radiologists: Emily Conant, M.D., University of Pennsylvania
Rene Shumak, M.D., University of Toronto
Melinda Staiger, M.D., Good Samaritan Hospital

Collaborating Physicists: Martin Yaffe, Ph.D., University of Toronto
Andrew Maidment, Ph.D., Thomas Jefferson University
Loren Niklason,, Ph.D., General Electric
Eugene Johnston, Ph.D., University of North Carolina
Dev Chakraborty, Ph.D., University of Pennsylvania
Chris Lynch, Ph.D., TREX Medical
Joel Gray, Ph.D., TREX Medical

OVERALL OBJECTIVES OF THIS MANUAL

This manual outlines the protocol and procedures for investigators and research assistants participating in the DAMD sponsored trial: "Clinical Evaluation of Digital Mammography".

PURPOSE AND HYPOTHESIS

Purpose: To date, clinical evaluations of DM have focused on demonstrating its basic *equivalence* to SFM, as is necessary to achieve marketing clearance by the FDA. With further, novel optimizations in system design, *improvement* in breast cancer detection using DM - the potential benefit - can be measured. The major goal of this Clinical Translational Research project is to perform a multicenter clinical study evaluating DM and allowing estimates of its sensitivity compared to SFM in women having moderately or markedly dense breasts who present for problem-solving mammography.

HYPOTHESES:

Primary: Optimized DM, as defined below, improves mammographic detection of lesions in radiodense breast tissue compared to SFM.

Secondary: Using optimized DM, radiologists' recommendations for additional imaging work-ups and biopsies for benign breast lesions are reduced, resulting in reduced costs associated with problem-solving mammography.

OBJECTIVES OF THIS RESEARCH

The primary objectives of this proposal are the technical characterization and clinical testing of digital mammography technology. The group's ultimate goal is to determine whether this new technology can replace film-screen mammography as the diagnostic modality of choice for breast cancer detection and breast lesion characterization in the clinical setting.

This proposal therefore contains two sets of goals: technical and clinical.

The technical goals are:

1) Characterize the imaging performance of the three types of digital mammography systems currently being marketed by the major US manufacturers (General Electric, Trex and Fischer).

2) Optimize technical parameters for operating DM systems with respect to x-ray beam/image acquisition, dose considerations, and image quality as a function of signal-to-noise ratio. Finalize operational and quality control routines for image acquisition.

The major clinical goals are:

1) Perform a scientifically rigorous cooperative trial at six clinical sites to demonstrate the improvements in detection, diagnosis and management offered by optimized DM. By performing a carefully constructed radiologist reader study, we will obtain estimates of false positive and true positive rates and hence, area under the receiver operating characteristic (ROC) curve for this population.

2) Evaluate radiologists' management decisions interpreting SFM versus DM images to determine whether more/fewer additional diagnostic studies are recommended with DM.

This multi-center collaboration is an extension of the pilot work completed during the HHS-sponsored pilot study, under the direction of Etta Pisano, M.D. We believe strongly that the women of North America will reap the benefits of continuing this strong and successful collaboration. The knowledge gained as a result of this work will be invaluable for women and their doctors in determining the appropriate clinical role for this potentially exciting new technology. We also believe strongly that the International Digital Mammography Development Group's prior collaborative history, along with our credentials in the field, ideally situate us to accomplish the very important work proposed here.

In addition, by working with industrial collaborators from General Electric, TREX Medical, and Fischer imaging, basic scientists and clinicians will set the quality standards for this technology in its infancy. Rather than waiting until 30 years after the introduction of the technology, as was the case for screen-film mammography, by establishing the International Digital Mammography Development Group, and by continuing the funding for its on-going support, federal funding agencies (DHS and DAMB) are ensuring that standards for the clinical performance of the equipment are set collectively and early in the evolution of the technology.

TECHNICAL EVALUATION/SYSTEM OPTIMIZATION: (months 1-5)

Our study will entail a brief (five months) optimization period of the DM systems, followed by a clinical trial comparing DM to SFM.

The investigator primarily responsible for oversight of this work is Mark B. Williams, Ph.D. at the University of Virginia. Dr. Williams will coordinate preparation of the required technical reports for this trial.

Task 1: Development of x-ray exposure techniques for the digital systems: Because the dynamic range of x-ray signals measured with DM systems greatly exceeds that of SFM systems, one of the most promising contributions of DM is improved imaging of patients with moderate to markedly dense breast tissue. For this study, we will focus on the operational parameters most likely to impact mammographic image quality in this population, namely: x-ray tube target material, filtration, tube voltage, and exposure level. At this point, the optimum choice of parameters is not obvious. Unlike SFM, where the exposure required is defined by the need to attain a specific optical density, there is more exposure flexibility with DM. Because the technology is new, and because the current FDA trials have required that images be acquired in a fashion as identical as possible to SFM, little work has been done to optimize x-ray exposure techniques for the DM receptors.

Task 1a. Identify DM exposure techniques for the clinical trial. One of our first tasks will be to develop a preliminary set of technique charts for clinical DM acquisition beginning in month 5.

Task 1b. Refine DM exposure techniques to optimize imaging performance. The goal is to determine, for each system, the combination of parameter choices that results in optimum imaging performance for a given imaging task, and to refine the preliminary technique charts for each that were developed under Task 1a.

FFDM System Quality Control (QC): The consortium physicists have developed a program to ensure uniform and consistent imaging performance from the DM units at the 6 clinical sites. Where applicable, performance evaluation will be based on ACR guidelines for SFM. Because of the specialized nature of DM systems, some tests will be modified and new guidelines for performance defined. For example, although useful to verify the stability of some aspects of DM detector performance, the standard ACR/MQSA mammography phantom does not provide a number of the imaging tasks needed for a full evaluation. Several investigators in this consortium have developed phantoms for DM QC. Because image data from a DM system is in numerical form, some QC tests can be made more automatic, objective and quantitative, reducing the time required to perform them. Experience gained from the DHHS-funded pilot study will be used to modify the frequency of QC test performance. Appendices C and D provide the QC protocol procedures for initial acceptance testing of equipment for participation in this trial and for ongoing quality control tests (phantom imaging and calibration) to be performed throughout the trial.

PROTOCOL FOR CLINICAL TRIAL

PARTICIPATING CLINICAL SITES

Institution	Machine Type	PI
Johns Hopkins University	TREX	Dr. Fajardo
University of North Carolina	Fischer	Dr. Pisano
University of Pennsylvania	GE	Dr. Conant
University of Toronto	Fischer	Dr. Shumak
Good Samaritan Hospital	TREX	Dr. Staiger

REQUIREMENT FOR PARTICIPATING CLINICAL SITES:

1. Experience performing at least 50 full field digital mammograms prior to the commencement of this trial.
2. Adequate acceptance testing of the digital mammography equipment by the consortium physicists.

ELIGIBILITY AND EXCLUSION CRITERIA FOR WOMEN PARTICIPATING IN THIS TRIAL

From consecutive women presenting for problem-solving mammography, those with moderately or markedly dense breasts will be candidates for one of three groups (1, 2, or 3) in this study if they meet the criteria shown in the tables below. Breast densities will be categorized according to the American College of Radiology Breast Imaging Reporting and Data System (BIRADS), and only breast compositions in categories 3 (heterogeneously dense) or 4 (extremely dense) will be eligible.

INCLUSION CRITERIA Total to be accrued = 1075	Group 1 n=252	Group 2 n=630	Group 3 n=193
Moderately or markedly dense breast tissue - BIRADS category 3 or 4	X	X	X
Palpable breast lesion, scheduled for surgical or large (11 or 14 gauge) core breast biopsy	X		
Nonpalpable breast lesion, scheduled for surgical or large (11 or 14 gauge) core breast biopsy		X	
Nonpalpable breast lesion, scheduled for diagnostic imaging work-up, but not for biopsy			X
Willing to undergo 4-view SFM and DM	X	X	X
Willing to undergo SFM surveillance for 2 years			X

Exclusion Criteria

Pregnant or believes she may be pregnant
Unable to give informed consent for any reasons (psychiatric or neurological disability, language barrier, etc.)
Prior mastectomy
Implants
Needle biopsy within 2 weeks prior to the eligibility mammogram
Group 3: unable, for any reason, to undergo follow-up SFM for 2 consecutive years after study entry.

This study has been designed to include patients with palpable breast lesions (Group 1) because the diagnostic work-ups of these women frequently include abnormal clinical breast examination findings, accompanied by negative SFM. This is one of the patient populations that may be significantly impacted by optimized DM. The purpose for enrolling women not undergoing breast biopsy is to provide a more clinically realistic set of cases for interpretation than one composed only of women having biopsy.

PATIENT POPULATIONS ELIGIBLE FOR FFDM TRIAL

FLOW CHART: ACCRUAL

PATIENT POPULATION OF INTEREST FOR FFDM TRIAL

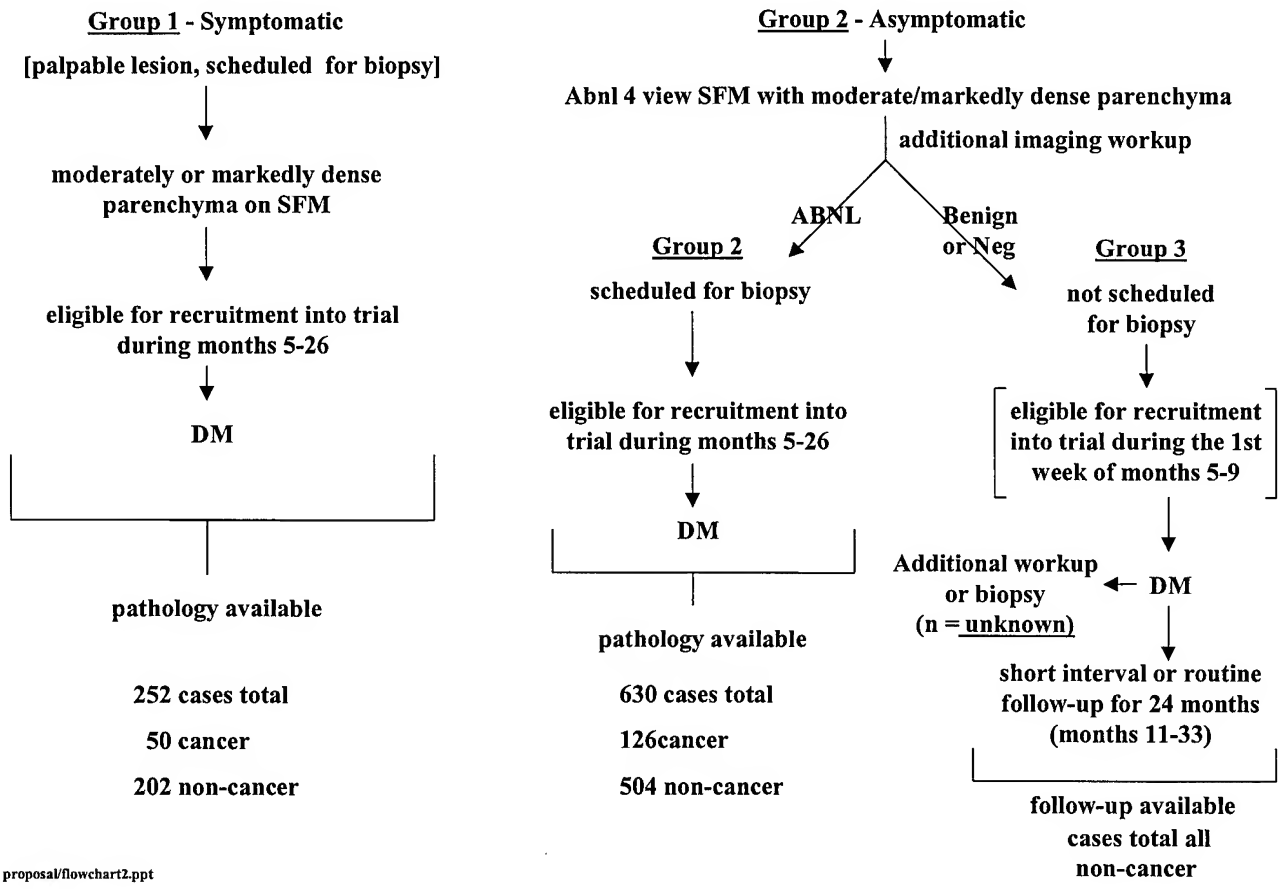

proposal/flowchart2.ppt

PROTOCOL FOR FFDM CLINICAL TRIAL: OVERVIEW OF DATA TO BE COLLECTED

NOTE: See Appendix A for printouts of all electronic forms to be used for acquiring data in this trial. All data will be collected on laptop computers equipped with software designed for this trial.

Enrollment Obligations:

Accrual is expected to begin on July 1, 1999

Each clinical site is contractually obligated to enroll a total of 179 women to this trial (42 into Group 1, 105 into Group 2, and 32 into Group 3.

NOTE: The opportunity exists to enroll additional patients above the contractual obligations and additional funds will be allocated to sites willing to accrue additional numbers of patients, especially GROUP 1 PATIENTS.

The expected enrollments at each site will be evaluated semi-annually. If a particular clinical site does not reach its target approval, funds will be redistributed to sites able to meet or exceed their target accruals.

Expected Enrollment for FFDM Clinical Trial:

Based on the numbers of women typically evaluated at each participating site and on the numbers of breast biopsies (palpable and nonpalpable) performed each month, we have conservatively estimated accrual assuming 50% enrollment of eligible recruits. We expect an average monthly accrual per site of 4 women into Group 1 and 10 women into Group 2 during study months 5 through 26. The pool of women eligible for Group 3 will require two-year mammographic follow-up. Therefore, this group will be accrued at a rate of 6 women per week per site, only during the first week of each month and only in study months 5 through 9 to complete accrual during year one and allow for mammographic follow-up during years 2 and 3. Based on our experience with the Radiological Diagnostic Oncology Group 5 study, we expect 65%-75% compliance with follow-up mammography for Group 3. Of 1075 total women recruited in this trial, 176 cancers (16 %) are expected.

RECRUITMENT & ENROLLMENT:

All subjects will be registered by laptop data entry and eligibility evaluation, using the ***Eligibility Checklists*** on the laptop computer (**DIG.EC.1.2** for patients in Groups 1 and 2 and **DIG.EC.3** for patients in Group 3. See hard copies of forms in ***Appendix A)***. Hard copies of all forms will be retained and filed for each patient enrolled or not enrolled in this trial at the originating clinical site. For tracking purposes, the statistical coordinating site will provide calendars to the enrolling sites indicating completed or outstanding data.

Sites will also receive a list of study numbers that are to be assigned to patients enrolled in the trial. Keep any data for a particular patient in a file folder labeled with the patient's study number. Hard copies of forms for each patient may also be filled out and retained by the originating site.

NOTE: Use the numbers on the list in order. Do not skip numbers. If you have any difficulty reading the numbers, contact Dr. Lin (UNC) at 919-966-8647.

Women scheduled for biopsy or problem-solving mammography who are recruited for this trial will have had a recent 4-view (bilateral craniocaudal and mediolateral oblique) screen-film mammogram (SFM). This mammogram must have been performed **within 1 month** of enrollment into this study. Otherwise, it must be repeated or the patient is not eligible.

After enrolling, they will have a 4-view Digital mammogram (DM).

The investigator-radiologist at each trial site will confirm the eligibility of consecutive patients by entering eligibility data for an individual patient into a laptop computer on the ***Eligibility Checklist Form*** (**DIG.EC.1.2**. for patient Groups 1 or 2; **DIG.EC.3** for Group 3 patients – see Appendix A) that will provide confirmation of eligibility status. After the eligibility status is confirmed, Group 1 & 2 patient's can be enrolled by completion of the ***Patient Enrollment Form*** on the laptop computer (**DIG.EN** form in Appendix A).

Patients with moderately dense or very dense breasts scheduled for biopsy (i.e., would be eligible for the study), but who are not enrolled for any reason (i.e., patient does not wish to enroll, equipment is not functioning, etc.) should also be tracked at the originating site. This is done by giving the patient a study number from your list and completing the ***Eligible Patients Not enrolled in the Digital Study*** form on the laptop computer (form **DIG.NE** in Appendix A).

NOTE: Group 3 patients are handled differently. See below.

Groups 1 & 2 Patients (having biopsy for palpable or nonpalpable lesions):

An eligible woman in Group 1 (palpable lesions) will be approached regarding her participation in this clinical trial by the recruiting radiologist or his/her designee at each institution when she presents for evaluation of palpable.

When an eligible Group 1 or 2 patient consents to enroll, an institutional-approved informed consent form will be completed and signed. After obtaining the enrollee's informed consent, an investigator-radiologist or research assistant will complete the ***Enrollment Form*** **(DIG.EN)** on the laptop computer. At this time, assign a study number to the patient from your printed list and record the patient's name on your study number list, next to the study number. For any patient that you enroll who has had a previous breast cancer, core biopsy or open surgical biopsy, the laptop computer will automatically take you to an additional data screen –***Prior Breast Cancer***

Form, Prior Core Needle Biopsy Form, or ***Prior Open Biopsy Form*** - so that you can enter this information (see **DIG.PBC, DIG.PCNB,** and **DIG.POB Forms** in Appendix A).

Remember, eligible subjects who are not enrolled (i.e., do not consent) will have minimal data collected on the ***Non-Enrollment Form*** **(DIG.NE).**

For each patient enrolled into any of the three patient groups, data regarding the woman's palpable breast lesion or her nonpalpable (mammographic) lesion will be recorded on the ***Clinical Film-Screen Interpretation/Clinically Relevant Lesion Form*** (form **DIG.SFM.LESION** in Appendix A). **NOTE: This form has been designed to use for both palpable and mammography (nonpalpable) breast lesions.**

Group 3 Patients - Accrual and Randomization Procedures:

NOTE: Randomization of women for inclusion in Group 3 will take place during the first week of months 5 through 9 (Nov. 99-Mar. 00) of patient enrollment only. During these weeks, consecutive women with dense breasts presenting for problem-solving (diagnostic) mammography who are not scheduled for biopsy will be identified by the recruiting radiologist or research assistant.

To enroll women into group 3, first enter data into the laptop computer trial on the ***Eligibility Checklist for Group 3 Patients.*** (form **DIG.EC.3**) to determine if they are eligible for the trial. If the patient is eligible for Group 3, you will next determine whether or not she is eligible for invitation into the trial by opening one of your site's randomization envelopes. Inside there will be a tag that says whether or not you should invite the patient to enroll. If the patient is designation as "invite", approach her regarding her desire to enter the study. If the patient consents to be in the study, she should sign your approved institutional consent form and you should complete the ***Patient Enrollment*** screen on the laptop computer (**DIG.EN** form – Appendix A). The patient will then have a routine, 4-view digital mammogram.

If the patient declines to enter the study OR if she is designated as "no invitation", complete the ***Eligible Patient Not Enrolled Form*** (form **DIG.NE** – Appendix A).

At each of the participating sites, this process is repeated for consecutive patients (with dense breasts having problem-solving mammography) until a total of 6 eligible women are successfully recruited during the week.

NOTE: All women eligible for patient Group 3 during the recruitment week will be assigned a study number from your study number sheet. Remember, during the weeks that women are being enrolled to Group 3, minimal basic demographic information about the ENTIRE problem-solving mammography population at each site will be collected to assess the representativeness of the enrolled patient sample from each site. This information will include age, and race of all women presenting for problem-solving mammography.

ALSO NOTE: Group 3 patients comprise lesions not going to biopsy that will instead be followed by interval mammography at 6, 12, and 24 months (as per the usual standard of care for probably benign nonpalpable, BIRADS 3 lesions detected by mammography). See section on follow-up below.

SUMMARY: Data Collected On All Patient Groups at the Time of Enrollment:

At the time of enrollment, the research assistant will interview the patient and enter patient data directly into a laptop computer using special data entry software designed for this study. The information entered at that time will include demographics and symptom information. This record will be labeled with the study number that identifies the patient and the clinical site from where she was recruited.

As discussed above, a log of ALL eligible patients must be kept at each site by assigning a study number and by completing the ***Non-Enrollment Form*** for any patient not enrolled. This will allow the representativeness of the patient sample from each site can be determined. This information will include age, and race of all women presenting for problem-solving mammography.

As discussed previously, for eligible patients consenting to enter the study, information regarding their past medical history will entered onto the laptop computer. Specifically, we will gather data on history of prior breast cancer (***Prior Breast Cancer Form*** – **DIG.PBC**), prior large-core breast biopsy (***Prior Core Needle Biopsy Form*** – **DIG.PCNB**), and prior open surgical breast biopsy (***Prior Open Biopsy Form*** – **DIG.POB**). These computer screen will automatically appear for a patient if you answer "YES" to questions about prior breast cancer/core biopsy/ surgical biopsy.

Screen-film Mammography (SFM):

All women enrolled in the trial must have had a SFM **within one month prior** to enrollment. At each site, the recruiting radiologist will be the clinical reader who identifies eligible women. The enrolling radiologist completes the ***"Clinical Screen-Film Interpretation/Clinically Relevant Lesion"*** form (**DIG.SFM.LESION**) based on the SFM or the clinical breast examination findings by entering the appropriate data onto the laptop computer.

This clinical interpretation will NOT be used as an experimental interpretation for the clinical trial. This data is collected so that information regarding lesions detected in the experimental setting that are NOT detected in the clinical setting might be relayed in a timely fashion to the local site radiologist, the woman and her physician.

NOTE: The Radiologist should first complete a paper copy of the **DIG.SFM.LESION** form and this information entered by the research assistant at a later time. The radiologist's original paper form should be kept on file at your site, with other data collected on each patient (i.e., the consent form). A copy of this form will be sent with the screen-film mammogram for over-reading and confirmation of the patient's eligibility status (see below).

SUBMITTING SCREEN-FILM MAMMOGRAMS FOR CONFIRMATION OF LESION ELIGIBILITY:

Participants' original SFMs will be copied at the clinical site for patient care use. The original films will then be sent to:

Etta Pisano, M.D.
U.N.C.
Dept. of Radiology
UNC-CH, CB 7510
509 Old Infirmary Bldg.
Chapel Hill, NC 27599-7510

The films should be shipped, in the film folder, to JHU via traceable courier (FedEx). Inexpensive (3rd day FedEx) is acceptable.

NOTE: Cases can be sent in batches every 2 weeks. They should include the original 4-view mammograms, labeled with the patient's study number and your clinical site number. Individual cases should be organized into separated file folders of envelopes. You should also include a copy of the **DIG.SFM.LESION** form completed by the radiologist with the films for each case.

After Dr. Pisano completes the Eligibility Confirmation Form and Information about the types of lesions present and their BIRADS assessment, she will mail the mammograms, the copy of the site radiologist's **DIG.SFM.LESION** form, and a copy of her over-reading form to Dr. Fajardo at Johns Hopkins University for a second review.

All original mammograms will be catalogued and secured at Johns Hopkins until the randomized case selection for the Reader Performance Study is completed.

If cases are found to be ineligible when the over-readings are performed, Dr. Fajardo will return the SF mammograms to the originating clinical site.

For eligible cases, if the originating site needs the SFM images at any time, they will be returned by FedEx. Dr. Fajardo will retrieve such cases at a later date for use in the Reader Study. Cases not selected for use in the Reader Performance Study will be returned to the originating institution prior to the Reader Study. All original mammograms used in the Reader Study will be returned to the originating sites at the completion of the trial.

SUBMITTING DIGITAL MAMMOGRAMS FOR ACHIVAL:

After consenting to participate, the woman will undergo 4-view DM (bilateral craniocaudal and mediolateral oblique). An electronic copy of each participant's DM will be forwarded to:

Allen McGruder
JHOC 4154A
Johns Hopkins Radiology
601 N. Caroline St.
Baltimore, MD 21287
(410) 955-7129
FAX 410-614-1079
E-mail: amcgru@jhmi.edu

The digital images should be shipped, in the film folder, to JHU via traceable courier (FedEx). Inexpensive (3rd day FedEx) is acceptable.

We would prefer that Digital Mammograms be sent on inexpensive CDs. However, we can accept studies on magneto-optical disc, Exabyte or DAT media. Please have a designated individual from your site (such as your physicist) contact Allen McGruder to discuss the media you intend to use. Expensive media such as Magneto-optical discs can be backed up on CD at Johns Hopkins and returned to your site for re-use.

The DM studies will be archived at JHU until randomized case selection for the reader performance trial is completed.

Risks, Benefits, and Corrective Actions to Minimize Risks:

NOTE: This section required by ARMY Data Safety Monitoring Board:

The immediate risks of this study are very low:

- The unlikely possibility of a breast hematoma or bruise from compression.
- The radiation exposure received by participating in this study is equivalent to an exposure of 0.05 rem (whole body).
- Another risk is the possibility that the digital mammogram might falsely indicate an abnormality that could cause unnecessary anxiety to subjects.
- In addition, it is possible in any study that side effects that are not now known could occur. Precautions will be taken to prevent harmful side effects, including regular monitoring of the digital mammography equipment.

Reporting of Serious and Unexpected Adverse Events:

Adverse experiences that are both serious and unexpected will be immediately reported by telephone to the USAMRMC Deputy Chief of Staff for Regulatory Compliance and Quality **(301-619-2165)** (non-duty hours call 301-619-2165 and send information by facsimile to **301-619-7803**). A written report will follow the initial telephone call within 3 working days. Address the written report to the U.S. Army Medical Research and Material Command, ATTN: MCMR-RCQ, 504 Scott Street, Fort Detrick, Maryland 21702-5012.

Patient Follow-up Information:

Group 1 Patients:
For participants in Group 1 the ***"Clinical Screen-Film Interpretation/Clinically Relevant Lesion"*** form **(DIG.SFM.LESION)** will be completed on the lap top computer. These forms will give information on the location of the nonpalpable lesion biopsied. Copies of their pathology reports, identified only by study number labels will be submitted to Dr.Fajardo at JHU who will catalog the receipt of these data (for site reimbursement purposes – see below – Pathology Review Protocol). The Pathology Findings from biopsy will be coded on the ***"Clinical Screen-Film Interpretation/Clinically Relevant Lesion"*** form **(DIG.SFM.LESION)** will be completed on the lap top computer as well.

Group 2 Patients:
For group 2 patients, the pathology results will be coded on the ***"Clinical Screen-Film Interpretation/Clinically Relevant Lesion"*** form **(DIG.SFM.LESION)** via laptop computer entry at the originating site following the core biopsy or open surgical biopsy procedure. Copies of pathology reports, identified only by study number labels will be submitted to Johns Hopkins for centralized pathology coding (see below– Pathology Review Protocol).

Group 3 Patients:
The majority of follow-up data in this group will comprise information obtained from the patient's 12 month and 24 month follow-up mammograms. For patients in the Group 3 (non-biopsy) study arm, information on the stability over time of breast lesions not biopsied will be entered onto ***Follow-up Mammography Forms*** **(DIG.MAM.FU)** at the time that the 12, and 24 month follow-up SFMs are performed. To encourage the submission of follow-up data, a portion of the participating sites' reimbursement per subject will be withheld until complete data are received.

If any Group 3 patient undergoes a breast biopsy during the follow-up period because of an adverse change on follow-up mammography (or for any other reason, such as physician or patient preference), data will be collected regarding the biopsy type using the ***"Clinical Screen-Film Interpretation/Clinically Relevant Lesion"*** form **(DIG.SFM.LESION)** to enter pathology onto the laptop computer.
A copy of the pathology report, labeled with the patient's study number will also be sent to Dr. Fajardo.

PATIENT CONFIDENTIALITY: Labeling of Mammographic Studies and Pathology Reports:

For all patients, after informed consent is obtained, the patient will be assigned a study number. A patient's screen-film images and pathology reports will be labeled with that number only, without other identifiers. All data sheets for the reader interpretation study for that patient will contain the same number, without other identifiers, to ensure patient confidentiality.

SUBMITTING PATHOLOGY REPORTS FOR PATHOLOGY REVIEW:

The pathology report for biopsied lesions will be mailed to Dr. Fajardo, at JHU who will coordinate coding sessions with Dr. Fred Askin, the consortium pathologist.

If any woman undergoes a breast biopsy during the months that this study is open after she is enrolled in the trial, that pathology report will be sent for inclusion in the database.

Laurie L. Fajardo, M.D.
Department of Radiology
Johns Hopkins Outpatient Center, Room 4006
601 N. Caroline St.
Baltimore, MD 21287
Contact telephone no.: 410-955-7095
FAX: 410-955-1079
Email: LFAJARDO@rad.jhu.edu

COMPUTER DATA SUBMISSION

Protocol For Sending Computer Back-up Data to the Statistical Coordinating Center at UNC:

ID NUMBERS AND THEIR MANAGEMENT

Each ID number consists of 4 digits and a check digit for a total of 5 digits. The check digit is derivable by an algorithm that will be programmed into the data-entry system. The algorithm detects several types of errors, including 100% detection of transposition of adjacent digits, a common error.

ID numbers will be allocated to centers at random, so that no center is allocated a block on consecutive ID numbers. A set of labels will be pre-printed for each ID number, and sent to the centers to be used as needed. Hand-writing of ID numbers should be avoided as much as possible. In addition, a list of the assigned ID numbers will be sent to each center to be completed by filling-in patients' names and hospital numbers as patients are recruited into the study. This will serve as the "patient enrollment list" at each center. \

DATA ENTRY

Data entry menus and screens will be setup at UNC. Since menus and forms will be similar to those used in the pilot study, training will be done via a conference call.

Questions that arise during the course of the study can be directed to the biostatistician, Dr. Bahjat Qaqish at (919) 966-7271 or programmer, Yuhua Lin at (919) 966-8647. The computer hardware (notebooks) and software should not be modified at the sites in any way. No new software of any kind should be installed (specific examples include network and Internet software and games). One person at each center will be designated to be in charge of data entry and backup procedures.

BACKUPS

A backup procedure will be programmed and should be performed at least once a day, but preferably several times during the day. A set of 5 disks labeled "Monday" through "Friday" will be used for backups on the respective days of the week. This allows recovery of up to 5 working days back. The backup disks should be kept in a secure location, not in the same office as the computers; preferably in a different building.
On any given day, only one disk will be in the same office as the data-entry notebook.

SUBMITTING BACK-UP DISCS OF COMPUTER DATA:

Using the back-up procedure described above, clinical sites will submit computer back-up discs every two weeks to the statistical coordinating center at UNC. Data back-up discs should be mailed to:

Yuhua Lin, Ph.D.
UNC Chapel Hill Biostatistics Dept.
20-012 Lineberger Comprehensive Cancer Center
CB#7295
Mason Farm Rd and West Drive
Chapel Hill, NC 27599-7515
919-966-8647
919-966-4244 (fax)
ylin@bios.unc.edu

READER PERFORMANCE STUDY

The reader trial will comprise 12 readers from the six clinical sites. The display of DM images may be accomplished using soft-copy display, on optimized workstation and CRT monitors.

Reader Training for DM Image Interpretation: Although, all radiologist readers will have experience in viewing digital mammograms, they will be "trained" with soft copy images on the image interpretation workstation prior to performing their interpretations for the Reader Trial. Twenty-five digital (soft-copy) and original screen-film will be prepared for training. Practice with completing the Reader Trial Interpretation Forms will also be completed.

Case Selection and Trial Design for the Reader Performance Study: From the total of 1075 cases, which will include about 176 cancers, the reader study will require 432 cases comprising: 144 biopsy-proven cases with cancers (selected from the cancer cases in Groups 1and 2); 144 biopsy-proven cases without cancer (selected from the non-cancer cases in Groups 1and 2); and 144 problem-solving mammography cases that did not go to biopsy (selected from Group 3).

The 12 readers will be grouped into two cohorts, A and B. The cases accrued at sites in cohort A will be read by readers from sites in cohort B, and vice versa. The following table defines cases to be read by each reader in each condition. Here the SFM and DM columns list the set of cases to be read.

Reader		Site	SFM	DM
1	A	1	3	4
2	A	1	3	4
3	A	2	3	4
4	A	2	4	3
5	A	3	4	3
6	A	3	4	3

Reader		Site	SFM	DM
7	B	4	1	2
8	B	4	1	2
9	B	5	1	2
10	B	5	2	1
11	B	6	2	1
12	B	6	2	1

Each of the four image sets will contain 108 cases (36 cancers, 36 biopsy without cancer, 36 non-cancer non-biopsy). Each reader will read a set of 108 SFM and a set of 108 DM cases during one interpretation session. Readers will not read cases originating from their site. To avoid recall bias, they will not read the DM and SFM images for an individual case. The design allows controlling for important nuisance variables and allows direct testing of the primary hypotheses.

RADIOLOGIST INTERPRETATION PROTOCOL

Experimental Readings of Film-screen Mammograms

The readings of the film-screen mammograms will be interpreted in the standard clinical fashion, using mammographic viewboxes with a magnifying glass. The assigned radiologist readers will have no prior familiarity with or information about the cases being read apart from that provided to them with the images on a printed copy of the Enrollment Form. The radiologist will examine the four-view mammogram (left and right medio-lateral oblique images and left and right cranio-caudal images) and record his or her interpretation of these images by completing ***Reader Study Interpretation Form***. When more than one lesion is detected, the ***Reader Study Interpretation Form – Additional Lesions*** will be completed (as many as required to address all findings on the mammogram).

Experimental Readings of Digital Mammograms

Soft-copy cranio-caudal and medio-lateral oblique digital mammograms will be interpreted similar to the conventional mammograms. After reading these images, the radiologist will render interpretations by completing the ***Reader Study Interpretation Form*** **(and** ***Reader Study Interpretation Form-Additional Lesions***, as needed). These interpretations will henceforth be known as the Experimental interpretations.

Experimental Interpretation Method

On the ***Reader Study Interpretation Forms***, the interpreting radiologists will answer yes or no to the following question for all mammograms: "Are there any radiological findings on this mammogram?" If the answer to this question is "yes", then the radiologist will note the location of each finding using ACR descriptors, namely, an o'clock location, an antero-posterior location, and woman's body side (i.e. right or left). The interpreting radiologist will also be asked to qualify the description of the finding using the ACR lexicon descriptor terms. The reader will then answer two additional questions for each finding. The first question about each finding is the following: Given the radiological features of this finding, which description best applies:

1: There is no finding or the finding is definitely not malignant.
2: The finding is probably not malignant.
3: The finding is possibly malignant.
4: The finding is probably malignant.
5: The finding is definitely malignant.

The second question about each finding is the following: Based only on the images and information currently available, what would you recommend for this finding?

1: No further work-up. Routine follow-up only.
2: No further work-up. Six month follow-up only.
3: Further work-up with additional mammographic views and/or ultrasound.
4: Further work-up with either percutaneous or open surgical biopsy.

Each reader will be assigned a unique identifying number so that his or her interpretations cannot be linked to him or her by name without access to the identifying codes. These codes will be included with his or her interpretations.

DISAGREEMENT RESOLUTION

Because multiple interpretations will be rendered of the same patient's studies, there will undoubtedly be some differences in opinion on the mammographic interpretation. Specifically, there may be "lesions" discovered by the study readers that will not have been detected by the clinical reader. When patients are enrolled into the study, they will be informed that they will not directly benefit from any extra readings of their images done at outside institutions. The delay in the interpretation study until the final year of this trial makes the probability of detection of a lesion that has not become clinically apparent in the interim low, but not zero, especially for patients enrolled at the end of the accrual period and whose images are re-read at the beginning of the interpretation period.

When disagreements are encountered, the clinical investigator radiologist will be contacted about any area identified by other readers as indeterminate, probably malignant or malignant that was not identified in the original interpretation or that was identified but considered probably benign or benign in that interpretation, by the local reader. The local reader can then review the images, together with whatever additional clinical and imaging information he or she possesses, to determine whether or not there is a real clinical concern, enough to justify contacting the patient and the patient's physician regarding the need for additional work-up.

Frequently, these areas of concern to the experimental readers will have been seen and are unchanged since prior mammograms that will be available to the local radiologists but not to the study interpreters.

The local radiologist will complete a **Mammography Assessment Disagreement Resolution Form** to document the actions taken regarding these types of disagreements. If there are lesions that are detected in this manner for which the patient ultimately undergoes biopsy (either core needle or open), the local radiologist will send a copy of the local pathology report to Dr. Fajardo at JHU.

APPENDIX C:

CASE REPORT/DATA FORMS

DIG.EN Patient Enrollment form for the Digital Study

Patient Name:	**MRN #:**
Study ID #:	**Center Name:**
Patient's Date of Birth: (mm/dd/yyyy) ☐☐ ☐☐ ☐☐☐☐	**Today's Date:** (mm/dd/yyyy) ☐☐ ☐☐ ☐☐☐☐
Enrolling Radiologist: (Please Print Name)	

To be completed by a **research assistant** at the time of **patient enrollment**.

~~Part A~~: Race/Ethnic Background
(please circle code)

W	White
H	Hispanic
AA	African American
AS	Asian
NA	Native American
NH	Native Hawaiian
O	Other: (please specify) ☐

~~Part B~~: Menopausal Status
(please circle code)

PR	Premenopausal
SM	Surgical Menopause
PO	Postmenopausal (last menses ≥ 1 year ago)
PE	Perimenopausal (last menses < 1 year ago)
U	Unknown

Date of last menses: ☐☐ ☐☐ ☐☐☐☐
mm dd yyyyy

~~Part B~~: History of Hormone Use
(please circle code)

Y	Yes
N	No
U	Unknown

If the patient has ~~no known history of hormone use~~, go to Part D (page 3). Otherwise, continue.

[redacted]

Hormone Use – Continued.

1. **Birth Control Pill Use?**
   (please circle code)

   Y Yes
   N No
   U Unknown **If patient has ~~no known history of birth control pill use~~, then go to Part C, question 2 (this page). Otherwise, continue.**

   Current or Former Use?
   (please circle code)

   C Current Use
   F Former Use

   Used for ☐☐ years and ☐☐ months.

   Age (in years) of first use: ☐☐

2. **Estrogen Replacement Therapy?**
   (please circle code)

   Y Yes
   N No
   U Unknown **If patient has ~~no known history of estrogen replacement therapy~~, then go to Part D (page 3). Otherwise, continue.**

   Current or Former Use?
   (please circle code)

   C Current Use
   F Former Use

   Used for ☐☐ years and ☐☐ months.

   Age (in years) of first use: ☐☐

Study ID:

~~Part D~~: Prior Diagnosis of Breast Cancer
(please circle code)

Y Yes
N No
U Unknown

How many prior diagnoses? ☐

~~Part E~~: Prior Breast Surgery or Procedures for Nonmalignant Conditions
(please circle code)

Y Yes
N No
U Unknown

1. Open Biopsy?
(please circle code)

Y Yes
N No
U Unknown

How many open biopsies? ☐

~~If yes~~, please complete Form DIG.POB for each prior open biopsy.

2. Core Needle Biopsy?
(please circle code)

Y Yes
N No
U Unknown

How many core needle biopsies? ☐

~~If Yes~~, please complete form DIG.PCNB for each prior needle biopsy.

[redacted]

Study ID:

3. Subcutaneous Mastectomy?
(please circle code)

Y Yes
N No
U Unknown

If YES, Right or Left Breast?
(please circle code)

R Right Breast
L Left Breast

4. Cyst Aspiration or FNA?
(please circle code)

Y Yes
N No
U Unknown

How many cyst aspirations or FNAs?

~~Part E~~: Risk Factors

Family History of Breast Cancer Among Patient's ~~BLOOD~~ Relatives?
(Do not include relatives by marriage.)
(please circle code)

Y Yes
N No
U Unknown **If patient has ~~no known history of breast cancer among blood relatives~~, go to the bottom of page 8.**

1. Please check all that apply and enter age at diagnosis.

☐ **Grandmother 1**
Age at diagnosis: ☐☐

☐ **Grandmother 2**
Age at Diagnosis: ☐☐

DIG.EN Patient Enrollment form for the Digital Study

Study ID:

☐ **Mother**
Age at diagnosis: ☐☐

☐ **Sister 1**
Age at diagnosis: ☐☐

☐ **Sister 2**
Age at diagnosis: ☐☐

☐ **Sister 3**
Age at diagnosis: ☐☐

☐ **Daughter 1**
Age at diagnosis: ☐☐

☐ **Daughter 2**
Age at diagnosis: ☐☐

☐ **Daughter 3**
Age at diagnosis: ☐☐

☐ **Other (please specify)** _____
Age at diagnosis: ☐☐

☐ **Other (please specify)** _____
Age at diagnosis: ☐☐

Number of full-term pregnancies: ☐☐

Age (in years) at first full term pregnancy: ☐☐

Age (in years) at menarche: ☐☐

Initials of person completing this form: ☐

DIG.NE Eligible Patients Not Enrolled in the Digital Study

Patient Name:	**MRN #:**
Study ID #:	**Center Name:**
Patient's Date of Birth: ☐☐ ☐☐ ☐☐☐☐ (mm/dd/yyyy)	**Today's Date:** ☐☐ ☐☐ ☐☐☐☐ (mm/dd/yyyy)
Enrolling Radiologist: (Please Print Name)	

This form is to be completed by a **research assistant** or the **recruiting radiologist** for each **eligible** patient who is **not enrolled** into the Digital clinical trial. An eligible patient is one who presents for problem-solving mammography, who is scheduled for breast biopsy, and who meets the eligibility criteria listed on **form DIG.EC.1.2 or DIG.EC.3**.

Race/Ethnic Background
(please circle code)

- **W** White
- **H** Hispanic
- **AA** African American
- **AS** Asian
- **NA** Native American
- **NH** Native Hawaiian
- **O** Other: _____ (please specify)

Type of Lesion:
(please circle code)

- **M** Mass
- **MC** Mass With Calcifications
- **C** Calcifications
- **AR** Architectural Distortion
- **AS** Asymmetric Density
- **DD** Dilated Duct
- **O** Other: _____ (please specify)

DIG.NE Eligible Patients Not Enrolled in the Digital Study

Reason Patient Was Not Enrolled in this Study:
(please circle code)

PR	Patient refused
P	Pregnancy
IC	Inform consent
NR	Not randomized to invitation (Group 3 only)
O	Other: _____ (please specify)

Initials of person completing this form: _____

DIG.EC.1.2 Eligibility Checklist for the Digital Study – Groups 1 & 2

Patient Name:	**MRN #:**
Study ID #:	**Center Name:**
Patient's Date of Birth: (mm/dd/yyyy) ☐☐ ☐☐ ☐☐☐☐	**Today's Date:** (mm/dd/yyyy) ☐☐ ☐☐ ☐☐☐☐
Enrolling Radiologist: (Please Print Name)	

This form is to be completed by a **research assistant** or the **recruiting radiologist** at the clinical site to determine patient eligibility for the Digital clinical trial.
A patient is eligible for entry into this study **if and only if** each answer circled is in uppercase and in boldface type.

1. Did the patient present to your clinic to undergo mammography for one of the following reasons: She had a breast problem that was detected on physical examination. She had a breast problem detected on a screening mammogram. She had a symptom in her breast (a dominant lump or suspicious nipple discharge). She had an abnormal mammogram that required follow-up.	**YES** no
2. Has a biopsy been recommended for her based on the mammographic or physical examination finding?	**YES** no
3. Is she scheduled for FNA or cyst aspiration only?	yes **NO**
4. Does the patient have ≥ 1/3 dense breast tissue? (Moderately or markedly radiodense.)	**YES** no
5. Has she had a mastectomy?	yes **NO**
6. Does she have breast implants?	yes **NO**
7. Is she pregnant or nursing or does she think she might be pregnant?	yes **NO**
8. Is she capable of giving informed consent?	**YES** no
9. Has she signed a consent form?	**YES** no
10. Has she/will she have undergone biopsy within the 12 weeks after her entry mammogram?	**YES** no

[redacted]

DIG.EC.1.2 Eligibility Checklist for the Digital Study – Groups 1 & 2

11. Is the patient <u>ELIGIBLE</u> for this study?
(please circle code)

Y Yes
N No

12. If the patient is eligible, has she consented to be <u>ENROLLED</u> in the study?

Y Yes → **Please complete Form DIG.EN**
N No → **Please complete Form DIG.NE**

DIG.EC.3 Eligibility Checklist for the Digital Study – Group 3

Patient Name:	**MRN #:**
Study ID #:	**Center Name:**
Patient's Date of Birth: (mm/dd/yyyy) ☐☐ ☐☐ ☐☐☐☐	**Today's Date:** (mm/dd/yyyy) ☐☐ ☐☐ ☐☐☐☐
Enrolling Radiologist: (Please Print Name)	

This form is to be completed by a **research assistant** or the **recruiting radiologist** at the clinical site to determine patient eligibility for the Digital clinical trial.
A patient is eligible for entry into this study **if and only if** each answer circled is in uppercase and in boldface type.

1. Did the patient present to your clinic to undergo mammography for one of the following reasons: She had a breast problem detected on a screening mammogram. She had an abnormal mammogram that required follow-up.	**YES** no
2. Has a biopsy been recommended for her based on a mammographic or physical examination finding?	yes **NO**
3. Is she scheduled for mammographic follow-up, without biopsy?	**YES** no
4. Does the patient have ≥ 1/3 dense breast tissue? (Moderate or markedly radiodense.)	**YES** no
5. Has she had a mastectomy?	yes **NO**
6. Does she have breast implants?	yes **NO**
7. Is she pregnant or nursing or does she think she might be pregnant?	yes **NO**
8. Can she undergo follow-up film-screen mammography at this facility or provide copies of mammograms for the next 2 years?	**YES** no
9. Is she capable of giving informed consent?	**YES** no

DIG.EC.3 Eligibility Checklist for the Digital Study – Group 3

10. Is the patient <u>ELIGIBLE</u> for this study?
(please circle code)

Y Yes
N No

11. If the patient is eligible, will she be invited for enrollment? (Open envelope.)

Y Yes
N No

12. If patient is eligible for invitation, has she consented to be <u>ENROLLED</u> in this study?

Y Yes → **Please complete Form DIG.EN**
N No → **Please complete Form DIG.NE**

DIG.SFM.LESION

Clinical Film-Screen Interpretation:
Clinically Relevant Lesion Form

Patient Name:	**Center Name:**
Study ID #:	**Today's Date:** (mm/dd/yyyy) ☐☐ ☐☐ ☐☐☐☐
Enrolling Radiologist: (Please Print Name)	

To be completed by the **clinical radiologist** (who determined the patient to be eligible for this clinical trial) to record his/her interpretation of the eligibility film-screen mammogram.

Information Regarding Patient's Eligibility Mammogram

Date performed: ☐☐ (mm) ☐☐ (dd) ☐☐☐☐ (yyyy)

Facility where mammogram performed: _____

Lesion # ☐ **of** ☐ (Note: complete this form for each clinically relevant lesion, both mammographic and palpable)

Density of Breast Parenchyma
(please circle code)

HD Heterogeneously Dense
XD Extremely Dense

Seen on Film-Screen Mammogram?
(please circle code)

Y Yes
N No

Palpable Lesion?
(please circle code)

Y Yes
N No

DIG.SFM.LESION

Clinical Film-Screen Interpretation:
Clinically Relevant Lesion Form

Type of Lesion?
(Please check whatever applies)

- ☐ **Mass**
- ☐ **Asymmetric Density**
- ☐ **Architectural Distortion**
- ☐ **Clusters of Calcification**

Right or Left Breast?
(please circle code)

- **R** Right Breast
- **L** Left Breast

Lesion Seen on
(Please check one applies)

☐ **Both Views**

1 ☐ **2** ☐ **3** ☐ **4** ☐ **5** ☐

6 ☐ **7** ☐ **8** ☐ **9** ☐ **10** ☐

11 ☐ **12** ☐ **AT** ☐ **SN** ☐

☐ **CC View**

Lateral ☐ **Medial** ☐ **Retroareolar** ☐

☐ **MLO view**

Superior ☐ **Retroareolar** ☐ **Inferior** ☐

AP Location: (Note: If you choose AT in b, only P can go with AT in c.)
(please circle code)

- **A** Anterior
- **C** Central
- **P** Posterior

DIG.SFM.LESION

Clinical Film-Screen Interpretation:
Clinically Relevant Lesion Form

Which description best applies?
(please circle code)

1	There are **no** findings or the finding is **definitely not** malignant.
2	The finding is **probably not** malignant.
3	The finding is **possibly** malignant.
4	The finding is **probably** malignant.
5	The finding is **definitely** malignant.

What is the final outcome of this lesion?
(please circle code)

1 **Biopsy**

Date performed

Core Biopsy → ☐☐ ☐☐ ☐☐☐☐

Surgical Biopsy → ☐☐ ☐☐ ☐☐☐☐

2 **Probably benign. Short term interval follow-up at 6-months.**

3 **Routine follow-up Imaging at 12 months.**

Is this the PRIMARY lesion that caused the patient to be included in the study?
(please circle code)

Y	Yes
N	No

Was this lesion MOST suspicious for which biopsy was recommended?

Y	Yes
N	No
NA	N/A (Group 3)

DIG.SFM.LESION

Clinical Film-Screen Interpretation:
Clinically Relevant Lesion Form

ARE YOU READY TO RECORD THE PATHOLOGY FINDING(S)?
(please circle code)

Y Yes
N No

ARE YOU READY TO CODE THE PATHOLOGY FINDING(S)?
(please circle code)

Y Yes
N No

☐☐ ☐☐ ☐☐ ☐☐

Initial of radiologist completing this form: ☐

DIG.PBC Prior Breast Cancer Form for the Digital Study

Patient Name:	**MRN#:**
Study ID #:	**Center Name:**
Patient's Date of Birth: ☐☐ ☐☐ ☐☐☐☐ (mm/dd/yyyy)	**Today's Date:** ☐☐ ☐☐ ☐☐☐☐ (mm/dd/yyyy)
Enrolling Radiologist: (please print name)	

Extension of **Form DIG.EN, Part D**. This form is only applicable when a patient has a prior diagnosis of breast cancer. The **research assistant** should complete one copy of this form for each diagnosis of breast cancer.

PRIOR DIAGNOSIS # ☐ of ☐:

a. Date of Diagnosis: ☐☐ ☐☐ ☐☐☐☐ (mm dd yyyy)

b. Right or Left Breast?
(please circle code)

R Right Breast
L Left Breast

c. Part of Breast Involved :
(please circle code)

UO Upper Outer Quadrant
UI Upper Inner Quadrant
LO Lower Outer Quadrant
LI Lower Inner Quadrant
AT Axillary Tail
CS Central or Sub-Areolar
U Unknown

d. O'Clock /Axillary Tail /Subareolar Nipple Location (1-12, AT, SN):
(check O'Clock location or AT, SN location)

1 ☐ **2** ☐ **3** ☐ **4** ☐ **5** ☐
6 ☐ **7** ☐ **8** ☐ **9** ☐ **10** ☐
11 ☐ **12** ☐ **AT** ☐ **SN** ☐

e. AP Location: (Note: If you choose AT in d, only P can go with AT in e.)
(please circle code)

A Anterior
C Central
P Posterior

[redacted]

f. Treatment Rendered:
(please check all that apply and indicate date received):

		mm	yyyy
☐	Unknown		
☐	None	☐☐	☐☐☐☐
☐	Lumpectomy	☐☐	☐☐☐☐
☐	Mastectomy	☐☐	☐☐☐☐
☐	Quadrantectomy	☐☐	☐☐☐☐
☐	Radiation Therapy	☐☐	☐☐☐☐
☐	Chemotherapy (last cycle)	☐☐	☐☐☐☐
☐	Other:	☐☐	☐☐☐☐

(please specify)

Initials of person completing this form: ☐

DIG.PCNB Prior Core Needle Biopsy Form for the Digital Study

Patient Name:	**MRN #:**
Study ID #:	**Center Name:**
Patient's Date of Birth: (mm/dd/yyyy) ☐☐ ☐☐ ☐☐☐☐	**Today's Date:** (mm/dd/yyyy) ☐☐ ☐☐ ☐☐☐☐
Enrolling Radiologist: (Please Print Name)	

Extension of **Form DIG.EN, Part E, question 2.** This form is only applicable when a patient has a prior core needle biopsy. The **research assistant** should complete one copy of this form for each core needle biopsy.

PRIOR CORE NEEDLE BIOPSY # ☐ of ☐ :

a. Date of Core Needle Biopsy: ☐☐ mm ☐☐ dd ☐☐☐☐ yyyy

b. Right or Left Breast?
(please circle code)

R Right Breast
L Left Breast

c. O'Clock /Axillary Tail /Subareolar Nipple Location (1-12, AT, SN):
(check O'Clock location or AT, SN location)

1	☐	**2**	☐	**3**	☐	**4**	☐	**5**	☐
6	☐	**7**	☐	**8**	☐	**9**	☐	**10**	☐
11	☐	**12**	☐	**AT**	☐	**SN**	☐		

d. AP Location: (Note: If you choose AT in c, only P can go with AT in d.)
(please circle code)

A Anterior
C Central
P Posterior

Initials of person completing this form: ☐

DIG.POB Prior Open Biopsy Form for the Digital Study

Patient Name:	**MRN #:**
Study ID #:	**Center Name:**
Patient's Date of Birth: (mm/dd/yyyy) ☐☐ ☐☐ ☐☐☐☐	**Today's Date:** (mm/dd/yyyy) ☐☐ ☐☐ ☐☐☐☐
Enrolling Radiologist: (Please Print Name)	

Extension of Form **DIG.EN, Part E, question 1**. This for is onlyh applicable when the patient has a prior open biopsy. The **research assistant** should complete one copy of this form for each open biopsy.

OPEN BIOPSY # ☐ of ☐:

a. Date of Open Biopsy: ☐☐ ☐☐ ☐☐☐☐
mm dd yyyy

b. Right or Left Breast?
(please circle code)

R Right Breast
L Left Breast

c. O'Clock /Axillary Tail /Subareolar Nipple Location (1-12, AT, SN):
(Check O'Clock location or AT, SN location)

1	☐	**2**	☐	**3**	☐	**4**	☐	**5**	☐
6	☐	**7**	☐	**8**	☐	**9**	☐	**10**	☐
11	☐	**12**	☐	**AT**	☐	**SN**	☐		

d. AP Location: (Note: If you choose AT in c, only P can go with AT in d.)
(please circle code)

A Anterior
C Central
P Posterior

Initials of person completing this form: ☐

APPENDIX D:

ABSTRACTS PRESENTED

The 1999 Radiologic Society of North America, Chicago, IL, November 27-December 3, 1999:

"Development of a quality control system for full-field digital mammography".
MJ Yaffe, MB Williams, LT Niklason, GE Mawdsley, AD Maidment, Radiology 209(P) (1999) 160.

The 5th International Workshop on Digital Mammography, Toronto, CA, June 11-14, 2000:

"Beam Optimization for Digital Mammography".
MB Williams, M More, V Venkatakrishnan, L Niklason, MJ Yaffe, G Mawdsley, A Bloomquist, A Maidment, D Chakraborty, C Kimme-Smith, LL Fajardo

"Accuracy of digital mammography vs. screen-film mammography in a diagnostic mammography population".
The International Digital Mammography Group

BEAM OPTIMIZATION FOR DIGITAL MAMMOGRAPHY

Mark B. Williams[*], Mitali More[*], Vaidehi Venkatakrishnan[%], Loren Niklason[^], Martin J. Yaffe[#], Gordon Mawdsley[#], Aili Bloomquist[#], Andrew Maidment[**], Dev Chakraborty[^^], Carolyn Kimme-Smith[##], and Laurie L. Fajardo[***]

* University of Virginia, [%]Beth Israel Hospital, ^General Electric Medical, [#]University of Toronto, **Thomas Jefferson University, ^^University of Pennsylvania, [##]UCLA, [***]Johns Hopkins University

1.0 Introduction

Criteria for optimization of tube voltage and external filtration in digital mammography (DM) differ from those used in screen-film mammography. This is because the separation of the processes of acquisition and display in the former permits the contrast of individual structures to be adjusted when the image is viewed. It is therefore possible to detect objects with low subject contrast provided that the image signal to noise ratio (SNR) is adequate. Thus, rather than maximization of contrast within the constraint of acceptable film darkening and patient dose, beam optimization in digital mammography requires maximization of the image SNR, constrained by acceptable patient dose.

The goal of this study is to identify, for each of several currently available DM systems, technique factors that result in the highest SNR per unit radiation dose, and to do so for a range of breast thickness and adipose/fibroglandular ratio. Data from three different early commercial DM systems, located at three different university test sites, are presented here. Each of these sites is participating in a coordinated clinical evaluation of the DM systems, and a major purpose of our study is to provide guidelines for technique factors to be used during the clinical evaluation.

To identify optimum technique factors, we have chosen the following figure of merit (FOM),

$$FOM = (SNR)^2/MGD,$$

where MGD is the mean dose to the glandular portion of the breast, and the SNR is as defined in section 2.2 below. This FOM is independent of exposure (in the x-ray quantum-limited regime of operation), and has been used previously by others in mammographic beam optimization studies (Jennings et al., 1993; Boone et al., 1990).

2.0 Materials and Methods

2.1 Data Acquisition

Three DM units from three different manufacturers were used in the study. The units from Fischer, GE, and Trex will hereafter be referred to as Systems 1, 2, and 3, respectively. A common set of phantoms was circulated between the physicists participating in the study. The phantoms were assembled from stacks of blocks of breast equivalent material (CIRS, Inc., Norfolk, VA). Nine different phantoms were assembled and imaged, simulating breasts of three different thicknesses (3 cm, 5 cm, and 7 cm), and three different attenuation equivalent adipose/fibroglandular mass ratios (30/70, 50/50, and 70/30). All blocks of a given phantom had the same adipose/fibroglandular ratio, except for two 5 mm thick blocks, common to all phantoms, that are 100% adipose equivalent. These blocks were placed at the top and bottom of the stack to simulate skin (see figure 1). In each phantom stack assembled, the centrally located block in the stack (the signal block) contained a series of test objects. For the data reported here, the test objects of interest were two stepwedges, one each of calcification equivalent and mass equivalent material. The mass equivalent stepwedge has the same x-ray attenuation as 100% glandular equivalent material, and the microcalcification equivalent step wedge is composed of calcium carbonate. Figure 2 is a schematic of a signal block showing the dimensions of the block and step wedges (other test objects present in the signal block have been omitted for clarity). The thickness of all signal blocks is 2 cm. Images were obtained in manual mode with the phantoms positioned at the chest wall edge of the receptor, centered left to right. Exposure time was selected to give approximately the same average pixel value in the phantom background area for each phantom/technique combination. For each combination two images were obtained with identical exposure times for the purpose of image subtraction, taking care not to move the phantom between the two exposures. At each site, entrance exposures (mR/mAs) and half value layers (HVLs) were measured for each target/filter/kVp combination used.

2.2 Image Analysis

Signal was defined as the difference between the average pixel values in a region of interest (ROI) centered on an individual step (but not including the step boundaries), and an equal sized ROI located immediately adjacent to the step, but containing only background. To quantify the image noise, the two images of a given phantom, obtained at a common technique, were subtracted. Image subtraction was performed to remove fixed pattern noise associated with phantom defects, detector nonuniformity, and the heel effect. Noise in a single image was defined as the rms pixel-to-pixel fluctuations in an ROI of 1109 x 511 pixels in the difference image, divided by the square root of two.

2.3 Calculation of MGD

Table I lists each of the target and filter combinations tested in the study. Also given for each target/filter combination are the range of kVps used, and the corresponding HVL range. In several cases, the same target/filter combination was available on more than one DM system. Table I lists the combined kVp and HVL ranges from all systems.

The MGD for each phantom was calculated using its known thickness and composition, and the measured HVL and mR/mAs values from each DM system. For Mo/Mo and Mo/Rh spectra, the parameterized dose tables of Sobol and Wu were utilized to obtain the glandular dose per unit exposure (Sobol and Wu, 1997). For the W/Al spectra, normalized (to entrance exposure) MGD values were obtained from the data of Stanton et al. (Stanton et al., 1984). Their data were extrapolated to 3 cm breast thickness, and interpolation between their published HVL curves was used to obtain correction factors for the particular glandular volume fractions (0.22, 0.40, and 0.61, corresponding to glandular mass fractions of 0.30, 0.50, and 0.70, respectively) used in our study. For the W/Rh spectra, the calculations of Boone were utilized, interpolating between his published HVL and adipose/fibroglandular composition values (Boone, 1999). All FOM values were obtained by dividing the square of the SNR by the MGD, expressed in units of 10^{-5} Gy (1 mrad).

3.0 Results

The measured HVL values for the seven specific target/filter combinations tested at the three sites, as a function of kVp, are shown in Figure 3. Figure 4 shows the corresponding normalized MGD, D_{gN}, calculated for each of the seven spectra, plotted versus the measured HVL. Similarly, Figure 5 shows D_{gN} for each target/filter combination tested, plotted versus kVp. The general tradeoff between loss of contrast and reduction in MGD with increasing kVp is illustrated in Figure 6. In this example, the measured contrast of the 0.3 mm thick (thickest) calcification step in shown for the 5 cm thick, 50/50 phantom.

For each of the three DM systems, SNR versus kVp, and the corresponding FOM values vs. kVp have been determined. Figures 7-12 show the results obtained for the 300

Table I

Target	**Filter**	**kVp range**	**HVL range (mm Al)**
Molybdenum	Molybdenum	22-35	0.26-0.43
Molybdenum	Rhodium	24-39	0.37-0.51
Rhodium	Rhodium	25-35	0.36-0.52
Tungsten	Aluminum	29-45	0.46-0.77
Tungsten	Rhodium	32-45	0.47-0.58

Target/filter combinations, kVp ranges, and HVL ranges of the systems tested. Two of the three mammographic systems used Mo/Mo and Mo/Rh combinations. In those cases, the kVp and HVL ranges given represent the pooled values from both systems.

micron thick step of the calcification stepwedge in the three 50/50 composition phantoms, for each of the three imaging systems. To illustrate the applicability of these data to objects, the dependence of the FOM on the step thickness for both types of stepwedges is presented in Figures 13 and 14. These data are from images obtained on System 3, using a Mo/Mo target/filter combination to image a 5 cm thick, 50/50 composition phantom. Finally, Figures 15-17 illustrate the effect on the FOM of changing breast composition, holding breast thickness fixed. These data were obtained using System 1, and signals were calculated using the 10 mm thick mass equivalent step.

4.0 Discussion and Conclusions

The analysis of SNR and FOM as a function of kVp, shown in Figures 7-12, indicates that although the image SNR tends to decrease monotonically for all systems with increasing kVp, the accompanying MGD reduction results in fairly flat FOM curves. Note, however, in the case of System 1, the SNR falls at low kVp. This is primarily due to tube loading, since it was not possible to obtain the same exit exposure at all kVps (that is, the tube output was insufficient to compensate for the lower transmission through the phantoms). Thus the falling SNR (and the falling MGD) with decreasing kVp are really consequences of falling exposure.

For a given phantom/technique combination, the SNR, and thus the *magnitude* of the FOM, increases with increasing step thickness for both types of stepwedge. However, the *shape* of the FOM vs. kVp curves for a given target/filter/phantom combination are essentially independent of step thickness, and are similar for mass and calcification equivalent signals. This is illustrated by the example shown in figures 13 and 14. This implies that the result of the optimization is not sensitively dependent on signal amplitude.

Figures 15-17 illustrate that, at least in the case of System 1, there is a clear advantage to using rhodium filtration for thin breasts, but that for breasts 5 cm or thicker, aluminum filtration becomes increasingly advantageous. Similar statements can be made for the molybdenum target systems tested, where molybdenum filtration was superior for 3 cm phantoms of all compositions, but rhodium filtration produced better results for 5 and 7 cm thick phantoms of all compositions. These data suggest that the choice of external filtration is potentially more significant in determination of the overall FOM of a DM system than is choice of tube voltage.

Fahrig and Yaffe developed a model for optimizing spectral shape in digital mammography, and used it to calculate kVp values producing maximum SNR at a fixed dose for W and Mo spectra (Fahrig and Yaffe, 1994). They found that, for a fixed MGD of 0.6 mGy (60 mrads), the peak SNR occurred in the 24-31 kVp range (W spectrum) and 25-29 kVp range (Mo spectrum) for 4 – 8 cm breast thickness, and 50/50 breast composition. Their results were the same, whether the lesion type modeled was infiltrating ductal carcinoma or microcalcification.

Jennings et al. used a computational approach to identify maximum FOM values (FOM = SNR^2/MGD) for a variety of target/filter combinations, and breast thicknesses. They found that for a Mo/Mo beam used to image 3-6 cm, 50/50 breasts, the FOM peaks at 27-

28 kVp, and changes slowly with changing kVp near the peak values. Very similar FOM vs. kVp curves were obtained for Mo/Mo, Mo/Rh, and W/Al spectra, applied to 6 cm thick, 50/50 composition breasts. The general trends in our data appear to be consistent with those of these previous studies.

One limitation of our study is that only large area (low frequency) signals were considered. Other test objects in the signal blocks (simulated microcalcifications, for example), may permit some spatial frequency-dependent optimization, but those data have not yet been analyzed. Conversely, noise was calculated from the RMS pixel-to-pixel variations. This is equivalent to estimating the area under the two dimensional noise power spectrum (NPS) out to the Nyquist frequency. Other valid scalar measures of noise, such as the low frequency NPS, would give different results. Finally, this paper does not discuss detector saturation effects, which are important when imaging thick, dense breasts.

ACCURACY OF DIGITAL MAMMOGRAPHY VS. SCREEN-FILM MAMMOGRAPHY IN A DIAGNOSTIC MAMMOGRAPHY POPULATION

The International Digital Mammography Group

Background and Significance

Screening mammography has proven to be an effective test in identifying early breast cancer. Large randomized trials have demonstrated that breast cancer mortality among screened women over 50 years old can be reduced up to 30% when compared with unscreened controls. [Kerlikowske 1995, Fletcher 1993, Nystrom 1993] The cancers found by mammography tend to be smaller and of less advanced stages than those found by breast physical examination or breast self-examination. Smaller and lower stage breast cancers tend to have better survival rates over time. [Letton 1996]

Unfortunately, approximately 10% of clinically obvious breast cancers are not visible with mammography. [Baker 1982, Brekelmans 1996, Burrell 1996A] This occurs most frequently in patients with large amounts of breast glandular tissue. [Baker 1982, Stomper 1989, Burrell 1996A, Hollingsworth 1993] The density of this tissue tends to obscure underlying pathology. Premenopausal women and women undergoing estrogen replacement therapy are more likely to have dense glandular breasts. This may partially explain why some randomized trials of mammography have failed to demonstrate a significant reduction in breast cancer mortality for women under 50 years old. Furthermore, tumor doubling times may be shorter in younger women. With current technology, for women under 50, the average interval between mammographically apparent disease and clinically apparent disease averages only 1.5 to 2 years. For women over 50, this interval averages 3.5 to 4 years. [Moskowitz 1986] The American College of Radiology (ACR) and the American Cancer Society (ACS), among other organizations, currently advocate screening mammography for women between 40 and 49 years old every one to two years. It is desirable to increase the sensitivity of mammography in these patients so that their cancers are apparent earlier. This earlier detection may result in significantly reduced mortality in this population. In the United States, 24% of breast cancers occur in women under 50 years of age and 24% of deaths from breast cancer occur in women whose diagnoses were made before age 50. This means that 41% of the years of life lost occur in this age group. [Smart 1990]

Another major issue raised by the advent of widely available screening mammography is the frequency of false positive interpretations. In fact, among nonpalpable lesions that are submitted to needle localization and open surgical biopsy, only 10-30% prove to be malignant. [Sickles 1991, Lidbrink 1996, Burrell 1996B] The biopsy yield is higher with very little sacrifice in sensitivity in centers in which six month follow-up mammography is judiciously used in place of biopsy for the majority of probably benign lesions. [Sickles

1991] Generally speaking, the medical morbidity from open biopsies and needle aspirations is minimal. [Helvie 1991] The monetary costs are quite high with approximately 32% of the total cost of screening caused by open biopsy for benign disease. [Cyrlak 1988] According to Eddy, if screening is performed on women under 50 years old, the total dollars spent for work-up for false positive mammograms in this age group alone will amount to $40,654,00 in 1984 dollars, in the year 2000. [Eddy 1988] Clearly, this expenditure is a significant drain on a burdened health care system. If a more specific technique were available, a large sum of money might be saved.

Digital mammography could be both more sensitive and specific than standard film-screen mammography. Although these systems employ new, sophisticated detector technology and their operation is largely under computer control, they still possess the essential components of mammography systems and must achieve the same (and potentially higher) imaging goals as those required in conventional (screen-film) mammography.

One fundamental difference between digital and screen-film mammography is that, while in screen-film mammography the functions of image acquisition and image display are inextricably linked through the sensitometric properties of the film, in digital mammography they are decoupled. This should provide one of the major advantages of digital mammography - the potential for optimization of both the acquisition stage and the display parameters rather than needing to accept the compromises imposed in conventional mammography, e.g. the limitation in exposure latitude as the display contrast gradient of the film is increased.. This may also have an impact on the exposure techniques that are chosen for imaging. In screen-film mammography these are based on two goals - attainment of a target optical density on the processed film and adequate penetration of as much of the breast as possible. The first is achieved by the use of the automatic exposure control, the second primarily by choice of the x-ray spectrum. The main objective, of necessity, is to achieve a certain level of image contrast in all areas of the breast. This may occur at the expense of signal-to-noise ratio (SNR) in the image, a fundamental property determining its information content.

In digital mammography, both image contrast and brightness can be controlled at the stage of image display and, therefore, there is no single image, but an enormous range of possibilities for how the image is displayed. For this reason, in digital mammography it seems more appropriate to optimize the acquisition technique for SNR rather than brightness or contrast, and therefore, use a measure of SNR as an index of imaging performance. In addition, the substantially wider dynamic range of the x-ray detector reduces the concern regarding variation in penetration of different regions of the breast and may change the weighting of considerations in determining the x-ray spectrum. The introduction of digital mammography will impose the need to develop new algorithms for optimization of exposure techniques.

Despite the differences between digital and conventional mammography, the basic concepts of image quality are unchanged , so that it is logical to extend the ideas and

methods of acceptance testing, quality control and image optimization originally developed for screen-film imaging to digital mammography rather than starting afresh.

Important factors in the acquisition stage that require assessment include: geometrical alignment of components of the imaging system in relation to breast positioning, spatial resolution and signal-to-noise properties. In the display stage, it is essential to monitor the performance of hardware components which are subject to deterioration and miscalibration as well as software components such as look-up tables and enhancement algorithms which must be optimized for the imaging task.

The advent of digital mammography offers the possibility of further improvements in early breast cancer detection and characterization. [Shtern 1992] Careful large-scale multicenter clinical trials must be performed to evaluate the new technology to assess its potential utility. This will require radiologist readers who have undergone training in how to interpret images that do not resemble standard film-screen images. Training sets must be developed to accomplish this goal. The reading studies must be carefully constructed so that the interpretation task closely mimics that which occurs in the clinical setting. Even small improvement in sensitivity or specificity (e.g. between 5 and 10%) are potentially clinically important since breast cancer is a common disease. Even a small increase in sensitivity might translate into many lives saved. Likewise, given the frequency of breast biopsy for benign diagnoses, a small increase in specificity could save a substantial amount of patient anxiety and money.

Obviously, these types of clinical trials and reading studies cannot be undertaken lightly. The expenditure of time and money required to do the "right" type of research is substantial. The development of digital mammography holds forth the possibility of tremendous improvement in the early diagnosis of breast cancer.

Materials and Methods

Patient Enrollment

Our goal was to perform a multicenter clinical pilot study to evaluate the diagnostic accuracy of digital mammography in the diagnostic (or problem-solving) mammography population. This project was seen as a pilot study, designed to provide estimates of the sensitivity and specificity of digital mammography compared to film-screen mammography in women who have dense breasts who present for problem-solving mammography. This project provided better estimates of the numbers of women required for a large-scale clinical trial, given the variability in radiologist interpretation performance. Such variability might be attributable to machine type and patient-related factors, among other unpredictable factors.

The study was carried out at 7 institutions, utilizing digital mammography units manufactured by three different companies (Fischer Imaging Senoscan® (Fischer Imaging Corporation, Denver, CO), the Fuji Medical Systems Computed Radiography for Mammography (Fuji Medical Systems USA, Stamford, CT), General Electric

Senographe 2000 D (General Electric Medical Systems, Milwaukee, WI) and the Trex Digital Mammography System (Trex Medical Corporation, Long Island, NY). The institutions, the type of digital mammography system utilizied and the number of patients enrolled at each site are shown in Table 1.

Table 1

Institution	Machine Type	Number Enrolled
University of Pennsylvania	General Electric	30
Massachusetts General Hospital	General Electric	22
University of Toronto /Mt. Sinai	Fischer	26
Thomas Jefferson	Trex	26
University of North Carolina	Fischer	48
Good Samaritan Hospital	Trex	30
University of Virginia	Trex	20

There were two groups of eligible women: Group A and Group B.

Group A consisted of all consecutive women with mammographically dense breasts who presented to the participating mammography clinics for problem-solving mammography and who were scheduled to undergo either open or percutaneous large core needle breast biopsy within the 12 weeks after the eligibility mammogram. Women with palpable and/or nonpalpable lesions were included in this group. Women who underwent ***only*** fine needle aspiration (FNA) or cyst aspiration as part of their work-up of an abnormal mammogram or physical examination, or women with only axillary abnormalities were ***not*** eligible.

Group B consisted of a random sample of women with mammographically dense breasts who presented to the participating mammography clinics for problem-solving

mammography and who were ***not*** scheduled to undergo biopsy and who were recommended for 1 year follow up.

Women who otherwise met the eligibility criteria were excluded if they were pregnant, or believed that they might be pregnant, they were unable to give informed consent for any reason, if they had prior mastectomy, if they had breast implants, or if they had reason for inability to undergo follow-up mammography at the participating institution for at least 2 years after study entry. Patients were also excluded if their screen-film mammogram was deemed to be of poor quality, if they had undergone FNA, cyst aspiration or biopsy within 6 months of the eligibility mammogram, and if the breast density was considered to be less than 20% of the total breast volume. At each institution, a radiologist determined the eligibility of the women presenting for problem-solving mammography, including deciding whether the patient has dense breasts by film-screen mammography. Randomization of women for inclusion in Group B took place during the final week of patient enrollment only.

After obtaining informed consent from the patient, a research assistant interviewed her regarding demographic and symptom information. In addition, data was collected at each of the local sites by a radiologist regarding the location of lesions detected through screen-film mammography and physical examination. In addition, breast pathology reports were collected and coded centrally by a single radiologist. (EDP)

All enrolled women underwent two-view mammograms (both cranio-caudal and medio-lateral oblique views) of both breasts using the available screen-film and digital mammography systems. For large-breasted women, as many cranio-caudal and medio-lateral oblique views as were deemed necessary to include each breast in its entirety were performed.

Collecting Matched Screen-Film Mammograms

In order to allow the use of all digital mammograms for all readers in the reader study, matched screen-film mammograms were collected from the UNC case files. To maximize comparability, the same inclusion criteria were applied to the screen-film

mammograms. Research assistants selected the analogue mammograms from the hospital clinical information system by reviewing records of women imaged at UNC more than one year but less than five years prior to the beginning of this study. Two hundred cases were selected based on their match to the digital mammograms for breast density, lesion type (mass, calcification, architectural distortion) and histopathological diagnosis. Normal mammograms with at least 1 year of follow-up, and no clinical or mammographic evidence of malignancy, were also selected.

Controlled Reader Study

The reader study for this project compared laser printed digital mammograms using the manufacturer's recommended printing algorithm with laser-printed image-processed digital mammograms, with original matched film-screen mammograms. The image processing algorithms that were tested in this study were Histogram-based Intensity Windowing and Contrast Limited Adaptive Histogram Equalization. A total of 18 (17 board-certified and 1 board-eligible) diagnostic radiologists read all 200 digital mammograms and 100 matched screen-film mammograms.

For the reader study, the digital mammograms of all of the women entered into the study were divided into 4 sets of cases, one set of 100 matching film screen mammograms and 3 sets of 200 digital mammograms. Each set of digital mammograms consisted of the entire collection of 200 digital cases in one processed format Each reader read one set of 100 film screen mammograms matched for inclusion criteria to the set of 200 digital mammograms and randomized for inclusion for each of the 18 readers. Each reader read

one set of 200 digital mammograms, in one of the 3 digital formats, randomized for each of the 18 readers. This allowed each of the 3 possible digital processed methods to be read by 6 of the 18 readers. The order of case presentation was counterbalanced and randomized for each reader.

Images were interpreted in the standard clinical fashion, using mammographic viewboxes with a magnifying glass. The assigned radiologist readers had no prior familiarity with or information about the cases being read.

A research assistant who was specially trained to perform this study directly supervised the experimental readings. Each reading session took place at the University of North Carolina. The experimental cases to be interpreted, both film-screen mammograms and digital mammograms, were prehung on multiviewers with appropriate masking. Readers interpreted cases for 45 minutes and took breaks as needed.

The interpreting radiologists answered yes or no to the following question for all mammograms: "Are there any radiologic findings on this mammogram?" If the answer to this question was "yes", then the radiologist noted the location of each finding using ACR descriptors, namely, an o'clock location, an antero-posterior location, and woman's body side (i.e. right or left). Each radiologist also graded each finding using the following scale:

1: There is no finding or the finding is definitely not malignant.
2: The finding is probably not malignant.
3: The finding is possibly malignant.
4: The finding is probably malignant.
5: The finding is definitely malignant.

In addition, the radiologist was asked to give a recommendation for each finding, as follows:

1: No further work-up. Routine follow-up only.

2: No further work-up. Six month follow-up only.

3: Further work-up with additional mammographic views and/or ultrasound.

4: Further work-up with either percutaneous or open surgical biopsy.

Data Analysis

A General Linear Multivariate Model analysis was used, with repeated measures tests based on the Geisser-Greenhouse test. Sensitivity, specificity and area under the ROC curve performance were measured for all readers.

Results

A total of 202 patients were enrolled into the study. The numbers of patients enrolled per each institution are shown in Table 1. Incomplete data was received on 2 patients so these were eliminated from the reader study. Of those included in the reader study, 165 were from Group A and 35 were from Group B.

References

Baker LH. 1982. Breast cancer detection demonstration project: five-year summary report. CA 32(4), 194-225.

Brekelmans CT, Van Gorp JM, Peeters PH, Collette HJ. 1996. Histopathology and growth rate of interval breast carcinoma. Characterization of different subgroups. Cancer 78(6): 1220-1228.

Burrell HC, Sibbering DM, Wilson AR, Pinder SE, Evans AJ, Yeoman LJ, Elston CW, Ellis IO, Blamey RW, Robertson JF. 1996A. Screening interval breast cancers: mammographic features and prognosis factors. Radiology 199(3): 811-817.

Burrell HC, Pinder SE, Wilson AR, Evans AJ, Yeoman LJ, Elston CW, Ellis IO. 1996B. The positive predictive value of mammographic signs: a review of 425 nonpalpable breast lesions. Clinical Radiology 51(4): 277-281.

Cyrlak D. 1988. Induced costs of low-cost screening mammography. Radiology 168: 661-663.

Eddy DM, Hasselblad V, McGwney W, Hendee WR. 1988. The value of mammography screening in women under age 50 years. JAMA 259:1512-1519.

Fletcher SW, Black W, Harris R, Rimer BK, Shapiro S. 1993. Report of the International Workshop on Screening for Breast Cancer. JNCI 85(20): 1644-56.

Helvie MA, Ikeda DM, Adler DD. 1991.Localization and needle aspiration of breast lesions: complications in 370 cases. AJR 157:711-714.

Hollingsworth AB, Taylor LD, Rhodes DC. 1993. Establishing a histologic basis for false- negative mammograms. American Journal of Surgery 166(6): 643-647.

Kerlikowske K, Grady D, Rubin SM, Sandrock C, Ernster VL. **1995.**Efficacy of screening mammography. A meta-analysis. JAMA 274(5): 381-382.

Letton AH, Mason EM, Rainshaw BJ. 1996. Twenty year review of a breast cancer screening project. Ninety-five percent survival of patients with nonpalpable breast cancers." Cancer 77(1): 104-106.

Lidbrink E, Elfving J, Fussell J, Jonsson E. 1996. Neglected aspects of false positive findings of mammography in breast cancer screening: analysis of false positive cases from the Stockholm trial. BMJ 312(7026): 273-276.

Moskowitz M. 1986. Breast cancer: Age-specific growth rates and screening strategies. Radiology 161,37-41.

Nystrom L, Rutqvist LE, Wall S, Lindgren A, Lindqvist M, Ryden S, Andersson I, Bjustam N, Fagerberg G, Fussell J. 1993. Breast Cancer Screening with mammography: Overview of Swedish Randomized trials. Lancet 342(8851): 973-8.

Shtern, F. 1992. Digital mammography and related technologies: a perspective from the National Cancer Institute. Radiology 183:629-630.

Sickles E. 1991. Periodic mammographic follow-up of probably benign lesions: results in 3,184 consecutive cases. Radiology 179(2):463-8.

Smart C. 1990. The role of mammography in the prevention of mortality from breast cancer. Cancer Prev. 1-16.

Stomper PC, Gelman RS. 1989. Mammography in symptomatic and asymptomatic patients. Hem/Onc Clinics NA, 3(4),611-640.

APPENDIX E:

MANUSCRIPTS IN PREPARATION

Radiologist Preferences for Digital Mammography Display

[To be submitted to *Radiology*]

The following grants partially supported this work:

Grey Scale Image Processing for Digital Mammography, National Cancer Institute, National Institutes of Health, Grant # RO1 CA60193-05

Multi-center Clinical Evaluation of Digital Mammography, Office of Women's Health, Department of Health and Human Services, Grant # 282-97-0078

Evaluation of Digital Mammography Display, U.S. Army Medical Research and Material Command, Grant # DAMD 17-94-J-4345

Enhancement and Analysis of Digital Mammograms. Canadian Breast Cancer Research Initiative, Grant #7289

Clinical Evaluation of digital Mammography. National Cancer Institute, National Institutes of Health. Grant # 1RO1CA60192

Measurement of Differential Image Quality to investigate two methods for evaluating differential image quality due To compression algorithms.
National Cancer Institute, National Institutes of Health. Grant # RO1-CA75145-01A1

Computer Analysis of Mammography Phantom Images (CAMPI): an Application to the Optimization and Evaluation of a Full-field Digital Mammographic Machine To apply two powerful image quality evaluation tools to a full field digital mammography machine. Office of Women's Health, Department of Health and Human Services, Grant # 282-97-0077

Abstract

Purpose: To determine the preferences of radiologists among eight different image processing algorithms applied to digital mammograms for the screening and diagnostic imaging tasks.

Materials and Methods: Twenty-eight images, representing pathologically proven cases obtained using three clinically available digital mammography units were processed and printed to film using Manual Intensity Windowing, Histogram-based Intensity Windowing, Mixture Model Intensity Windowing, Peripheral Equalization, MUSICA, Contrast Limited Adaptive Histogram Equalization, Trex® processing and Unsharp masking. Twelve radiologist observers compared the processed digital images to the screen-film mammograms of the same patient for breast cancer screening and breast lesion diagnosis.

Results: For the screening task, screen-film mammograms were preferred to all digital presentations, but Trex and MUSICA processed images were not statistically different in acceptability. All printed digital images were preferred to screen-film radiographs for the diagnosis of masses with Unsharp Masking processed mammograms statistically significantly preferred. For the diagnosis of calcifications, no digital algorithm was preferred to screen-film mammograms.

Conclusions: When digital mammograms were preferred to screen-film mammograms, radiologists selected different digital processing algorithms for each of three mammography reading tasks, and for different lesion types. Softcopy display will eventually allow this option more easily.

Key Words: Digital mammography, image processing, display

Background and Significance

Digital mammograms can be printed to film or displayed on a monitor. Typically, laser-printed films can display 4000X5000 pixels at 12 bits of grey scale. Although currently most radiologists are more comfortable with these printed images, the disadvantages of film display for digital mammography are obvious. Once an image is printed, it can no longer be manipulated, and any information available in the digital data but not captured in the printed image will therefore be lost.

With currently available high luminance, high resolution monitors (2000X2500 pixels) (1), for many digital mammograms, only a portion of the breast can be displayed at one time at full resolution. In addition, comparing prior with current and left with right images is difficult. Roaming, zooming and grey level manipulation of the digital images with the computer, while possible, is not trivial to learn, and can be inefficient and time-consuming. Memory requirements for on-line interpretation are currently prohibitive. More practical displays with short, clinically acceptable display times for the entire set of images, including comparison images, are needed before digital mammography can reach its full potential. Exploration of this issue was the purpose of a recent working group meeting jointly sponsored by the Office of Women's Health and the National Cancer Institute. (2)

Given the present limitations of soft-copy technology and radiologist preferences, digital mammography will most likely be displayed on film for the next few years at least. Therefore, exactly how the images should be printed is an important issue. Even if softcopy display is utilized, it is important to determine how the images should be

viewed for optimal visualization of different lesion types in breasts of different radiographic density.

This is the first study to systematically explore the utility of displaying printed digital mammograms using 8 different image processing algorithms. We sought to determine the preferences of radiologists for algorithms for the two main tasks in mammography: lesion detection (screening) and characterization (diagnosis).

Methods

Image Production

Radiologist investigators at four participating institutions (EDP, LLF, DK and EC) selected unilateral digital mammograms for inclusion in the study. Studies were deemed eligible for inclusion if there were mammographic findings present and the screen-film image of the same patient was available for comparison. The cases were obtained using three different full field digital mammography devices: 10 cases from the Trex Digital Mammography System (Trex Medical Corporation, Long Island, NY), 10 cases from the Fischer SenoScan (Fischer Imaging Corporation, Denver, CO), and 8 cases from the General Electric Senographe 2000 D (General Electric Medical Systems, Milwaukee, WI).

Study cases were selected from all available digital mammograms available at the involved institutions. Coinvestigators were requested to select mammograms containing findings, i.e. masses or calcifications, preferably in patients with dense breasts. The findings were either pathologically proven or were considered benign by virtue of mammographic stability for at least 6 months. The goal was to obtain 10 cases

for each manufacturer, but only 8 cases were contributed from the General Electric system.

The raw digital data was transmitted to the University of North Carolina, and to other participating institutions for image processing purposes, by Exabyte 8mm tape (Exabyte Corporation, Boulder, CO), or over the internet using File Transfer Protocols (FTP). Exabyte tapes were read using an Exabyte 8mm Tape Drive (Exabyte Corporation, Boulder, CO).

For Trex images, the image size was 4800x6400 pixels with 40 micron pixel size. For GE images, the image size was 1800x2304 pixels with 100 micron pixel size. For Fischer images, the image size was 3072x4800 pixels with 50 micron pixel size. All three units produce images with 16 bits/pixel.

All images were processed using each of 8 different algorithms: Manual Intensity Windowing (MIW), Histogram-based Intensity Windowing (HIW), Mixture Model Intensity Windowing (MMIW), Contrast Limited Adaptive Histogram Equalization (CLAHE), MUSICA (Agfa®), Unsharp Masking(UM), Peripheral Equalization (PE) and Trex® processing. The details regarding how these algorithms were applied for this study are described in Appendix 1.

All images were maintained at their original contrast and spatial resolution during processing. HIW, MIW, MMIW, and Trex processed images were printed to film without subsequent contrast manipulation of any type. CLAHE, PE and UM images were manually intensity windowed by an experienced mammography technologist before printing. MUSICA images were intensity windowed over a fixed range (0-4095 grey

values). A single Orwin Model 1654 high brightness (100ftL) monitor (Orwin Associates, Inc., Amityville, NY), utilizing a Dome Md5Sun Display Card (Dome Imaging, Waltham, MA) and a Sun UltraSparc model 2200 computer (Sun Microsystems, San Jose, CA) was used for all manual intensity windowing. Both the monitor and display card have a display matrix size of 2048 x 2560 pixels.

All images except those with Trex processing were printed on Kodak Ektascan HN film (Eastman Kodak Company, Rochester, NY) using a Kodak 2180 EktaScan Laser Film Printer® (Eastman Kodak Company, Rochester, NY). This printer is capable of 12 bits/pixel. Images that contained a bit range wider than that of the printer were linearly remapped to the range of the printer. Images were bilinearly interpolated by the Kodak printer to its maximum spatial resolution, with a 50 micron pixel size and a matrix of 4096 x 5120, and printed by the Kodak printer at this resolution. The laser film was processed using a Konica Medical Film Processor QX-400 (Konica Medical Corporation, Norcross, GA).

Trex processed images were printed on Agfa Scopix LT-2B helium-neon film using an Agfa LR5200 film printer (Agfa Division of Bayer Corporation, Ridgefield, NJ). This printer is capable of 8 bits per pixel. The matrix size for this printer is 4776x5944 pixels, and it has a 40 micron pixel size. Films were processed using a Kodak RP-Xomat processor (Eastman Kodak Corporation, Rochester, NY).

Trex mammograms were cropped from 4800x6400 pixels to fit the printer matrix size. Fischer and GE images were scaled up using interpolation by factors of 1.35 and 3.5 respectively. All printers and monitors used in this study were calibrated to comply

with the DICOM grey scale display function standard. (American College of Radiology, Reston, VA and National Electrical Manufacturers Association, Roslyn, VA). (3)

Of the 224 processed digital mammograms, 3(1.3%) could not be printed because of printer software errors. These were excluded from the study. In addition, all printed digital images were reviewed for quality by an expert breast imager who did not participate in the ranking of the images. Four (1.8%) images were deemed of very poor quality and were excluded for that reason. Thus, a total of 7 (3.1%) digital mammograms of the original 224 prepared were not included in the study.

Preference Study

A total of 65 lesions were identified and circled on the two views of a single version of the digital printed image of the patient's digital mammogram. A written description of each of the circled lesions was also prepared. This description included histologic information about the lesion, if that was available. Other lesions were presumed to be benign by virtue of a minimum of one year of mammographic stability with no clinical findings.

Tables Ia, Ib and Ic give a complete description of the images included in this study. Each case rated had at least 1 and up to 6 lesions to evaluate. Cases included only pathologically proven lesions (2 GE, 5 Trex and 2 Fischer), only presumed benign lesions (3 GE and 5 Fischer) and both types of lesions (3 GE, 5 Trex and 3 Fischer).

Twelve radiologists, all Mammography Quality Standards Act (MQSA) qualified mammography interpreters, independently participated as readers in this study. Written

instructions were provided to each radiologist prior to the study. Appropriate masking of the viewboxes was utilized throughout.

The 28 cases were presented to each reader in random order by a research assistant. The craniocaudal images of each patient were presented first, followed by the mediolateral oblique images. The 8 processed digital mammograms were presented randomly within each case to each reader. Readers were also provided with the corresponding screen-film mammogram on the same patient, the annotated printed digital mammogram of the same view (lesions circled and numbered), and the description of the histologic findings for each case. The radiologists hung the annotated image on the top viewbox panel of a standard mammography lightbox (Mammography Illuminator, Two Tier Desktop, Picker International, Inc., Norcross, GA). The screen-film mammogram and one of the eight digital processed mammogram to be rated were hung on the lower viewbox panel. Radiologists were provided with and encouraged to use a magnifying glass.

First, radiologists were asked to rate the visibility and characterizability of each lesion on the processed digital image with respect to its depiction on the corresponding screen-film mammogram. Radiologists were instructed to use their expert judgement in determining which areas on the screen-film image corresponded to the lesions seen on the digital images, taking into account differences in positioning, compression, and other factors. Utilizing all relevant clinical information, readers were asked to consider whether the processed digital image allowed sufficient visualization and characterization of each lesion so that the correct diagnosis could be reached. Each lesion on the digital mammogram was rated on a 5-point scale as much better, better,

the same, worse or much worse than its screen-film counterpart (+2,+1,0,-1 or –2, respectively) with respect to visibility and characterizability. No magnification films or spot radiographs were provided to the readers.

Next, the radiologists were asked to rate the digital processed image as much better, better, the same, worse or much worse than the corresponding screen-film image for the purpose of screening (+2,+1,0,-1 or –2, respectively). For this task, they were asked to consider whether the digital image allowed sufficient visualization of all relevant anatomic structures for effective breast cancer screening. They were instructed to disregard artifacts that occurred outside the borders of the breast in making this judgment. Again, craniocaudal images were rated first, followed by mediolateral oblique images.

The radiologists completed the tasks in the order in which they were presented. To limit the effects of fatigue, short breaks (at least 5 minutes) were required after every 50 minutes of work. The radiologists also took additional breaks as needed. On average, the radiologists required 5 hours to evaluate all images.

A research assistant recorded the radiologist's ratings for each processed digital image, as well as any other comments the radiologist made about the cases and/or the digital processing algorithms. The research assistant then manually entered the data into a Microsoft® Excel spreadsheet (Microsoft Corporation, Redmond, WA).

In sum, a total of 8 processed images for each of the 28 cases, minus the 7 images that were excluded, were compared to screen-film images by 12 radiologists. The total number of images viewed per radiologist was 441 (8 algorithms x 28 cases x 2

views = 448, minus the 7 images that were not scored). The cases contained a total of 65 lesions, 29 that were pathologically proven and 36 that were presumed benign. For the diagnostic task, there was one score per lesion for each of the two views for each of the eight algorithms less the scores on the 18 lesions in the 7 missing images for each of the twelve readers (((65 lesions X 2 views X 8 algorithms) – 18 missing lesions that were not scored) X 12 readers) for a total of 12264 diagnostic scores collected. For the screening task, there were 2 views of 28 cases with 8 algorithms per case, minus the seven missing images, by 12 readers, (((28 X 2 X 8) – 7) X 12) for a total of 5292 screening scores collected. Therefore, a total of 17556 scores were requested from the 12 readers (12264 + 5292).

As some readers intentionally or accidentally failed to rate one or more lesions, the dataset was incomplete. Some of the missing values were incurred when a reader was unable to detect a lesion on either the screen-film mammogram or on the digital image, and was therefore unable to rate it. Missing scores for lesions not visible on screen-film were assigned scores of +2. To avoid possible bias towards digital due to positioning differences, the two cases for which scores were resolved in this manner were excluded from the final analyses (although including them did not change results). Missing scores for lesions not visible on the digital image were assigned scores of –2. Cases so affected were retained in all analyses. Other missing scores were due to accidental oversights by the reader and the research assistant.

Statistical Methods

All primary and exploratory analyses were conducted separately within the three mammography machines.

The primary analysis focused on the data for the diagnostic task, and consisted of two parts. First, a mean for each processing method by lesion type combination was calculated by averaging over reader, case, breast view, and lesion. Lesion types considered were calcifications and masses; masses with calcifications were classified as masses. Each of these 16 means (8 processing methods by 2 lesion types) was tested as equal to zero, corresponding to a null hypothesis of no difference in radiologist preference between the printed digital image and the screen-film mammogram. Per the Bonferroni technique for multiple comparisons, each test was evaluated at α =.01/16 =.000625, for an overall Type I error rate of .01 for this set of tests.

In the second part of the primary analysis, model assumptions were verified and the data were analyzed by the Analysis of Variance (ANOVA) technique. The design for this two-way factorial repeated measures ANOVA included lesion type, processing method, and their interaction. The test of method by lesion type interaction was conducted first, followed by step-down tests of the simple main effect of processing method within each lesion type. Within each of the two lesion types, there are (8 choose 2)=28 pairwise comparisons among the digital processing methods, for a total of (28*2)=56 tests. Per the Bonferroni technique, each test was evaluated at the α=.04/56=.000714285 level, resulting in an overall Type I error rate of .04 for this set of

tests. Note that the overall Type I error rate for the complete primary analysis *within each machine* is (.01 + .04) = .05.

The exploratory analysis of the screening task data mirrored the primary analysis. First, a mean for each processing method by lesion type combination was calculated by averaging over reader, case and breast view. Lesion types considered were again calcifications and masses; masses with calcifications were classified as masses. Each of these 16 means (8 processing methods by 2 lesion types) was tested as equal to zero, corresponding to a null hypothesis of no difference in radiologist preference between the printed digital image and the screen-film mammogram with respect to breast cancer screening. Per the Bonferroni technique for multiple comparisons, each test was evaluated at α =.01/16 =.000625, for an overall Type I error rate of .01 for this set of tests. However, as this analysis is exploratory, p-values must be interpreted as descriptive statistics only.

In the second part of the exploratory analysis, model assumptions were verified and the data were analyzed by the Analysis of Variance (ANOVA) technique. The design for this two-way factorial repeated measures ANOVA included lesion type, processing method, and their interaction. The test of method by lesion type interaction was conducted first, followed by stepdown tests of the simple main effect of processing method within each lesion type. Within each of the two lesion types, there are (8 choose 2)=28 pairwise comparisons among the digital processing methods, for a total of (28*2)=56 tests. Per the Bonferroni multiple comparisons procedure, each test was

evaluated at the α=.04/56=.000714285 level, resulting in an overall Type I error rate of .04 for this set of tests.

Finally, all method by lesion type means were centered by subtracting the overall mean score for that machine. Centered means were computed for both the primary and exploratory analyses. In order to discourage comparison of mean scores among the different mammography machines, only the centered means will be presented in the results section. However, note that all p-values presented pertain to tests of the uncentered data.

All statistical analyses were performed using SAS Software, Version 6.12. (SAS Institute, Cary, NC.)

Results

Primary Analysis: Diagnostic Mammography Scores

Tables II and III show radiologist ratings of the digital processing algorithms with respect to the screen-film mammogram for the diagnostic mammography tasks. Ratings are presented by machine type. For all Tables, Machine A is the Fischer SenoScan, Machine B is The General Electric Senographe 2000D, and Machine C is the Trex Digital Mammography System.

For each machine, there was a strongly statistically significant relationship between lesion type and image processing algorithm preference for the lesion characterization, or diagnostic mammography, task (p=0.0002 for Fischer, 0.0024 for GE and 0.0338 for Trex). That is to say, for each machine, radiologists preferred

different algorithms for the mass characterization and calcification characterization tasks.

Fischer Results

For the diagnostic evaluation of masses (including masses with calcifications), all printed digital mammograms were preferred to the screen-film mammograms for all eight processing algorithms. Musica, Trex, PE, UM and CLAHE were significantly preferred at the α =.01/16 =.000625 level. The machine-centered means for these algorithms were 0.37, 0.35, 0.32, 0.43 and 0.40, respectively.

For the diagnostic evaluation of calcifications, three of the eight printed processed digital mammograms, Trex processing, HIW, and MMIW, were rated as slightly better or equivalent to the screen-film mammograms (0.15, 0.07 and 0.03 machine-centered means respectively). These differences did not reach statistical significance. The screen-film image was significantly favored over the MIW and PE processed digital images, with $p<.000625$ (.01/16). The machine-centered means for these algorithms were -0.39 and -0.69, respectively.

GE Results

For the mass diagnostic task, the UM processed digital image was slightly but not statistically significantly preferred to the screen-film image. The machine-centered mean score for UM was 0.18. The screen-film mammogram was statistically

significantly preferred over the Trex processed image at the α =.01/16 =.000625 level; the machine-centered mean score for Trex was -0.27.

For the calcifications diagnostic task, the MIW, HIW, UM, MMIW processed images were all slightly preferred to the screen-film image. However, no digital processing algorithm was statistically significantly preferred. The machine-centered means for MIW, HIW, UM and MMIW were 0.19, 0.34, 0.30 and 0.28, respectively. The screen-film mammogram was statistically significantly preferred over the PE processed image at the α =.01/16 =.000625 level; the machine-centered mean score for PE was -0.48.

Trex Results

For the mass diagnostic task, all processed digital images except MMIW were preferred to the screen-film mammogram, with the Trex and HIW images statistically significantly preferred at the α =.01/16 =.000625 level. Machine-centered means for Trex and HIW were 0.53 and 0.57, respectively. The screen-film mammogram was preferred to the MMIW image, but not significantly. The machine-centered mean for MMIW was 0.17.

For the diagnostic evaluation of calcifications, the screen-film radiograph was statistically significantly preferred over all eight processed digital images at the α=.01/16 =.000625 level. The machine-centered mean scores ranged from –0.23 for the Trex processing algorithm to –0.75 for the PE method. These results were statistically significant for all eight algorithms ($p<.01/16$ or .000625).

Secondary Analysis: Overall Screening Score

Tables IV and V show radiologist ratings of the digital processing algorithms with respect to the screen-film mammogram for the screening mammography tasks. Ratings are presented by machine type.

There was a relationship between lesion type and image processing algorithm preference for each machine for the lesion detection, or screening mammography, score (p=0.0169 for Fischer, 0.1025 for GE and 0.0165 for Trex). Since this is an exploratory analysis, p-values may only be interpreted as descriptive statistics, and not as tests of significance.

Fischer Results

For the detection of both masses and calcifications, only Trex processed-digital radiographs were preferred to screen-film mammograms, although they were not strongly preferred. Machine-centered means for Trex processing of Fischer images were 0.84 for masses and 1.0 for calcifications. The screen-film image was strongly preferred over the MMIW-processed images for both mass and calcification detection. Machine-centered means for MMIW were -0.5 and –1.0 for mass and calcification detection, respectively. The screen-film image was also strongly preferred over MIW, PE and UM for the detection of calcifications (machine-centered means of -0.27, -0.37 and -0.16, respectively). All tests were assessed at the α = .01/16 = 0.000625 level.

GE Results

For the detection of both masses and calcifications, the screen-film mammograms were preferred to the printed digital radiographs for all processing algorithms. For masses, the machine-centered mean scores ranged from 0.44 for the Musica algorithm down to -0.48 for Trex. For calcifications, the machine-centered means ranged from 0.38 for Musica down to -0.41 for PE. All p-values were less than .01/16=0.000625 except Musica and HIW for masses, and Musica and MIW for calcifications.

Trex Results

The Trex-processed digital radiograph for the detection of masses was the only processing method preferred to the screen-film mammogram, but it was not strongly preferred ($p>.000625$). The Trex machine-centered mean for mass detection was 0.91. The screen-film mammogram was preferred to all other processed digital images for the detection of masses; centered means ranged from 0.91 for Trex down to –0.64 for MMIW. The screen-film mammogram was preferred to all eight processed digital images for the detection of calcifications; centered means ranged from 0.39 for Musica to –0.64 for CLAHE. P-values were less than 01/16=.000625 for all algorithms except Trex and MUSICA for both lesion types.

Discussion

Our results strongly indicate that radiologists prefer different processed versions of the digital mammogram depending on the task, the lesion type and the machine type.

This conclusion suggests that digital mammograms would best be displayed using monitor systems that allow flexibility and easy, quick access to different processed versions of the images. If soft-copy interpretation is to become clinically practicable, ergonomic issues regarding image display using monitor systems must be overcome.

Undoubtedly, habit and experience influenced the preference of radiologists for screen-film images over processed digital images in many cases. A prior preference study, that attempted to exactly match the appearance of the screen-film mammograms through manual intensity windowing, showed that radiologists preferred digital mammography to screen-film. (6) Of course, such matching might not allow the full benefits of digital mammography to be realized.

This study is limited by the fact that it was a preference study and not a quantitative measure of how well the radiologists performed. Radiologists gave their opinions on which images would improve their performance. Certainly they made educated guesses, but a performance study would have been better at determining how mammographic interpretation would be affected by image processing. This study is a good first step, however. A performance study would require many more cases and would have been too expensive and unwieldy if 8 algorithms were tested. This experiment allows us to run the next study as a performance study, with more cases and fewer algorithms to test.

In addition, this study is limited in that the diagnostic mammography task did not include available compression and magnification views. However, since this affected both modalities equally, it should not have significantly altered our results.

Clearly, the entire universe of image processing algorithms has not been tested. We chose those algorithms that were available to us that are in clinical use, or that we believed might have clinical utility, and about which we had expertise. Perhaps wavelets or one of its derivatives or an algorithm yet to be developed might have performed better than all of those tested and the screen-film mammogram for all three tasks. In addition, a combination of algorithms, such as would be available with a softcopy display system, might allow for even better diagnostic performance and might have been the most preferred by the radiologists.

In addition, since we included such a small number of cases and different lesions were imaged with each of the three systems, we believe that the direct comparison of the results achieved by the three machines is not reasonable at this time. That is to say, we believe that the mean scores that the radiologists gave the various units for the various tasks should NOT be directly compared. We believe that we cannot justify statements about how the three units compare for the diagnosis or detection of masses or calcifications based on this preliminary study alone. For example, clearly the algorithms that were tested did not allow optimal calcification characterization with the Trex digital images, and optimal calcification and mass detection with the GE digital images. We believe that these results reflect more on the limitations of the algorithms tested than on the detectors themselves. In addition, because the Trex images were printed with a different type of film, printer and processor than the GE and Fischer images, some of the differences between the Trex and the other images could be attributable to these factors.

[redacted]

We did omit seven images from the total processed image data set either because they could not be printed or they were deemed to be of poor quality. We believe that the size of any bias that was introduced into the study due to this factor was quite small, given that the omitted images only represented 3.1% of the total sample prepared.

In fact, these results strongly suggest that each digital mammography manufacturer should determine which algorithms to use for optimal digital mammography display for each mammographic task. These results will help in guiding those decisions. Clearly, some sort of objective performance measure (7,8), rather than an aesthetic assessment, should be used by the manufacturers in guiding the selection of image processing algorithms. We believe that image processing might significantly enhance the achievable accuracy of digital mammography. Conversely, choices based on producing digital mammograms that closely resemble screen-film radiographs might limit the results that can be achieved with this new technology.

Finally, we could not determine in this study whether other factors, such as breast density, patient age, location of the lesion within the breast and other variables such as softcopy display, would influence radiologist preferences regarding the algorithms. The role of these factors will have to be evaluated in future studies.

Appendix 1

Manual Intensity Windowing (MIW)

For MIW, an expert mammography technologist manually intensity windowed the digital mammograms on an Orwin Model 1654 high brightness (100ftL) monitor (Orwin Associates, Amityville, NY), utilizing a Dome Md5Sun Display Card (Dome Imaging, Waltham, MA) and a Sun UltraSparc model 2200 computer (Sun Microsystems, San Jose, California). Both the monitor and display card have a display matrix size of 2048x2560 pixels. The intensity windowing software was interactive, and the technologist could choose either a linear or asymmetric sigmoidal within-window intensity mapping curve shape.

Histogram-Based Intensity Windowing (HIW)

In HIW, the histogram for each individual mammogram in a study is automatically analyzed in terms of its peaks and troughs. All components of the breast tissue, such as the parenchyma, fatty areas and skin edge portions, are recognized from these histogram features. With this method, contrast over the selected range of values of breast tissue is enhanced via simple intensity windowing.

Mixture-Model Intensity Windowing (MMIW)

MMIW uses a combination of geometric (i.e., intensity gradient-magnitude ridge traversal) and statistical (i.e., Gaussian mixture modeling) techniques. This method isolates the radiographically dense component in each mammogram and based on

statistical characteristics of this isolated region sets the parameters of an asymmetric sigmoidal intensity mapping function.

Contrast Limited Adaptive Histogram Equalization (CLAHE)

Contrast Limited Adaptive Histogram Equalization (CLAHE) is a variant of Adaptive Histogram Equalization (AHE). In AHE, the histogram is calculated for the contextual region of a pixel, and the transformation provides the pixel a new intensity which is proportional to its rank in the intensity histogram. It is designed to provide higher contrast for pixel intensities which occur more frequently and to provide a single displayed image in which contrasts in all parts of the range of recorded intensities can be sensitively perceived. CLAHE limits the contrast increase factor produced by AHE to a user-specified unit. The CLAHE parameter settings (clip 4, region size 32) used in this study were based on prior published experiments. (7)

MUSICA

MUSICA processing is a multiscale wavelet-based contrast enhancement technique developed by Agfa® (Agfa Division of Bayer Corporation, Ridgefield Park, NJ). It involves variable enhancement of various spatial scale components of the image, followed by additive reconstruction. MUSICA processing was performed on an Agfa image processing workstation. Three of its four image processing parameters, namely Edge Contrast, Latitude Reduction and Noise Reduction were turned off by setting their levels to 0. The parameter for MUSICA was set to a maximum level of 5.

Unsharp Masking (UM)

Unsharp Masking is a technique used for crispening edges. A signal proportional to the unsharp, or low-passed filtered (blurred), version of the image is subtracted from the original image to yield a "sharpened" resulting image. The final image is produced by combining the original image (50% weighting) and the high-pass images (50% weighting). In our experiment a region size of 600x600 pixels was used for the calculation of the low-pass image.

Peripheral Equalization (PE)

IN PE, thickness differences between the periphery of the breast and the center portions are smoothed out so that the range of intensity values is accessible within the same narrow portion of the density look-up table. The thickness of the breast is approximated by using a smoothed version of the mammogram with resolution of about 3mm. The perimeter of the breast is determined by a simple threshold applied to the smoothed image, and grown to a few millimeters outside the breast. Masking of pixels outside this area is applied to remove detector flat-fielding artifacts. The thickness effect is removed essentially by dividing the original image values by those in the smoothed image. The correction is only applied within 3 cm of the periphery of the breast, while areas within the center of the breast are left at their original values. A damping factor, which limits the magnitude of the correction, is applied to the pixels immediately adjacent to the edge of the breast to reduce ringing. (8).

Trex Processing

The Trex processing used in this study is the proprietary processing applied as part of the Trex full-field digital mammography system. The algorithm is a weighted unsharp masking based on histogram data.

Acknowledgments

The authors gratefully acknowledges the contributions of the following individuals in support of this work: Faina Shtern of the Office of Women's Health, Department of Health and Human Services, Michelle Picarro, Michael Tesic, Ruth Grafton, Pat Campbell and Morgan Nields of Fischer Imaging Corporation, Beale Opsahl-Ong of General Electric Corporate Research and Development, Lim Cheung and Richard Bird of Trex Medical Corporation, Art Haus, Theresa Bogucki and Jeff Byng of Eastman Kodak, Willem Van Reit , Charles Augello and John Landry of Agfa; Jenny Harrison, Patty Barbour, Lisa Quamme, Kerrie Kurgat, Mark Kramer, Sheldon Earp, Anna Cleveland, Sanjay Sthapit, and Joseph K.T. Lee of the University of North Carolina, Wendy Kurutz of Good Samaritan Hospital; Denise McDonald of the University of Pennsylvania; Anoma Gunasekara of the University of Toronto; Lisa Sparacino of Thomas Jefferson University; Jayne Cormier of Massachusetts General Hospital; Claire Poyet and Karen Seaton of Wake Radiology, Raleigh, NC, Elizabeth Eagle and Rebecca Kennedy of Greensboro Radiology, and Mary Baldwin of the University of Virginia.

This work would not have been possible without the generous support of Fischer Imaging Corporation, General Electric Medical Systems, Trex Medical Corporation, Eastman Kodak Corporation and the Agfa Division of Bayer Corporation.

References

1. Weibrecht M, Spekowius G, Quadflieg P, Blume H. Image quality assessment of monochrome monitors for medical soft copy display. SPIE 1997; 3031:232-244.

2. Shtern F and Winfield D. (eds.) Report of the Working Group on Digital Mammography: Digital Displays and Workstation Design. March 9-10, 1998. Public Health Service Office of Women's Health and National Cancer Institute Document.

3. http://www.nema.org/standards/DICOM.HTM

4. Moore RH, Kopans DB, Niklason LT, et al. Initial Clinical Experience with Full-field Digital Mammography. [abstract] Radiology 1997; 205(P): 274.

5. Pisano ED, Zong S, Hemminger BM, et al. Contrast limited adaptive histogram equalization image processing to improve the detection of simulated spiculations in dense mammograms. J of Dig Imaging 1998; 11(4):193-200.

6. Pisano ED, Chandramouli J, Hemminger BM, et al. Does intensity windowing improve the detection of simulated calcifications in dense mammograms? J of Dig Imaging 1997; 10(2):79-84.

7. Pizer SM. Psychovisual issues in the display of medical images. In: Hoehne KH, ed. Pictorial Information Systems In Medicine. Berlin: Springer-Verlag, 1985; 211-234,.

8. Byng JW, Critten JP, Yaffe MJ. Thickness equalization processing for mammographic images. Radiology 1997; 203:564-568.

Table Ia. Case Types: Pathologically Proven Lesions. N=29

Machine	# of cases	Masses		Calcifications		Architectural Distortions	
		Cancer	Noncancer	Cancer	Noncancer	Cancer	Noncancer
General Electric	5	4	2	1	1		
TREX	10	4	5	2	4		
Fischer	5	1	2	1	1		1

Table Ib. Case Types: Lesions presumed benign due to stability. N=36.

Machine	# of cases	Masses	Calcifications	Architectural Distortions
General Electric	6	7	5	1
TREX	5	3	3	1
Fischer	8	5	10	1

Table Ic. Case Types: Histologic diagnoses for Pathologically Proven Lesions*

Cancers	**Masses**	**Calcs**	**AD^**
Infiltrating Ductal Carcinoma	6	0	0
Ductal Carcinoma in Situ	1	4	0
Infiltrating Lobular Carcinoma	2	0	0
Noncancers			
Atypical Ductal Hyperplasia	1	2	0
Fibrocystic Change	1	2	0
Cyst	3	0	0
Fibroadenoma	2	0	0
LCIS** and Atypical Lobular Hyperplasia	1	1	0
Intraductal Papilloma	1	0	0
Atrophy	0	1	0
Chronic Inflammation and Fibrosis	0	0	1

AD^ = Architectural Distortion

LCIS** = Lobular Carcinoma in Situ.

*The total number of pathologically proven lesions is not equal to the number of cases because some cases had more than one lesion and some cases had 0 pathologically proven lesions.

Table II. Radiologist Preference Mean Scores +/- Standard Deviation for Image Processing Algorithms applied to Printed Digital Mammograms Relative to Screen-film Mammograms for Mass Characterization.

Algorithm	Machine A	Machine B	Machine C
MUSICA	0.37+/-0.34	0.03+/-0.20	0.24+/-0.14
Trex Processing	0.35+/-0.28	-0.27+/-0.27	0.53+/-0.19
MIW	0.21+/-0.26	0.04+/-0.22	0.42+/-0.19
HIW	0.20+/-0.34	-0.03+/-0.26	0.57+/-0.28
PE	0.32+/-0.24	-0.02+/-0.22	0.33+/-0.30
UM	0.43+/-0.30*	0.18+/-0.26	0.47+/-0.23
CLAHE	0.40+/-0.19*	-0.11+/-0.18	0.44+/-0.19
MMIW	0.13+/-0.29	-0.09+/-0.24	0.17+/-0.16

*Mean score statistically significantly better than screen-film mammogram
p<.000625 or 0.01/16
Meaningful comparisons between machine types is not possible using these data.

Table III. Radiologist Preference Mean Scores +/- Standard Deviation for Image Processing Algorithms applied to Printed Digital Mammograms Relative to Screen-film Mammograms for Calcification Characterization

Algorithm	Machine A	Machine B	Machine C
MUSICA	-0.34+/-0.24	-0.02+/-0.24	-0.32+/-0.18**
Trex Processing	0.15+/-0.24	-0.23+/-0.31	-0.23+/-0.22
MIW	-0.39+/-0.19**	0.19+/-0.36	-0.44+/-0.19**
HIW	0.03+/-0.24	0.34+/-0.40	-0.42+/-0.29**
PE	-0.69+/-0.38**	-0.48+/-0.22**	-0.75+/-0.16**
UM	-0.11+/-0.28	0.30+/-0.44	-0.51+/-0.11**
CLAHE	-0.31+/-0.25	0.05+/-0.32	-0.56+/-0.17**
MMIW	0.07+/-0.28	0.28+/-0.38	-0.64+/-0.19**

**Mean score statistically significantly worse than screen-film mammogram
$p<.000625$ or 0.01/16

Meaningful comparisons between machine types is not possible using these data.

Table IV. Radiologist Preference Mean Scores +/- Standard Deviation for Image Processing Algorithms applied to Printed Digital Mammograms Relative to Screen-film Mammograms for Mass Screening Task

Algorithm	Machine A	Machine B	Machine C
MUSICA	0.41+/-0.47	0.44+/-0.58	0.51+/-0.49
Trex Processing	0.84+/-0.34	-0.48+/-0.45**	0.91+/-0.42
MIW	-0.14+/-0.71	0.11+/-0.39**	0.11+/-0.37**
HIW	0.09+/-0.57	0.26+/-0.48	0.12+/-0.45**
PE	0.07+/-0.47	-0.24+/-0.26**	-0.22+/-0.43**
UM	0.09+/-0.78	-0.04+/-0.49**	0.02+/-0.38**
CLAHE	0.06+/-0.47	-0.05+/-0.39**	-0.11+/-0.36**
MMIW	-0.50+/-0.59**	0.01+/-0.54**	-0.64+/-0.37**

**Mean score much worse than screen-film mammogram
p<.000625 or 0.01/16

Meaningful comparisons between machine types is not possible using these data.

Table V. Radiologist Preference Mean Scores +/- Standard Deviation for Image Processing Algorithms applied to Printed Digital Mammograms Relative to Screen-film Mammograms for Calcification Screening Task.

Algorithm	Machine A	Machine B	Machine C
MUSICA	0.32+/-0.50	0.38+/-0.47	0.39+/-0.46
Trex Processing	1.00+/-0.34	0.13+/-0.45**	0.28+/-0.38
MIW	-0.27+/-0.35**	0.31+/-0.38	0.04+/-0.40**
HIW	-0.10+/-0.61	0.15+/-0.48**	0.12+/-0.34**
PE	-0.37+/-0.47**	-0.41+/-0.36**	-0.38+/-0.40**
UM	-0.16+/-0.46**	-0.29+/-0.51**	-0.38+/-0.36**
CLAHE	-0.10+/-0.57	0.11+/-0.45**	-0.64+/-0.29**
MMIW	-1.00+/-0.34**	-0.29+/-0.42**	-0.59+/-0.45**

**Mean score statistically significantly worse than screen-film mammogram
p<.000625 or 0.01/16

Meaningful comparisons between machine types is not possible using these data.

Figure Legends

Figure 1a.

Photographic magnification of a craniocaudal view of a screen-film mammogram (1a).

Figure 1b.

A photographic magnification of a digital mammogram of the same region of the same breast imaged with a General Electric Senographe 2000 D (1b,c and d), processed with HIW. The clustered calcifications (arrows) seen in these images were needle-localized and surgically proven to be atypical ductal hyperplasia. The automated windowing algorithms, (MMIW, HIW, CLAHE) and MIW, the algorithms that somewhat compromise visibility of the skin for greater contrast in dense areas, all scored better than screen-film for calcification characterization for this case. The algorithms that are designed to improve contrast while maintaining skin visibility either were equivalent to screen-film (TREX processing) or worse (Unsharp Masking, MUSICA, and PE). (Case provided by Daniel Kopans of Massachusetts General Hospital).

Figure 1c.

Same digital mammogram processed with CLAHE.

Figure 1d.

Same digital mammogram processed with MIW.

Figure 2a.

This photographic magnification of a Fischer SenoScan® craniocaudal digital mammogram, processed with Unsharp Masking, shows a moderately well circumscribed mass in the far lateral portion of the breast, just below the skin, (arrow), that proved to be a simple cyst by ultrasound-guided fine needle aspiration. Because of its location at the periphery of the breast, the lesion is not even visible on some of the algorithms that cause reduced visibility of subcutaneous detail to allow improved penetration and contrast for the densest areas (MIW, MMIW and HIW).

Figure 2b.

The same area of the digital mammogram processed with CLAHE.

Figure 3a.

This photographic magnification of the subareolar region of a screen-film mammogram reveals a partially circumscribed, partially obscured nonpalpable mass (arrows) that had been visible for over 1 year by mammography and was therefore presumed benign. (Case provided by Emily Conant, MD of the University of Pennsylvania.)

Figure 3b.

The General Electric Senographe 2000 D digital mammogram of the same lesion (arrows) displayed after processing with Unsharp Masking, an algorithm preferred by

study radiologists for mass characterization with GE images. Note the improved border conspicuity over the screen-film image.

Figure 3c.

Digital mammogram of the same lesion (arrows) displayed using MIW processing.

Figure 3d.

Digital mammogram of the same lesion displayed using MUSICA processing.

Figure 4a.

This photographic magnification of a mediolateral oblique screen-film mammogram shows a spiculated mass in the axillary tail that proved by core biopsy and subsequent mastectomy to be infiltrating lobular carcinoma and lobular carcinoma in situ. (Case provided by the Mark Williams, pH of the University of Virginia and Laurie Fajardo, MD of Johns Hopkins University.)

Figure 4b.

Trex Digital Mammography System digital mammogram of the same lesion, processed with MUSICA. For this lesion, all digital images had higher mean scores than did the screen-film mammogram, probably because the spiculations on the anterior margin of the mass are more obvious on the digital images. The five processed digital images, 4b-4f, are shown in their order of preference to the radiologists for this particular case.

Figure 4c.

Processed with CLAHE.

Figure 4d.

Processed with HIW.

Figure 4e.

Processed with MIW.

Figure 4f.

Processed with Trex processing.

Image Processing Algorithms For Digital Mammography
-A Pictorial Essay

[To be Submitted to *Radiographics*]

This work was supported in part by National Cancer Institute RO1 CA60193-05; Office of Women's Health, Department of Health and Human Services, # 282-97-0078; U.S. Army Medical Research and Material Command, # DAMD 17-94-J-4345, Canadian Breast Cancer Research Initiative #7289; National Cancer Institute 1RO1CA6019, National Cancer Institute RO1-CA75145-01A1 and National Cancer Institute RO1-CA60183.

ABSTRACT

This article demonstrates the use of image processing algorithms with digital mammograms. Four illustrative cases obtained using three different digital mammography units show the advantages and disadvantages of seven different display algorithms for the specific tasks required in breast imaging – diagnosis and screening. This paper will elucidate why different algorithms may be useful for different tasks. The use of multiple algorithms for digital mammography display will necessitate the development of softcopy workstations for this modality.

Summary Statement
This article demonstrates the use of image processing algorithms with digital mammograms.

INTRODUCTION

The effectiveness of digital mammography in breast cancer detection is currently under investigation. This imaging modality separates image acquisition and image display, which allows for optimization of both.

In screen-film mammography, film serves as the medium for both image acquisition and display. Screen-film mammography offers limited detection capability of low contrast lesions in dense breasts. This poses a problem for the estimated 40% of women with dense breasts who receive mammograms (1). In this population, diagnosis often requires additional imaging, which results in more radiation exposure for the patient. When additional images fail to provide useful diagnostic information, a decision must be made as to whether the suspicious regions require biopsy or short or long term follow-up. Because of the expense and the risk associated with additional radiation exposure and surgery, any method of image presentation that increases the diagnostic conspicuity of lesions in breast tissue, but especially in dense tissue, would be a significant advance.

Digital mammography systems, unlike screen-film mammography systems, allow for manipulation of fine differences in image contrast through the use of image processing algorithms. As a result, very subtle differences between abnormal and normal but dense tissue can be made more obvious. The purpose of this paper is to illustrate the appearance of various image processing algorithms for display of digital mammograms and to discuss how these algorithms may affect the ability of radiologists to interpret the images.

Cases Used in this Paper

The four cases used in this paper to demonstrate the image processing algorithms were selected to show the range of types of mammographic lesions and the potential advantages and disadvantages of the different display algorithms. Figures 1a, 2a, 3a and 4a show the screen-film radiographs of these four patients. All digital mammograms in this paper were acquired under research protocols approved by the Investigational Review Boards at the involved institutions.

Figure 1a shows a photographic magnification of a partially obscured and partially circumscribed mass that proved to be a simple cyst by ultrasound and needle aspiration. The accompanying digital mammogram, displayed with 7 different image processing algorithms in Figures 1b-1h, was acquired at the University of North Carolina using the Fischer SenoScan full field digital mammography unit (Fischer Imaging Corporation, Denver, CO).

Figure 2a shows a screen-film mammogram of a breast with two indistinct masses. Photographic magnification of the screen-film mammogram of the larger mass is provided in Figure 2b. Both masses proved to be infiltrating ductal carcinoma with accompanying ductal carcinoma in situ (DCIS) by needle-localized open surgical biopsy. Figures 2c through 2f show the same patient's digital mammogram, which was acquired at Massachusetts General Hospital using the General Electric Senographe 2000D full field digital mammography system (General Electric Medical Systems, Schenectady, NY).

Figures 3a and 3b show a screen-film mammogram of a palpable spiculated mass that proved to be infiltrating ductal carcinoma with associated cribiform and solid-type DCIS at open surgical biopsy. Figures 3c and 3d show the Fischer SenoScan digital mammogram of the same patient, acquired at the University of North Carolina.

Figure 4a is a photographic magnification of a screen-film mammogram containing a pleomorphic cluster of calcifications that proved to be atrophic breast tissue at stereotactically-guided core biopsy. Figures 4b-4h show the same patient's digital mammogram from a Trex Digital Mammography System (Trex Medical Imaging Corporation, Danbury, CT), acquired at the University of Virginia.

Brief Overview of the Digital Mammography Systems

The GE system produces images with a spatial resolution of 100 microns per pixel that have a total matrix size of 1800 x 2304 pixels. Trex images are 41 microns per pixel with a display matrix size of 4800 x 6400 pixels. Fischer images are 54 microns per pixel with an image size of 3072 x 4800 pixels. The smaller the number of microns per pixel, the smaller the features that can be measured in the image produced. As for contrast resolution, the Trex and GE units offer 14 bits per pixel while the Fischer unit offers 12 bits per pixel. Increasing contrast gradation provides the opportunity to distinguish finer and finer density differences between features in the image. However,

the ability of a human observer to distinguish finer and finer gradations of gray may not always be possible due to visual perception and display device limitations. Detailed descriptions of the image acquisition hardware are provided elsewhere. (2)

Image Processing Algorithms Illustrated

Each manufacturer has developed image processing algorithms to use with its acquisition system. In addition, there are a number of algorithms that have been developed by independent investigators for use with digital mammograms. Specifically, the seven algorithms that are demonstrated in this paper are Manual Intensity Windowing (MIW), Histogram-based Intensity Windowing (HIW), Mixture-Model Intensity Windowing (MMIW), Contrast-Limited Adaptive Histogram Equalization (CLAHE), Unsharp Masking (UM), Peripheral Equalization (PE), and Trex proprietary processing.

Intensity Windowing Algorithms (IW)

Intensity windowing algorithms act on individual pixels within an image. A small portion of the full intensity range of an image is selected and then remapped to the full intensity range of the display device. This allows for the selection of specific intensity values of interest. For example, intensity values that represent abnormal tissue and dense but normal tissue are selected to allow for the exaggeration of small differences in intensity values between the two objects, thus potentially increasing the conspicuity of any abnormal regions. The three versions of IW demonstrated in this paper are Manual Intensity Windowing (MIW), Histogram-based Intensity Windowing (HIW), and Mixture-Model Intensity Windowing (MMIW). These algorithms differ in how intensity values of interest are selected.

Manual Intensity Windowing (MIW)

Manual Intensity Windowing was performed by an expert mammography technologist who interactively adjusted the contrast levels as appropriate for each image using an Orwin 1654 high brightness monitor (Orwin Associates, Amityville, NY) and a Sun Ultra Sparc 2200 (Sun Microsystems, San Jose, CA). The goal of this algorithm is to manually reproduce the appearance of a screen-film mammogram.

Figures 1b, 2c and 4b all illustrate this algorithm applied to the selected cases. These images readily demonstrate how similar in appearance the digital mammograms can be to standard screen-film mammograms of the same patients. For Figure 2c, the center of the large mass is very light. This is because of the technologist's selection of a window that allowed visualization of both lesions in the image. Both lesions were obvious to her trained eyes. In order to keep the smaller lesion from appearing less

obvious or even disappearing completely, she windowed the larger lesion so it was slightly lighter than ideal.

This case points out the obvious limitation of this interactive windowing algorithm. It is operator dependent. A less experienced operator might choose different windows that could obscure some of the visible pathology.

Histogram-based Intensity Windowing (HIW)

Histogram-based Intensity Windowing (HIW) is a variant of the intensity windowing (IW) image processing algorithm. Intensity windowing allows for a selected sub-range of the image intensity values to receive the full contrast of the display device. All parts of the image with values outside the selected intensity window range are set to black (less than the low end of the intensity window range) or white (higher than the maximum value in the intensity window range). HIW customizes standard intensity windowing by individually selecting the intensity window range for each image by statistically analyzing the histogram of each image, and locating the "humps" or modes of the histogram, and determining which modes represent the different breast tissue types (fatty, dense, muscle) or other parts of the image (background, labels). From these known modes in the histogram, an automatic selection of an intensity window range is made based upon percentile position within the composite breast tissue class (i.e. fatty, dense and muscle) that allows windowing over the overall breast tissue that is present in that woman. For example, if the woman's breast is mainly fatty, the window selected will allow the full range of contrast across the part of the histogram representing the fatty portions of the breast. If the breast is mixed fatty and dense, the window will be selected by the portions of the histogram that represent those areas. Theoretically, this should improve the detection of mammographic features compared with fixed intensity windowing, which cannot adapt to individual images. The adaptability of HIW to individual breast types is especially appropriate for digitally acquired mammograms, because the breast tissue is always imaged with reasonable contrast, but the range of digital values containing the breast tissue can vary significantly depending on acquisition parameters. An example of how the window is tailored for an individual histogram with HIW is shown in Figure 5.

Figures 1c and 4c demonstrate this automated windowing algorithm. For the cyst in Figure 1c, notice the improved conspicuity of the lesion edge on the digital radiograph compared to the screen-film mammogram shown in Figure 1a. Part of the difference in visibility in the lesion border and the accompanying benign calcifications is attributable to differences in positioning and compression. There is some loss of detail outside the dense parts of this image compared to the screen-film image and to the other digital mammogram presentations. This might detract from the use of this algorithm for screening.

Mixture-Model Intensity Windowing (MMIW)

Mixture-Model Intensity Windowing provides regions-specific intensity window settings for mammograms. It operates by automatically identifying the five major regions in a mammogram: background, uncompressed fat, fatty, dense, and muscle. It identifies these regions using a combination of geometric (i.e., gradient magnitude ridge traversal) and statistical (i.e., Gaussian mixture modeling) techniques. Once these regions have been identified, their histograms can be selectively analyzed to determine region-specific intensity window settings. For this study, MMIW was used to determine intensity window settings specific to the dense regions in mammogram. [3]

The steps of MMIW are illustrated in Figures 6a through 6d. In Figure 6a, the major regions of a mammogram have been labeled. Since mammograms are formed via projection, these region labels reflect the prominent tissue present at that location; not the absolute quantities of the multiple tissues that affected x-ray absorption at each point. In Figure 6b, the regions have been labeled and the image has been automatically cropped to reduce the portion of background in the image. Having identified these regions, the intensity histogram of each region can be calculated. The mean and standard deviation of the intensities in each region are used to parameterize a sigmoidal intensity window function. Those functions (mapping recorded intensity to displayed intensity) for each region are shown in Figure 6c. The result of applying the dense-region-specific intensity window function to the entire image produces the image shown in Figure 6d. Each image in this paper was processed using it own, MMIW-defined, dense-region-specific intensity window function.

Figures 1d, 2d, 2e and 4d demonstrate digital mammograms with MMIW applied. For all three cases, this algorithm enhances the visibility of the lesion borders against the fatty background. However, the mixed parenchymal densities that abut the lesion are lost in some cases. This effect is most dramatic at the edges of the mammogram, as shown in Figure 2d. Clearly, if this type of statistical sampling of the image is utilized to determine an optimal intensity window, an additional algorithm that enhances the visibility of the periphery of the breast should be used to rescue information that is lost at the low density subcutaneous regions of the breast.

Both HIW and MMIW algorithms might be useful on a workstation. At the touch of a button, radiologists could request a processed digital mammogram that allows them to see through the densest portions of the breast. Neither would probably be acceptable for the display of screening mammograms, however, since information in the peripheral and fatty areas of the breast is not visible when these algorithms are applied.

Contrast Limited Adaptive Histogram Equalization (CLAHE)

Contrast Limited Adaptive Histogram Equalization is a special class of Adaptive Histogram Equalization (AHE). Processing an image with AHE maximizes the contrast

throughout an image, by adaptively enhancing the contrast of each pixel relative to its local neighborhood. This produces improved contrast for all levels of contrast (small and large) in the original image. For AHE to enhance local contrast, histograms are calculated for small regional areas of pixels, producing local histograms. These local histograms are then equalized or remapped from the often narrow range of intensity values indicative of a central pixel and its closest neighbors to the full range of intensity values available in the display.

CLAHE limits the maximum contrast adjustment that can be made to any local histogram. This is useful so that the resulting image does not become too noisy. The size of the neighbor region is controlled through the region size parameter. Smaller regions can better enhance the contrast of smaller spatial scale structures. The CLAHE parameter settings (clip 4, region size 32) used in these sample digital mammograms were selected based on previous experiments (4). After CLAHE was applied, Manual Intensity Windowing was used so that the contrast of the resulting image more closely approximated standard screen-film mammography. Figure 7 provides a graphic illustration of how clipping with CLAHE redistributes the pixels in an image.

Figures 1e and 4e demonstrate CLAHE-processed digital mammograms. The lesions in these images do appear very obvious compared to background and the image detail is very good. However, note also the obvious visualization of graininess in the digital images. This is due to the enhanced visibility of both image signal and image noise by this algorithm. Again, this algorithm might be helpful in allowing radiologists to see subtle edge information, such as spiculation. It might degrade performance in the screening setting by enhancing the visibility of nuisance information that could simulate calcifications.

Unsharp Masking (UM)

Unsharp masking (5) is a technique whereby a low-pass filtered version of the original image is created and the image values that result are subsequently multiplied by a weighting factor and subtracted from the original image. The final image preserves much of the detail of the original image, but large structures are presented with less contrast, thereby reducing the dynamic range required to display the image. In preliminary experiments, a variety of low-pass filters where tested using kernel sizes from 2 mm^2 to 33 mm^2. Similarly, a variety of weighting factors were tested. A boxcar filter with a window size of 16 mm^2 and a weighting factor of 0.8 were found to optimally compress dynamic range, while preserving necessary structures in the breast and minimizing artifacts. A kernel size based upon area was chosen so that comparison between manufacturers was possible in spite of differences in pixel size. The image data were then rescaled and an offset was added, as necessary, to approximately match the distribution of gray levels in the unprocessed and unsharp masked images. Manual Intensity windowing was then applied to the resultant image to adjust the contrast to levels more closely approximating standard screen-film mammography. Figure 8 schematically illustrates how UM is applied to the digital image.

Figures 1f, 2f, 3c and 3d demonstrate UM applied to digital mammograms. The sharpness of the borders of the mass lesions is enhanced, as is the intended effect of this algorithm. The spiculations in the Fischer digital mammogram, seen in Figures 3c and 3d, are rendered especially evident. Of course, Figure 2f illustrates how even an indistinct mass can appear more circumscribed when this algorithm is applied, obviously an undesirable outcome if this were to lead to inappropriate patient follow-up instead of biopsy.

Peripheral Equalization (PE)

Peripheral Equalization is a technique that enhances visualization of tissue located near the periphery of the breast. (6, 7)

There are variations in thickness of the breast tissue under compression during image acquisition. The outer edges of the breast, which are thinner than the interior, are typically over-penetrated by x-rays at acquisition. Although the digital acquisition system should have adequate dynamic range to record this information precisely, the limited latitude of the laser film necessitates a compromise in image display. If the central parenchyma is presented with high contrast, then the peripheral tissue will appear very black on the film and may be difficult to distinguish visibly from the black film background. (Figure 9.)

In PE, a low-pass spatial filter is applied to the image to create a blurred "mask" that represents primarily the coarsest variations in signal which are related to variations in breast thickness. This mask is scaled from 0 to 1 and the mammogram is divided by the mask values on a pixel-by-pixel basis. (Figures 10a, 10b and 11) The algorithm is constrained to act only on pixels that lie within the breast and where the breast thickness is changing. There are also constraints placed on the total amount of enhancement to avoid disturbing artifacts at the skin line. The result is that the digital values of pixels located near the periphery are changed so that the absolute intensities of the image become "flatter" across the mammogram. The local contrasts between pixels located near each other, representing compositional variations in tissue are not suppressed. In fact, because the part of the dynamic range of the film required to represent thickness changes is no longer required, it is now possible to increase the overall contrast of the image if desired. For the illustrations in this paper, after PE was applied, Manual Intensity Windowing was used to adjust the resultant image contrast.

Figures 1g and 4g demonstrate this image processing algorithm. Both calcification and mass details are well depicted in these images. In addition, as is especially evident in Figure 1g, the peripheral information in the surrounding breast is preserved. This algorithm might be effective in the screening setting since it preserves image features in all breast locations. However, there does appear to be some flattening of image contrast in the nonperipheral portions of the mammograms when this algorithm is applied.

Trex-Processing

Trex-processing was developed by Trex Medical Imaging Corporation for use with the Trex Digital Mammography System. This method utilizes a form of histogram-based unsharp masking.

This algorithm is demonstrated in Figures 4h and 4i. As can be seen from these images, the algorithm allows visualization of both lesion detail and breast edge information. This is achieved with some reduction of image contrast, however, as seen in this case when the Trex-processed version is compared to the other processed versions of the same image.

Summary

It is obvious from the illustrated cases that different digital image processing algorithms are likely to be useful for different tasks. Characterization of lesions and screening will most probably require a uniquely adapted image-processing algorithm to provide the best presentation for visualization of different image features. In addition, different types of lesions, masses and calcifications, might benefit from specifically tailored algorithms. This will not be easily achieved unless the current method of displaying mammograms on film is replaced by a softcopy display system.

Given the added costs, the efficacy of digital mammography will ultimately depend upon improved diagnostic accuracy over conventional screen-film mammography. The development and assessment of image processing methods that allow for detection and characterization of individual lesion types will be instrumental in the acceptance of this new technology.

References

1. Shtern, F. Digital mammography and related technologies: a perspective from the National Cancer Institute. Radiology. 1992; 183: 629-630.

2. Feig SA, Yaffe MJ. Current Status of Digital Mammography. Seminars in US, CT and MRI. 1996; 17: 424-443.

3. Aylward SR, Hemminger BM, Pisano ED. Mixture modeling for digital mammogram display and analysis. In: Karssemeijer N, Thijssen M, Hendriks J, van Erning, eds. Digital Mammography Nijmegen, 1998. Dordrecht: Kluwer Academic Publishers, 1998; 305-312.

4. Pisano ED, Zong S, Hemminger BM, DeLuca M, Johnston RE, Muller K, Braeuning MP, Pizer S. Contrast Limited Adaptive Histogram Equalization Image Processing to Improve the Detection of Simulated Spiculations in Dense Mammograms. Journal of Digital Imaging. 1998; 11(4): 193-200.

5. Chan HP, Vyborny CJ, MacMahon H, et al. Digital mammography ROC studies of the effects of pixel size and unsharp-mask filtering on the detection of subtle microcalcifications. Investigative Radiology. 1987; 22: 581-589.

6. Byng, J.W., Critten J.P. and Yaffe, M.J. Thickness equalization processing for mammographic images. Radiology 1997; 203:564-568.

7. Bick U, Giger ML, Schmidt RA, Nishikawa RM, Doi K: Density correction of peripheral breast tissue on digital mammograms. RadioGraphics 16, 403-411, 1996.

LEGENDS

Figure 1a: This is a photographic magnification of a craniocaudal screen-film mammogram of a cyst.

Figure 1b: Photographic magnification of the Fischer digital mammogram, processed with Manual Intensity Windowing (MIW).

Figure 1c: Photographic magnification of the Fischer digital mammogram, processed with Histogram-based Intensity Windowing (HIW).

Figure 1d: Photographic magnification of the Fischer digital mammogram, processed with Mixture-Model Intensity Windowing (MMIW), showing the same lesion as seen in Figure 1a.

Figure 1e: Photographic magnification of the Fischer digital mammogram, processed with Contrast Limited Adaptive Histogram Equalization (CLAHE).

Figure 1f: Photographic magnification of the Fischer digital mammogram, processed with Unsharp Masking (UM). (Algorithm provided by Andrew Maidment, PhD of Thomas Jefferson University).

Figure 1g: Photographic magnification of the Fischer digital mammogram, processed with Peripheral Equalization (PE). (Algorithm provided by Martin Yaffe, PhD and Gordon Mawdsley, PhD of the University of Toronto)

Figure 2a: This mediolateral oblique screen-film mammogram shows two masses, (arrows) which both proved to be infiltrating ductal carcinoma with associated ductal carcinoma in situ at open surgical biopsy. (Courtesy of Daniel Kopans, MD, of Massachusetts General Hospital.)

Figure 2b: Photographic magnification of the screen-film image of the large inferior carcinoma.

Figure 2c: A photographic magnification of the larger lesion seen on the digital mammogram, displayed with MIW.

Figure 2d: This General Electric digital mammogram, processed with Mixture-Model Intensity Windowing (MMIW), shows both cancers very well.

Figure 2e: A photographic magnification of the larger lesion seen on the digital mammogram, displayed with MMIW.

Figure 2f: A photographic magnification of the larger lesion seen on the digital mammogram, displayed with UM. (Algorithm provided by Andrew Maidment, PhD of Thomas Jefferson University.)

Figure 3a: This mediolateral oblique screen-film mammogram shows a spiculated mass in the axillary portion of the breast, an infiltrating ductal carcinoma with associated cribiform and solid-type ductal carcinoma in situ at open surgical biopsy.

Figure 3b: A photographic magnification of the lesion seen on the screen-film mammogram.

Figure 3c: The Fischer digital mediolateral oblique mammogram, displayed using Unsharp Masking. (Algorithm provided by Andrew Maidment, PhD of Thomas Jefferson University.)

Figure 3d: A photographic magnification of the lesion seen on the digital mammogram, displayed with Unsharp Masking. (Algorithm provided by Andrew Maidment, PhD of Thomas Jefferson University.)

Figure 4a: This photographic magnification of a screen-film mammogram revealed a cluster of calcifications, which proved to be atrophic breast tissue at core biopsy. (Case provided by the University of Virginia and Laurie Fajardo of Johns Hopkins University.)

Figure 4b: The MIW processed digital mammogram with photographic magnification of the clustered calcifications.

Figure 4c: The HIW processed digital mammogram.
Figure 4d: The MMIW processed digital mammogram.

Figure 4e: The CLAHE-processed digital mammogram.

Figure 4f: The UM processed digital mammogram. (Algorithm provided by Andrew Maidment, PhD of Thomas Jefferson University.)

Figure 4g: The PE processed digital mammogram. (Algorithm provided by Martin Yaffe, PhD and Gordon Mawdsley, PhD, of the University of Toronto.)

Figure 4h: The digital mammogram with Trex proprietary processing applied.

Figure 4i: A photographic magnification of the lesion as seen with the Trex processing.

Figure 5: The histogram for a digital mammogram is shown. The range of intensity values representing breast tissue is seen on the right. These are automatically recognized by HIW. HIW then chooses a display range based on this breast tissue range. In this example a 30% to 100% range is chosen. Then the display devices output range is mapped to the selected intensity window range (30% location maps to black, 100% location maps to white).

Figure 6a: Figures 6a through 6d demonstrate the application of MMIW to digital mammograms. Figure 6a shows a digital mammogram with its various components labeled. "M" is pectoral muscle. "F" is fat. "UF" is uncompressed fat. "D" is dense breast tissue. "Bkg" is background.

Figure 6b: This figure shows the same image after cropping and segmentation. The muscle, dense, compressed fat, and uncompressed fat portions of the image are each identified by different portions of the gray scale of the image.

Figure 6c: This graph demonstrates how the recorded intensity of the different regions in the image is mapped to different displayed intensities in Figure 6d.

Figure 6d: This image shows the same mammogram as is shown in Figure 6a after MMIW is automatically applied.

Figure 7: This graph demonstrates how CLAHE redistributes the mapped intensities of the pixels in an image.

Figure 8: Illustration of Unsharp Masking in which a weighted, low-pass filtered image is subtracted from the original image. For consistency in display, the data are then rescaled and an offset is added when necessary.

Figure 9: Schematic illustration of the compressed breast. Under compression the breast is considered to consist of two regions, one of approximately uniform thickness referred to as the central region, and a margin, where thickness varies. In the margin, variation in transmitted x-ray fluence occurs due to changes in both breast thickness and composition.

Figure 10a: A smoothed representation of the image, s(x,y), is obtained from a low-pass filtering operation. The low-pass filter (shown schematically in 1 dimension) is a first order Butterworth filter with a cutoff frequency of 0.05 cycles/mm.

Figure 10b: Figure 8(b) Overview of the thickness equalization processing technique. For each point in the margin, the smoothed image is used to determine a correction factor.

Figure 11: A profile of brightness as a function of position across a line of the original and corrected images. The vertical lines identify the margin. Note the reduction in the range of levels in the corrected data, as a result of the adjustment in the margin.